The Dissertation Committee for Jessica Ann Plante Certifies that this is the approved version of the following dissertation:

Impact of West Nile Virus Envelope Domain III Surface Loop Residues on Antigenicity and Virulence

Committee:

David W.C. Beasley, PhD

Alan D.T. Barrett, PhD

James C. Lee, PhD

Theodore C. Pierson, PhD

Robert B. Tesh, MD

Dean, Graduate School

Impact of West Nile Virus Envelope Domain III Surface Loop Residues on Antigenicity and Virulence

by

Jessica Ann Plante, B.S.

Dissertation

Presented to the Faculty of the Graduate School of

The University of Texas Medical Branch

in Partial Fulfillment

of the Requirements

for the Degree of

Doctor of Philosophy

The University of Texas Medical Branch

September 2013

Dedication

I dedicate this dissertation to my parents, Linda Ann Lewis and Charles David Lewis, and to my husband, Kenneth Steven Plante. My parents always encouraged my love of science and learning, whether that meant asking me what I learned that day in class or spending their weekend driving me to science seminars for children. I never would have had the confidence to apply to graduate school or the drive to finish it without you. Ken, you have been the one rock solid thing that I could depend on in graduate school. You put things in perspective when I get frustrated, celebrate with me when things go right, and you are my best sounding board when I need help solving a problem. I love you all so much. I could not have accomplished any of this without your love and support.

Acknowledgements

Many thanks are due to my mentor, Dr. David Beasley, who has patiently taught me how to work in a virology lab and has kindly encouraged me on my way to becoming an independent scientist. The other members of the Beasley lab, namely Dr. Shuliu Zhang, Josef Lopez, Maricela Ramos, Alexander McAuley, and Evgeniy Bovshik, have been instrumental in teaching me new techniques and helping me perform experiments. Shuliu spent countless hours giving me hands-on training and was always kind to me; without her help I would have been lost with many of the techniques that were essential to completing this dissertation. I would like to thank my committee members, Drs. Alan Barrett, James Lee, Theodore Pierson, and Robert Tesh. They have generously helped me with their time, advice, and reagents. Finally, I would like to thank my two main funding sources, the Sealy Center for Vaccine Development pre-doctoral fellowship from Dr. Alan Barrett and the T-32 Biodefense Training program from Dr. Scott Weaver.

Impact of West Nile Virus Envelope Domain III Surface Loop Residues on Antigenicity and Virulence

Publication No._____

Jessica Ann Plante, Ph.D.

The University of Texas Medical Branch, 2013

Supervisor: David W.C. Beasley

West Nile virus (WNV) is an encephalitic flavivirus that is maintained worldwide in a transmission cycle between birds and mosquitoes. Domain III of its envelope protein is the target of highly specific and potently neutralizing antibodies, and is thought to bind the host cell receptors. To determine the role of individual surface loop residues in the function and antigenicty of WNV EIII, a panel of mutants was generated. Changes in antibody neutralization, *in vitro* replication kinetics, and *in vivo* virulence were characterized. In general, it was found that diversity in the surface loops was well tolerated and that all surface loop residues had at least some contribution to antigenicity. Residue T332 was especially important from an antigenic standpoint. Changes at T332 resulted in escape from neutralization by monoclonal and polyclonal antibodies both *in vitro* and *in vivo*. Changes at residues G331, D333, and N368 resulted in attenuation, suggesting a possible functional patch involved in receptor binding.

TABLE OF CONTENTS

List of Tables

List of Figures

List of Abbreviations

AST	Average survival time
DEF	Duck embryo fibroblast
CPE	Cytopathic effect
DC-SIGN	Dendritic Cell-Specific ICAM-3 Grabbing Non-integrin
DC-SIGNR	DC-SIGN Related
DENV	Dengue virus
DENV-1	Dengue virus type 1
DENV-2	Dengue virus type 2
DENV-3	Dengue virus type 3
DENV-4	Dengue virus type 4
DPBS	Dulbecco's phosphate buffered saline
E	Envelope protein
EIII	Envelope domain III protein
ELISA	Enzyme-Linked Immunosorbent Assay
ILHV	Ilheus virus
IP	Intraperitoneal
IPTG	Isopropylthio-β-galactoside
JEV	Japanese encephalitis virus
KFDV	Kyasanur Forest disease virus
LB	Luria broth
LD_{50}	50% Lethal dose
LGTV	Langat virus
MOI	Multiplicity of infection
MVEV	Murray Valley encephalitis virus
PAGE	Poly-acrylamide gel electrophoresis
PFU	Plaque forming unit
POWV	Powassan virus
PRNT	Plaque reduction neutralization test
SD	Standard deviation
SLEV	Saint Louis encephalitis virus
TBEV	Tick-borne encephalitis virus
WNF	West Nile fever
WNV	West Nile virus
YFV	Yellow fever virus
X-GAL	5-bromo-4-chloro-3-indolyl β-D-galactopyranoside

Chapter 1: Background

WEST NILE VIRUS DISTRIBUTION AND PHYLOGENY

West Nile virus (WNV) is a member of the family *Flaviviridae* and the genus *Flavivirus*. Within the flaviviruses, WNV is a member of the Japanese encephalitis virus (JEV) serogroup along with Murray Valley encephalitis virus (MVEV) and Saint Louis encephalitis virus (SLEV).(1) For many decades outbreaks of WNV disease in humans were mild, caused almost exclusively by members of lineage 1, and were largely restricted to Africa and Israel with some scattered cases in Europe.(2-12) Then, in 1999, a lineage 1 strain of WNV with increased virulence in birds was transported from Israel to New York, and rapidly established an endemic cycle in North America.(13-15) By the end of 2012 there had been 37,088 confirmed cases of human WNV disease in the United States, of which 20,892 were West Nile fever (WNF), 16,196 were neuroinvasive, and 1,549 were fatal.(16) WNV has also spread to Central and South America, although there have been far fewer human cases of WNV-associated disease.(17-21) Possible explanations include pre-existing antibodies to related flaviviruses and the increased diversity and decreased population density of birds in these tropical regions.(22, 23)

In addition to the spread of lineage 1 WNV strains into the Americas, lineage 2 has recently acquired a more virulent phenotype and caused significant human disease in Europe and the Mediterranean. Lineage 2 was detected in Hungary in 1994, then in Russia in 2007.(24, 25) WNV harvested from birds and mosquito pools during the early stages of the initial 2010 outbreak in Greece had acquired the T249P mutation in the WNV NS3 helicase associated with increased avian virulence in the lineage 1 strains introduced to New York.(26, 27) Pathogenic lineage 2 WNV has since spread to Italy(28)

Up to five more lineages of WNV have been proposed, but they contain far fewer isolates and it is less well defined whether some of these proposed lineages represent lineages of WNV or separate species of viruses.(29, 30) Lineage 3 WNV is represented by the Rabensberg strain which was isolated from mosquito pools in the Czech Republic in 1997, 1999, and 2003.(31-33) The Rabensberg strain replicates in C6/36 cells but not Vero E6, DF-1, BHK, or Hek293 cells.(29) Further efforts revealed that WNV Rabensberg could be made to replicate in Vero and E6 cells at 28°C but not 37°C, while it could replicate in C6/36 cells at either temperature.(34) It was also able to be maintained in mosquitoes via vertical transmission, but poorly disseminated suggesting that it may not be efficiently spread via horizontal transmission.(29) Lineage 4 originally consisted of a single isolate collected from a tick in Russia in 1988, but other lineage 4 strains have since been isolated from mosquitoes and frogs in the same region.(35-37) Lineage 5 contains WNV isolates from India previously classified as lineage 1c which have been proposed to constitute a separate lineage due to genetic and antigenic variation.(38) It has also been proposed that Kunjin virus, a close relative of WNV from Australia, may be lineage 6 of WNV and that Koutango virus, a close relative of WNV from Africa, may be lineage 7 of WNV.(39) Finally, nucleic acid from a single mosquito pool in Spain was determined to be a new WNV lineage that does not group with the seven previously described lineages, leading to its tentative assignment as the sole member of WNV lineage 8.(40)

WNV REPLICATION

Transmission Cycle

The main amplifying hosts of WNV are birds. There is some evidence that WNV can be passed directly between birds with no need for a mosquito intermediary, likely through grooming, contact with excrement, or ingestion of infected carcasses.(41, 42) Susceptibility to WNV infection is widespread among avian species, having been

detected in 332 species in the United States.(43) This ability to infect such a wide range of hosts may explain the worldwide distribution of WNV. Laboratory experiments demonstrated that passerine birds tend to be extremely competent hosts, reaching peak titers averaging $9.5\log_{10}$ plaque forming units (pfu)/ml by 2-4 days post-infection.(42) Extreme mortality in birds, first seen in Israel in 1998 and later a hallmark of the spread of WNV through North America in 1999, was one of the indicators that the North American strain originated in the middle east.(13-15, 44, 45) This change is thought to be caused by a T249P mutation in the NS3 helicase gene, resulting in earlier onset of viremia, 10,000-fold higher viremia, longer duration viremia, increased mortality, and lower average survival time (AST) in the American crow.(46) This T249P mutation in NS3 has also been associated with the emergence of virulent lineage 2 WNV in Greece.(26) The susceptibility of the American crow does appear to be declining, perhaps due to the intense selective pressure for naturally resistant bird populations since 1999.(47) Although other vertebrates such as rabbits, squirrels, and alligators and chipmunks do develop viremia upon WNV infection that approached or exceeds the presume threshold for mosquito infectivity, their importance in the natural transmission cycle is poorly defined.(48-50)

WNV is transmitted by mosquitoes and has been detected in 65 species in the United States.(51) The most important are thought to be members of the *Culex* genus. Specifically, *Culex pipiens* has been implicated in the eastern United States and *Culex tarsalis* and *Culex quinquifasciatus* have been implicated in the western United States. One key feature that makes *Culex* mosquitoes important in the spread of WNV is their selection of both humans and birds for blood feeding.(52-54) *Culex* mosquitoes are estimated to deliver 10^4-10^6pfu of virus to the host when they feed, and a host must in turn have a viremia of over 10^5pfu/ml to infect a naive mosquito.(55-57) This is why humans, who typically develop a viremia closer to 10^3pfu/ml, are considered dead-end hosts.(58) In addition to female mosquitoes acquiring WNV infection by feeding on an

infected host, female and male mosquitoes can acquire WNV infection via vertical transmission, and vertically infected females can horizontally transmit WNV to a vertebrate host.(59-61) Emergence of the WN02 genotype in the United States, characterized by a V159A mutation in the αA' α-helix of domain I in the envelope protein (see Figure 2), is attributed to a shortening the extrinsic incubation period in mosquitoes from seven days to five days.(62-64) The impact of V159A may be due to displacement of the carbohydrate bound to N154, which is shifted by the αA' α-helix that contains residue 159 (see the section 'Structure and Function of WNV E' for more details).(65) The precise timing and rate of dissemination in mosquitoes appears to be sensitive to factors such as age and weather, with warmer temperatures leading to more rapid dissemination.(66, 67)

Hard ticks can be infected by WNV and can maintain that infection during the transition from one life stage to the next, but they are incapable of transmitting WNV to a naïve vertebrate under experimental conditions.(68, 69) Soft ticks, on the other hand, have been collected from the field with WNV infections and have been experimentally shown to transmit WNV infection to a naïve vertebrate.(70, 71)

Replication Cycle

The first step in WNV infection of a cell is binding to the host receptor, but the identity of that receptor is not well defined. One possibility is the lectin dendritic cell-specific ICAM-3 grabbing non-integrin (DC-SIGN), which is found on dendritic cells and macrophages, and/or its endothelial cell homolog, DC-SIGN-related (DC-SIGNR).(72-74) Both DC-SIGN and DC-SIGNR are receptors for dengue virus (DENV).(75, 76) Expression of DC-SIGN and DC-SIGNR both increased WNV infection in cell lines, but the effect of DC-SIGNR was stronger and more consistent across cell types (i.e. DC-SIGNR substantially increased WNV infection of K562, Raji, SupT1, BHK, 293T, and CHO-K1 cells, but DC-SIGN caused only a modest increase in

WNV infection in all cell lines but Raji, which had the highest levels of DC-SIGN expression). Binding to DC-SIGN was more dependent on mannose-rich glycosylation than binding to DC-SIGNR. DC-SIGNR binding, however, did require glycosylation, as removal of both the prM and envelope (E) glycosylation sites eliminated DC-SIGNR binding.(77) Interestingly, when an additional N-linked glycosylation site was introduced to WNV E at residue D67N, infection was increased by both DC-SIGN and DC-SIGNR. This D67N glycosylation site is naturally present in DENV, which is also able to efficiently bind both DC-SIGN and DC-SIGNR.(78) However, a THP cell line that must express DC-SIGN for successful DENV infection is able to be infected by WNV with or without DC-SIGN expression, indicating that DC-SIGN/DC-SIGNR is not the exclusive receptor for WNV.(76)

One potential alternative is the integrin $\alpha_v\beta_3$. Antibodies against either α_v or β_3 reduced WNV binding, soluble $\alpha_v\beta_3$ reduced WNV entry into Vero cells, and either expressing β_3 or silencing $\alpha_v\beta_3$ increasing or decreases WNV infection, respectively.(79) Interestingly, like DC-SIGN/DC-SIGNR, WNV binding to $\alpha_v\beta_3$ may require glycosylation.(80) This is despite the finding that $\alpha_v\beta_3$ was bound by envelope domain III (EIII), which has no glycosylation site.(81) However, WNV is capable of infecting multiple cell lines that do not express $\alpha_v\beta_3$ integrin, so it, too, cannot be the exclusive receptor for WNV.(77, 82) It is possible that integrins are involved, not in binding or internalization, but in replication.(83)

Electron microscopy shows that within 0.5-3 minutes after binding to the receptor WNV enters the cell via clatherin-dependent endocytosis and the resulting endosome traffics to the perinuclear region near the endoplasmic reticulum.(84, 85) Upon endosome acidification, the E dimers dissociate and the fusion loops in domain II of the monomers swing outward to embed themselves in the endosomal membrane. This forms a trimer of E, which stabilizes when EIII folds back toward domain II and the stem region at the C-terminal end of EIII moves into a hydrophobic groove the runs up the length of E

in the newly formed trimer. This rearrangement by E brings the endosomal and viral membranes together and forming the fusion pore (Figure 1).(86) Further details regarding the structure of E are located in the 'Structure and Function of WNV E' section of this dissertation.

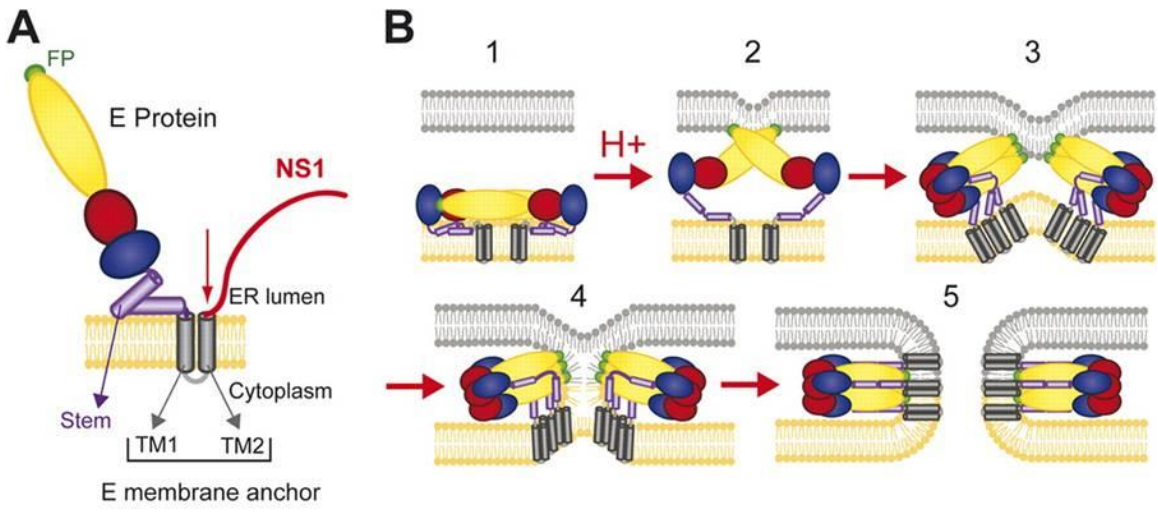

Figure 1: Schematic of Flavivirus Envelope During Membrane Fusion

Figure 1A: Diagram of flavivirus E and its attachment to the viral membrane. Figure 1B: Schematic of pH-induced rearrangement of E resulting in formation of a fusion pore. Red = domain I. Yellow = domain II. Blue = domain III. Figure from Fritz *et al*., reproduced with permission . See Appendix C.(86)

The WNV genome that is released from the pore is an 11kb, single-stranded, positive-sense strand of RNA with a 5' m^7GpppAmp cap but no 3' poly-A tail. The structural genes (C, prM, and E) are located at the 5' end of the genome, and the non-structural genes (NS1, NS2A, NS2B, NS3, NS4A, NS4B, and NS5) are located at the 3' end of the genome. Upon entering the cytoplasm, the WNV RNA genome is translated as a single polypeptide.(87) The polyprotein is cleaved into its three structural and seven nonstructural proteins by the NS2B/NS3 viral protease and host proteases.(88-90) The WNV RNA genome and the negative-sense template strand are transcribed by the NS5 RNA-dependent RNA polymerase, with production skewed toward the production of positive sense genomic RNA.(91-96) Two potential assembly and maturation sites for the WNV virion have been observed. The virus may rarely assemble near the plasma

membrane and acquire its lipid bilayer during its release from the cell via budding.(97) More commonly, the virus may assemble on the cytoplasmic surface of the endoplasmic reticulum and acquire its lipid bilayer by budding into the lumen of the ER, then be transported to the plasma membrane in a vesicle and exit the cell using the secretory pathway.(98) Between the assembly and release steps, low pH triggers the cleavage of 'pr' from M, changing the positions of E from a protruding to a flat dimer to form the smooth, mature virion.(99) Complete cleavage of all pr fragments from all M protein, however, is not necessary.(100)

WNV DISEASE IN HUMANS

Course of Infection

WNV is typically acquired by mosquito bite and is therefore first introduced either into a capillary, allowing it to directly seed a systemic infection, or to the epidermis. The mosquito feeding itself alters the environment into which WNV is initially introduced, and experiments in mice have shown that feeding by uninfected mosquitoes immediately prior to intradermal inoculation can accelerate both death and neuroinvasion.(101) These effects are thought to be due to a local response to the mosquito saliva.(102) Following the initial inoculation, WNV replicates in the local keratinocytes and in Langerhans cells, which then migrate to the local draining lymph node.(103, 104) WNV then replicates in the lymph node and disseminates through the blood to peripheral organs. Tissue samples from fatally infected humans confirm that WNV can spread to many peripheral organs including the spleen, kidneys, liver, lungs, stomach, and intestines, but that not all organs will be infected in all cases.(105-107)

There are several mechanisms by which WNV may potentially enter the central nervous system. One possibility is axonal retrograde transport from the dorsal root ganglia neurons of the peripheral nervous system that are responsible for sensing pressure.(108) Similarly, WNV may infect olfactory neurons, thus spreading to the

olfactory bulb and the rest of the central nervous system.(109) WNV may infect the epithelium of the choroid plexus, thus gaining access to the cerebrospinal fluid and from there the central nervous system.(110) Similarly, WNV may infect the brain microvascular endothelial cells of the blood brain barrier, providing access to the central nervous system without disturbing the integrity of the blood brain barrier.(111) Other potential methods of crossing the blood brain barrier include the 'Trojan horse' method using infected T cells or the disruption of blood brain barrier integrity by upregulating matrix metalloproteinases or TNF-α.(112-119) Inside the central nervous system, WNV infection kills neurons by both apoptosis and necrosis.(120, 121)

WNV Symptoms

A serological survey revealed that approximately one in five WNV-infected humans will develop WNF and one in 150 WNV-infected humans will develop neuroinvasive disease.(122) Death occurs in approximately one in ten neuroinvasive cases.(123) The major risk factor for developing neuroinvasive disease following WNV infection was being over 65 years old.(122) Risk factors for developing the milder WNF are less well defined. One study found that the odds of developing WNF are actually inversely correlated with age, but this finding was not repeated in other studies.(124-126) The onset of disease for WNV is typically 2-14 days post-infection.(17) The incubation period for WNV in humans ranged from 2-21 days for transfusion-associated infection, with individuals who were immunosuppressed due to organ transplants having a higher average incubation period.(127)

Symptoms of WNF are typically non-specific. The most common reported symptoms are headache and weakness, and over half of WNF patients also report a rash, fever, and/or muscle pain. Although WNF is typically self-limiting and acute symptoms resolve in a week, fatigue can persist.(17) Neuroinvasive disease result in acute flaccid paralysis, encephalitis, or meningitis. The majority of patients with neuroinvasive

disease develop the non-specific symptoms of fever, headache, nausea, neck pain, vomiting, malagia, and chills and the neurologic symptom of tremors. Encephalitic patients also experience nuchal rigidity (a stiff neck), while meningitis patients are more likely to experience confusion and Parkinson-like symptoms.(128) Autopsy results showed widespread inflammation in the spinal cord and brainstem along with glial nodules and neuron loss.(129, 130)

ANTI-WNV ANTIBODIES

Kinetics and Common Targets of the Anti-WNV Antibody Response

The antibody response to WNV infection is of interest because neutralizing antibody is generally accepted as a reliable correlate of protection.(131, 132) It is also necessary for protection, as demonstrated by the lethality of WNV in mice lacking mature B cells and the protection conferred upon those mice with the passive transfer of heat-inactivated immune serum.(133) IgM antibody, produced in mice by 4 days post-infection, is necessary for protection. Binding IgM titers are a good predictor of survival outcome, and C57BL/6 mice lacking the ability to generate secreted IgM are more susceptible to lethal WNV infection and develop higher viral loads than wild-type C57BL/6 mice.(133, 134) IgG is protective in mice, but it is not typically detected until the virus has been cleared from the peripheral organs and infected the CNS, which should be essentially inaccessible to IgG.(133, 135) Similarly, in viremic human blood donors, IgM was detected approximately 4 days after the detection of WNV RNA and IgG was detected approximately 8 days after the detection of WNV RNA.(136)

Studies with monoclonal antibodies against WNV EIII demonstrate that they tend to be specific and potently neutralizing, but their role in a natural infection is not as clear.(65, 137-140) In a C56BL/6 model of infection, the IgG response to EIII constitutes approximately 25% of the total, while convalescent serum from human patients showed that the IgG response to E constitutes 80% of the total but antibodies

against EIII constitute only 8% of the anti-E response. In contrast, nearly half of the anti-E antibodies bind the fusion loop region of EII.(132) When looking specifically and antibodies that bind the surface loops of EIII the difference between the mouse model and the human response is more dramatic, with anti-EIII surface loop antibodies comprising 20% of the anti-E IgG in mice but less than 2% in humans.(135) However, despite their low abundance, anti-EIII antibodies do tend to be potently neutralizing, and it has been demonstrated that using EIII as a boost (instead of an EIII-exclusive EIII vaccination schedule), can effectively raise the level of neutralizing antibodies induced against this important target.(141)

EIII Epitope Mapping

Many anti-WNV EIII monoclonal antibodies are available, and their epitopes have been mapped using diverse methods such as yeast display libraries, the selection and nucleotide sequencing of neutralization-resistant mutants, and structural analysis of antibody bound to WNV proteins or virions. One example is 5H10, an antibody used extensively in this dissertation. 5H10 was initially mapped to EIII due to its binding to recombinant EIII protein in a Western blot.(138) This epitope was further refined by the selection of neutralization-resistant variants which encoded changes at residues 307, 330, and 332, all of which are located in the surface loops of EIII. Subsequent neutralization assays with both naturally occurring and engineered variants in the surface loop residues confirmed the importance of the initially identified residues and suggest a possible role for the neighboring residues 331 and 333.(139, 140) The importance of residues 307, 330, and 332 was subsequently confirmed by ELISA using recombinant EIII proteins with engineered mutations at those residues.(139, 142) The role of 331 and 333 was confirmed by Western blot with infected cell lysates.(140) The importance of the N-terminal and BC loops did not correspond to importance for residue 367 of the

neighboring DE loop (see the 'Structure and Function of WNV E' section of this dissertation for more details regarding the WNV EIII surface loops).(143)

Another monoclonal antibody used in this dissertation is 7H2, and is epitope was mapped in a similar way to that of 5H10. The 7H2 epitope was also localized to EIII using a Western blot with recombinant EIII protein. Although 7H2-resistant plaques were not initially purified and sequenced, the ability of 7H2 to neutralize WNV variants selected for resistance to other monoclonal antibodies demonstrated that 307 and 332, and to a lesser extent 330, impact 7H2-mediated neutralization.(138) The importance of 307, 330, and 332 was subsequently demonstrated by ELISA using recombinant EIII protein.(139, 142) Engineered WNV mutants used in neutralization assays and Western blots with infected cell lysates suggested that, like 5H10, the 7H2 epitope may include residues 331 and 333.(140) Once again, changes to residue 367 in the DE loop had no apparent impact on 7H2 binding.(143)

Another WNV EIII antibody for which epitope mapping has been extensively reported is E16. An overview of E16 epitope mapping is included here; more details are available in the 'Mechanisms of Neutralization' and 'Critical Antigenic Residues in WNV EIII' sections of this dissertation. A yeast display library demonstrated that changes to residues 306, 307, 330, and 332, but not to residues 310, 315, 381, 394, or 396 resulted in moderate to strong loss of binding by E16. Note that for residue 332, the yeast-displayed T332M mutant resulted in strong loss of binding but the T332A and T332V mutants did not.(137) Following initial mapping with a yeast display library, E16 was crystallized with recombinant WNV EIII, and E16 was found to contact EIII at residues 302, 306-309, 330-333, 365-368, and 389-391, thus confirming and expanding upon the epitope identified by yeast display. Overlaying this structure onto a cryo-electron microscopy reconstruction of the WNV virion revealed that steric hindrance would prevent E16 from binding to EIII oriented about the 5-fold axis of symmetry, thus restricting E16 to the 120 copies of E involved in the 2-fold and 3-fold axes of

symmetry.(65) The importance of residues 307 and 332 in particular to E16 neutralization was later confirmed by the *in vivo* selection of E16 neutralization-resistant mutants.(144)

Mechanisms of Neutralization

Despite the relative abundance of anti-WNV antibodies and epitope mapping studies, the exact mechanisms of neutralization have been defined in only a few cases. Surprisingly, despite the purported role of WNV EIII in receptor binding and the neutralizing potency of antibodies that bind WNV EIII, none of the anti-WNV EIII antibodies have been demonstrated to function by preventing binding to the cell. There have certainly been examples of anti-EIII antibodies blocking attachment in other flaviviruses such as DENV-2, and as more studies are done in this area there may well be anti-WNV EIII antibodies that are shown to block binding.(145, 146) Antibodies that bind to WNV EI and WNV EII have been suggested to prevent binding to cells based on differential neutralizing capacity in cell lines displaying different potential receptor molecules.(147)

One anti-WNV antibody for which the mechanism of neutralization has been studied is E16. Structural analysis of E16 in complex with recombinant EIII protein revealed a binding footprint in the surface loops of EIII, with some extension into the EI/EIII linker (namely residue Y302).(65) This allows E16 to bind WNV E oriented at the 2-fold and 3-fold axes of symmetry, but prevents binding at the 5-fold axes of symmetry, thus rendering 60 of 180 copies of E inaccessible to E16 binding. E16, however, remains potently neutralizing despite its inability to bind the 5-fold axis, requiring only ~30 bound copies to render WNV 50% neutralized and ~54 bound copies to render WNV essentially completely neutralized.(148) Given that E16 binds the surface loops of EIII, it would be logical to hypothesize that E16 neutralizes WNV by preventing attachment to the host cell receptor(s). However, E16 is only weakly able to

block WNV attachment to Vero cells.(65, 149) More detailed studies revealed that E16-bound WNV is able to bind and enter cells and that the endosomes formed during entry do acidify, but that WNV is unable to fuse with the membrane upon acidification.(149) This suggests that E16 prevents the pH-induced rearrangement of E from dimers to trimers, thus preventing fusion with the endosomal membrane. This mechanism of neutralization may be due to the binding of E16 to the EI/EIII linker.

The mechanism of neutralization has also been determined for the human-derived monoclonal antibodies CR4348 and CR4354.(150) CR4348 binds a complex epitope that includes residues from all three structural domains of E and requires the cross-linking of two E monomeres.(151) CR4354 is also unable to bind recombinant E protein monomers, perhaps because its epitope in the flexible EI/EII hinge region is conformationally different in a recombinant protein than it is in a whole virion. Similarly to E16, both CR4348 and CR4354 fail to block attachment but do prevent fusion, presumably by preventing the rearrangement of E from dimers to trimers.(150) Thus, three different anti-WNV monoclonal antibodies with three distinct epitopes all seem to neutralize virus by preventing the structural rearrangement of E associated with pH-induced fusion.

WNV VACCINES AND THERAPEUTICS

Therapeutics

There is currently no approved, specific therapeutic for WNV infection; only palliative care is available. The two potential treatments that have advanced to human clinical trials are both antibody-based. Omr-IgG-am is normal human IgG taken from healthy donors. An initial study in mice demonstrated that IgG from Israeli donors with high anti-WNV antibody titers was able to protect 100% of mice when administered 1 and 2 or 2 and 3 days post-challenge. By comparison, serum from American donors with low anti-WNV antibody titers offered no protection against lethal challenge.(152) The

human IgG was also able to protect immunesuppressed mice.(153) Use of intravenous immunoglobulin in human patients has been limited, and results have been mixed but promising.(154-158) In addition to intravenous immunoglobulin, an monoclonal antibody that binds the surface loops of EIII, called E16 or MGAWN1, has been developed. Early results in a mouse model were quite promising, with 80-90% survival demonstrated in mice when administered up to five days post-challenge.(137) An intriguing study in hamsters confirmed that E16 can protect against mortality and further demonstrated that animals that survived infection with E16 treatment had less cognitive impairment that untreated survivors nearly a month after recovery.(159) The humanized E16 antibody has been shown to be safe in humans, but efficacy data is not yet available.(160) The epitope of E16 has been well mapped, and the potential for escape fromE16 neutralization has been documented (see 'Critical Antigenic Residues in WNV EIII' for details).

Vaccines

WNV EIII VACCINES

Five studies of WNV EIII as a potential vaccine have been published(161-165). The initial investigation of WNV EIII as a potential vaccine was performed by Chu *et al* in 2007. This group used recombinant EIII protein to vaccinate BALB/C mice, and although the vaccinated mice were not themselves challenged, Chu *et al* demonstrated that the resulting sera was able to protect 100% of 2-day-old pups from lethal IC challenge by WNV. This serum was also able to confer 83% protection against a parallel challenge with JEV Nakayama.(161) A subsequent group demonstrated that recombinant WNV EIII could protect 80% of vaccinated C57BL/6 mice from lethal intraperitoneal (IP) WNV challenge and 60% of vaccinated mice from lethal IP JEV Beijing-1 challenge.(162) The most recent investigation of WNV EIII recombinant protein as a vaccinating antigen resulted in 100% protection of Swiss mice from WNV IP challenge,

although the control mice had 50-83% survival depending on whether or not they received adjuvant with their PBS. A passive transfer experiment using 4-day-old pups showed that the resulting immune sera was protective and showed no signs of antibody-dependent enhancement even at sub-neutralizing concentrations. Finally, this study demonstrated that EIII vaccination is able to confer protection from mother to pups and that breast milk contributes more to this protection than trans-placental immunity.(163)

In addition to the use of recombinant protein, WNV EIII vaccines have also been investigated using plasmid DNA and VLP systems. The plasmid DNA was able to protect up to 80% of mice and showed a marked difference in protection based on the method of vaccination (IM syringe injection or ID gene gun injection). This protection was also able to be conferred via passive transfer.(164) The VLP study showed the most promising results, with all vaccinated mice surviving lethal challenge after three doses regardless of the use of adjuvant, compared to no survivors in the sham-vaccinated group.(165)

Of note, these studies have collectively demonstrated protection in three different strains of mouse (Swiss, BALB/c, and C57BL/6) and have utilized multiple combinations of adjuvants, dosing schedules, and vaccine platforms (recombinant protein, VLP, and plasmid DNA). However, in all cases the amino acid sequence of the immunizing EIII antigen was a perfect match to the EIII sequence of the challenge virus. In fact, with the exception of the Chu *et al* study which used the lineage 2 Sarafend strain, all other studies utilized the same lineage 1 NY99 sequence for generating their EIII antigens. No effort has been made to address the impact of EIII diversity on the protective capacity of a WNV EIII-based vaccine.

EIII VACCINES FOR NON-WNV FLAVIVIRUSES

Many groups have investigated EIII as a potential vaccine platform for flaviviruses other than WNV, namely JEV and DENV. EIII is especially attractive as a

vaccine component for DENV because it is a target of highly specific, potently neutralizing antibodies, which should be a substantial advantage when designing a vaccine where antibody dependent enhancement is a concern.(145, 166-171) Two studies of EIII as a potential DENV vaccine are especially relevant because they address the impact of naturally occurring EIII variation on the protection afforded by an EIII-based vaccine.

The first studies compares EIII vaccination from two different strains of dengue virus type 3 (DENV-3), a genotype III Latin American strain and a genotype IV Asian strain. The two differ at four residues in EIII: 301, 329, 383, and 391. A dot blot using serum from naturally infected humans from Cuba and the two recombinant proteins resulted in binding to the the genotype III Latin American EIII but not the genotype IV Asian EIII, indicating that the differences in EIII sequence do have an antigenic impact. Next, the levels of binding and neutralizing antibodies that each EIII protein are able to elicit in mice were measured by enzyme-linked immunosorbent assay (ELISA) and plaque reduction neutralization test (PRNT), respectively. The ELISA results showed that the genotype III Latin American EIII protein was able to induce a stronger binding antibody response than the genotype IV Asian EIII protein, even though the capture antigen used in the ELISA matched the genotype IV Asian strain. This indicated that the Latin American genotype III strain may be more immunogenic. Next, PRNT assays were carried out using a virus that matched the genotype III Latin American strain at residues 301, 383, and 391 and matched the genotype IV Asian strain at residue 329. The average $PRNT_{50}$ titer from the mice vaccinated with the genotype III Latin American strain of EIII were higher, indicating that the exact sequence of the immunizing EIII protein is an important factor in determining which strains will be effectively neutralized. Finally, vaccinated mice were challenged intracerebrally with the genotype IV Asian strain of DENV-3. The heterologous protection from the genotype III Latin American strain of EIII conferred a higher rate of protection against morbidity than the homologous

genotype IV Asian strain did. Taken together, these results indicate that small changes in the sequence of EIII can have a large impact on both immunogenicity and antigenicity, and that this should be considered when designing an EIII vaccine for a virus with naturally occurring EIII diversity.(172)

In a similar experiment involving dengue EIII vaccination, *Macaca fascicularis* monkeys were vaccinated with EIII from either dengue virus type 1 (DENV-1) or dengue virus type 2 (DENV-2) and PRNT assays were conducted using that anti-EIII serum. For DENV-1, the vaccinating EIII strain was from genotype V and the PRNTs were conducted using the corresponding genotype V strain or a type IV strain. The two DENV-1 strains differ by a single residue, 359, located in EIII. Control serum from a monkey infected with whole virus gave similar PRNT titers against both DENV-1 strains. The EIII vaccinated monkey, however, generated a 7-fold stronger heterologous neutralizing response compared to its homologous neutralizing response. In a parallel experiment with DENV-2, monkeys were vaccinated with EIII from an Asian genotype strain and PRNTs were run against the homologous Asian genotype strain, a different Asian genotype strain, or an American genotype strain. In this case, the Asian and American genotype strains were different at residue 390, located in EIII. PRNT results for the DENV-2 EIII vaccinated monkeys revealed that the serum could neutralize all thee strains, but that neutralization of the American genotype strain was approximately 4-fold higher than neutralization of the homologous Asian genotype strain. Like the experiments with DENV-3 EIII vaccinated mice, this work demonstrated that small changes in EIII can have important impacts on antigenicity.(173)

VETERINARY WNV VACCINES

Four equine vaccines for WNV have been developed. The first to be licensed was WN-Innovator, a formalin-inactivated whole virus vaccine.(174) The RecombiTEK rWNV vaccine is based on a recombinant canarypox virus that expresses the prM/E

proteins of WNV NY99. It has been shown to significantly decrease clinical signs and eliminate viremia in horses.(175, 176) PreveNile, a Yellow fever virus 17D backbone that again expresses the prM/E proteins of WNV, was approved for use but subsequently recalled due to adverse events in vaccinated horses and is now used as a killed vaccine.(177) Finally, a plasmid DNA vaccine expressing the prM/E proteins of WNV has been developed and licensed but not marketed for use in horses.(178) Of note, all of these veterinary vaccines use either whole virus or whole prM/E proteins (as opposed to the many EIII-based vaccines detailed in this chapter).

STRUCTURE AND FUNCTION OF WNV E

The cryo-electron microscopy structure of the WNV virion reveals that, like other flaviviruses, each WNV particle contains 180 copies of E arranged in head-to-tail homodimers that lay flat on the surface of a mature virion (Figure 2A).(179) Recall that E must also be able to form the spiked dimmers of the immature virion and the spiked trimers of the membrane-fused virion in order for WNV to complete is replication cycle; see the 'Cellcular Replication Cycle' section for more details. The E protein itself has three distinct structural domains (Figure 2B). Domain I is the central linker connecting domains II and III, and it is made up of 9 stranded (A_0-I_0) β-barrel. In addition to its role as the linker between domains II and III, domain I contains the critical N154 glycosylation site. This N-linked glycosylation site is not found in every strain of WNV but is critical to mouse neuroinvasion and virulence, interactions with DC-SIGNR, early production of TNFα in infected macrophages, mosquito dissemination and transmission, replication in birds, and virus infectivity(77, 180-188) Domain II contains the highly conserved fusion loop, which is essential for membrane fusion, at its far end. Domain III, the putative receptor binding domain and focus of this dissertation, is a seven stranded (A-G) structure with an Ig-G-like fold.(63, 189) Solution structures of recombinant domain III confirm that, although the overall folds of flavivirus EIII proteins are quite

similar, the exact properties of the surface exposed residues are unique to each virus.(142) Also, the mosquito-borne flavivirus EIII proteins more closely resemble each other than they do the tick-borne flavivirus EIII proteins and are generally less stable than the tick-borne flavivirus EIII proteins, which may explain why mosquito-borne flaviviruses are generally less stable in the environment.(190) There are several lines of evidence for the hypothesized function of WNV EIII as the receptor binding domain. Recombinant WNV EIII blocks WNV entry into Vero and C6/36 cells in a dose-dependent manner.(191) Similarly, WNV EIII blocks WNV binding to the proposed receptor avb3 integrin in a dose-dependent manner.(81) Finally, changes at residue 332 in WNV EIII are associated with differential binding of membrane receptor preparations prepared from mouse brains, further pointing to the role of EIII in receptor binding.(138)

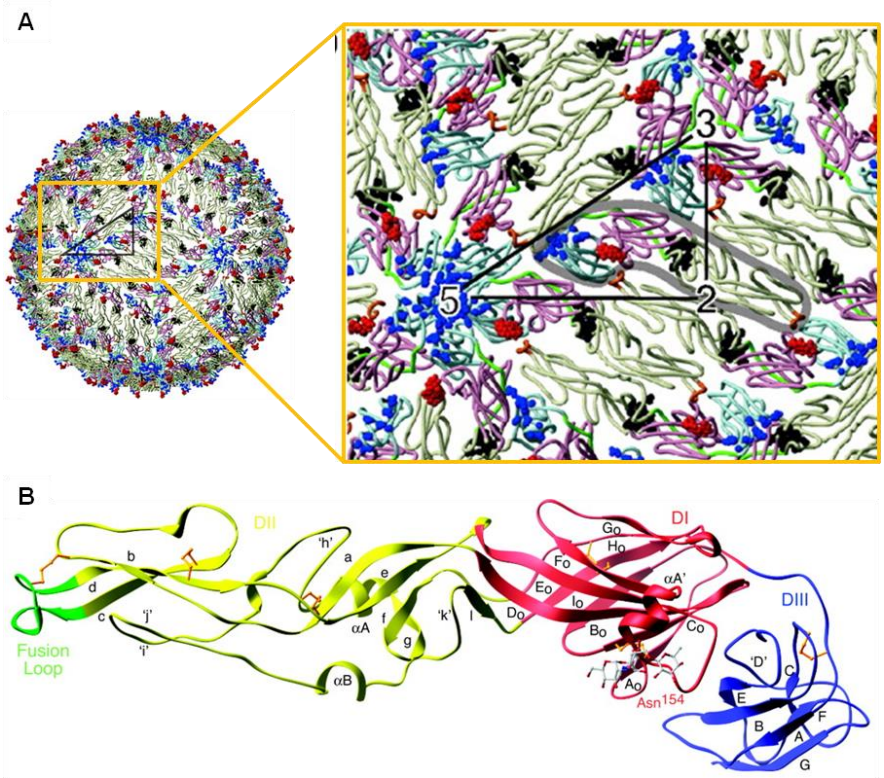

Figure 2: Structure of WNV Envelope Protein

Figure 2A shows the arrangement of WNV E based on the known structure of the dengue virion. The 2-fold, 3-fold, and 5-fold axes of symmetry are highlighted in the enlargement. EIII = blue. Fusion loop = green. Glycan = red. Images from Kanai *et al.*, used with permission (See Appendix C).(189) Figure 2B shows the structure of WNV E with the strands labeled. EI = red. EII = yellow. EIII = blue. Fusion loop = green. Image from Nybakken *et al.*, used with permission (See Appendix C).(63)

CRITICAL ANTIGENIC RESIDUES IN WNV EIII

Residue S306

The antigenic role of residue S306 was discovered by crystallography and a yeast display library.(65, 137) When recombinant WNV EIII and the Fab fragment of the E16 monoclonal antibody were crystallized and their structure determined, S306 was found to be in the binding footprint of the antibody. Specifically, residue S306 has contact with two E16 residues via van der Waals forces, one E16 residue via direct hydrogen bonding, and three E16 residues via water-mediated hydrogen bonding.(65) Other evidence for the role of S306 in antibody binding comes from a yeast display library that expresses WNV EIII with a S306L mutation. This mutation moderately or strongly inhibited binding by five of ten strongly neutralizing monoclonal antibodies including E16, E27, E40, E43, and E49 but not E24, E33, E34, E47, or E58.(137) Of note, none of the experiments pointing to S306 as a critical antigenic determinant included changes at that residue in the context of an infectious virus, and there is no known natural diversity at this residue.

Residue K307

The antigenic role of residue K307 had been demonstrated by crystallography, yeast display, and the selection of neutralization-resistant mutants. The same crystallography experiment that demonstrated the importance of residue S306 also pointed to an important role for residue K307. Specifically, residue K307 contacts the E16 Fab fragment at five residues via van der Waals contacts, two residues via direct hydrogen bonds, and three contacts via water-mediated hydrogen bonds.(65) The importance of residue K307 in antibody binding was further confirmed with a yeast display library that contained WNV EIII with K307E, K307N, and K307R substitutions. All three substitutions had widespread impact on the binding ability of the ten strongly neutralizing antibodies tested: E16, E24, E27, E33, E34, E40, E43, E47, E49, and E58.

The K307E mutant strongly inhibited binding by all ten antibodies, the K307N mutant strongly inhibited binding by all but E16 (which was still moderately inhibited), and the K307R mutant strongly or moderately inhibited binding by all but E24.(137)

In addition to the recombinant protein and yeast display library, the importance of residue K307 was confirmed by the selection of neutralization-resistant mutants. A K307R mutant in a NY99 backbone was selected for *in vitro* resistance to the monoclonal antibody 5C5, and a K307R mutant in a strain H-442 backbone was selected for *in vitro* resistance to the monoclonal antibody 5H10. In both cases, the K307R mutation conferred strong resistance to *in vitro* neutralization by the monoclonal antibodies 3A3, 5C5, and 5H10, and moderate escape resistance to *in vitro* neutralization by the monoclonal antibody 7H2. These results were supported by ELISA results demonstrating that binding of 7H2 to recombinant WNV EIII with a K307R mutation was roughly 2-fold lower than binding to wild-type WNV EIII. The binding of 3A3, 5C5, and 5H10 to WNV EIII with a K307R mutation was roughly 5-10-fold lower binding to wild-type WNV EIII.(138, 142) In a separate experiment that characterized the antigenicity of K307R, the K307R mutation in a NY99 backbone was found to have only moderate impact on the *in vitro* neutralization of E16, which is consistent with the moderate reduction in E16 binding to a K307R mutant in a yeast display library described earlier.(144) The K307R mutants had minimal impact on virulence when delivered IP to 3-4-week-old Swiss Webster mice and did not disrupt binding to a mouse brain tissue membrane receptor preparation.(138, 142)

Similarly to K307R, a K307N mutant was selected for resistance to *in vitro* 5H10 neutralization on an H-442 backbone. The antigenic properties of the K307N mutant were similar to those of the K307R mutant, resulting in moderate loss of 7H2 neutralization and strong loss of 3A3, 5C5, and 5H10 neutralization. The K307N mutant did not disrupt binding to a mouse brain tissue membrane receptor preparation, but unlike K307R, the K307N mutation was very mildly attenuating in Swiss Webster mice.(138)

The antigenic importance of a K307E mutation was demonstrated by the *in vivo* loss of protection by the monoclonal antibody E16. Swiss Webster mice were treated with 100μg humanized E16 monoclonal antibody and challenged with 100pfu of virus one day later. The antibody was able to protect 100% of the wild-type-challenged mice, but only 10% of K307E-challenged mice. In addition to the ability of a K307E mutation to confer *in vivo* resistance to neutralization, it was also demonstrated that K307E mutants can be selected from a wild-type population under the selective pressure of a monoclonal antibody therapy *in vivo*. When B cell- and T cell-deficient RAG mice were challenged with 100pfu of WNV NY2000 (which is identical to WNV NY99 in the sequence of its E gene) and treated with 500μg of humanized E16 antibody at 1, 14, and 28 days post-infection, two of the mice that succumbed were found to have WNV with a K307E mutation in their brains. A K307E mutant was similarly recovered from a Swiss Webster mouse treated one day pre-challenge with 100μg humanized E16 and challenged with 10,000pfu of WNV NY99. The ability of the K307E mutation in the *in vivo*-selected K307E mutants to resist E16 neutralization was confirmed via PRNT.(144)

Residue T330

The antigenic role of residue T330 has been demonstrated by crystallography, yeast display, and characterization of neutralization-resistant mutants and viruses with engineered substitutions at residue T330. The crystallography data showed that residue T330 in a recombinant WNV EIII protein contacts the Fab fragment of the E16 antibody at four residues via van der Waals forces and three residues via water mediated hydrogen bonds, but does not contact E16 via any direct hydrogen bonds.(65) Residue T330 was also found to be important to antibody binding using a yeast display library expressing WNV EIII with a T330I mutation. This mutation strongly or moderately inhibited binding by nine of ten strongly neutralizing antibodies tested: E16, E24, E33, E34, E40, E43, E47, E49, and E58.(137)

The impact of the T330I mutation was also evaluated as a neutralization-resistant NY99 variant selected in the presence of the 5H10 antibody and as a mutation deliberately added to a NY99 infectious clone. The T330I mutation resulted in strong escape from neutralization by 3A3.(138, 142) Neutralization by the 5H10 antibody gave more mixed results, with the engineered T330I mutant resulting in 56% loss of neutralization and the plaque purified T330I mutants resulting in 71-83% loss of neutralization.(138, 140, 142) The antigenic impact of T330I on 7H2 was moderate, and the impact on 5C5 was weak.(138, 140, 142) Antibody binding was also assessed using both a Western blot with infected cell lysates and an ELISA with WNV EIII recombinant proteins. All three antibodies assessed by the Western blot (5H10, 7H2, and 5C5) were unable to bind the WNV T330I cell lysate.(140) The ELISA results more closely resembled the neutralization results, with T330I resulting in a moderate loss of binding by 7H2 and 5C5 and a strong loss of binding by 5H10 and 3A3.(142) Despite these *in vitro* suggestions of a role of T330I in escape from neutralization, a T330I mutation in a NY99 backbone was not able to decrease the protective capacity of humanize E16 antibody administered either pre- or post-challenge in mice.(144) In contrast to its antigenic impact, the T330I mutation had minimal functional impact. Binding to a mouse brain tissue membrane receptor preparation, replication kinetics in Vero cells, and mouse virulence were essentially unaffected.(138, 140, 144)

The impact of a T330A mutation has also been assessed using the NY99 infectious clone. Unlike the T330I mutation, T330A had minimal impact on neutralization and binding by 5H10, 7H2, and 5C5. Similarly to the T330I mutation, T330A had minimal impact on viral growth kinetics in Vero cells and mouse virulence.(140)

Residue T332

Residue T332 is perhaps the most well-characterized antigenic determinant in WNV EIII. Crystallography demonstrated that residue T332 in recombinant WNV EIII contacts the Fab fragment of the monoclonal antibody E16 at six residues via van der Waals forces, two residues via direct hydrogen bonding, and three residues via water mediated hydrogen bonds.(65) A yeast display library demonstrated that residue T332 can have widespread antigenic impact, but that the identity of the amino acid substitution is quite important. The T332A and T332V substitutions result in strong or moderate escape from binding by three of ten monoclonal antibodies tested. Both T332A and T332V result in escape from E24 and E58, but only T332A escapes from E33 and only T332V escaped from E27. The T332M substitution, on the other hand, results in widespread escape from binding to nine of the ten monoclonal antibodies tested: E16, E24, E33, E34, E40, E43, E47, E49, and E58.(137)

Unlike the other antigenic determinants detailed in this chapter, residue T332 has been evaluated in the context of naturally occurring variation. One strain (ISR53) has a naturally occurring T332A and two strains (MAD88 and SA58) have a naturally occurring T332K. The ISR53 strain is a member of lineage 1 and has no other variation in EIII, and the MAD88 and SA58 strains are members of lineage 2 and have naturally occurring L312A and A369S variations. The antigenic impact of L312 and A369 were thought to be minimal due to the lack of neutralization loss demonstrated by other strains that varied from NY99 at residues L312 or A369. The ISR53 strain (T332A) had moderate loss of neutralization by 5H10 and 5C5, and weak loss of neutralization by 7H2, but was strongly neutralized by polyclonal serum against WNV EIII and whole WNV. The MAD88 and SA58 strains (T332K), on the other hand, had essentially total loss of neutralization by all three monoclonal antibodies (5H10, 5C5, 7H2) and the anti-WNV EIII serum, but remained strongly neutralized by serum against whole WNV.(139)

The importance of the T332K variant SA58 in neutralization was clearly demonstrated *in vivo* using the humanized E16 monoclonal antibody. Whereas treatment with E16 pre- or post-challenge was able to protect against death with NY99, it was unable to protect against an SA58 challenge. Changing residue 332 from the natural SA58 lysine to a NY99 threonine restores protection by E16.(144) In the case of the monoclonal antibodies 5H10, 5C5, and 7H2, binding ability closely mimicked neutralizing ability, but serum against WNV EIII was able to bind in a Western blot regardless of neutralizing activity, perhaps due to the display of epitopes in the Western blot that would not be exposed in an infectious particle. ELISA results with mutant WNV EIII proteins confirmed the moderate loss of monoclonal binding to T332A and the total loss of binding to T332K.(139)

In addition to the naturally occurring T332A variant (ISR53), the impact of T332A has been evaluated by the introduction of T332A into a NY99 infectious clone. The T332A substitution reduced neutralization by 7H2 and 5H10 by approximately 50% and reduced neutralization by 5C5 by approximately 30%. These results are roughly similar to the neutralization information gathered for ISR53.(140) The T332A mutation did not have any effect on *in vivo* protection or *in vitro* neutralization by the humanized E16 antibody.(144) Western blot binding levels roughly correspond to neutralization levels for 7H2, 5H10, and 5C5. Mouse virulence and growth in Vero cells were essentially unaffected by the T332A mutation.(140)

Like T332A, the role of T332K has been assessed in a NY99 infectious clone in addition to naturally occurring variants (MAD88 and SA58). Like SA58 with its natural T332K, a NY99 virus with a T332K mutation is able to significantly decrease the *in vivo* protection conferred by humanized E16 antibody in a mouse model.(144) Also like SA58 and MAD88, NY99 T332K is not neutralized or bound *in vitro* by the monoclonal antibodies 5C5, 5H10, or 7H2. The T332K mutation did not functionally impact the

NY99 virus, as it retained the Vero growth and mouse virulence phenotypes of the wild-type NY99.(140)

The final T332 mutation evaluated using infectious virus was T332M. The T332M mutant demonstrated strong escape from 5H10 and moderate reduction in neutralization by 5C5 and 7H2. The binding and neutralization phenotype corresponded well for 5H10 and 5C5, but 7H2 was unable to bind NY99 T332M in a Western blot despite retaining moderate neutralization.(140) Treatment with humanized E16 antibody, either pre- or post-challenge, was able to protect mice from lethal NY99 T332M infection. However, the T332M mutation did reduce *in vitro* neutralization by E16 and when mice were treated with 100μg and then challenged with 10,000pfu of wild-type NY99, one of the mice that succumbed to infection had virus with the T332M mutation in its brain.(144) The T332M mutation had minimal impact on both replication in Vero cells and virulence in mice.(140)

Residue A367

Residue A367 does appear to have some antigenic role, although it seems to be involved in an epitope that is distinct from the other antigenic determinants discussed in this chapter. The crystallography data revealed that A367 in recombinant WNV EIII protein contacts that Fab fragment of the E16 antibody at three residues via van der Waals forces, one residue via direct hydrogen bonding, and no residues via water mediated hydrogen bonding.(65) However, despite this contact, no A367 mutants were selected from a yeast display library using any of the ten screening antibodies, including E16.(137)

When grown in the presence of the monoclonal antibody 5E8, a neutralization-resistant mutant was selected and found to have an A367V substitution. Subsequent neutralization experiments with this A367V mutant demonstrated that A367V impacts neutralization by 5E8 but not 3A3, 5C5, 5H10, or 7H2. The A367V mutation affected

5E8 binding as well as neutralization as demonstrated in an ELISA using recombinant WNV EIII. Mouse virulence was unaffected by the A367V mutation.(143)

Naturally Occurring Variation at Known Antigenic Determinants and Neighboring Residues

Of the five known antigenic determinants in WNV EIII and their six neighboring residues, only three had any naturally occurring variation (Table 1). The N-terminal loop residues (C305, S306, K307, and A308) had no amino acid variation at all. In the BC loop (T330, G331, T332, and D333), only T332 had any naturally occurring variation. There were strains with T332A, T332K, T332M, and T332S. All of these amino acid substitutions were attainable with a single nucleotide change from the wild-type threonine codon. The T332K variants were found in lineage 2 viruses and in a single lineage 1 virus, while theT332A, T332M, and T332S variants were all found in lineage 1 viruses.(192-197) In the DE loop, the two neighboring residues (T366 and N368) had naturally occurring variation, but the known antigenic determinant (A367) did not. The only T366 variant, T366A, occurred in conjunction with a T332K variant in a lineage 1 virus.(194) Both of the N368 variants were N368D, and both were in lineage 1 strains.(195, 198)

Table 1: Naturally Occurring Variation in Known WNV EIII Antigenic Determinants and Their Neighboring Residues

Summary of all available WNV sequences in GenBank with variation from the dominant NY99 amino acid at a known antigenic determinant or a neighboring residue. X = amino acid unable to be determined from sequence.

Residue	Variant	Accession #	Strain	Lineage	Source	Location	Year	Additional EIII Changes	Ref.
332	332A	HM051416.1	Goldblum	1	Human	Israel	1953	None	191
332	332K	AF45403.3	H-442 (a.k.a. SA58)	2	Human	South Africa	1958	L312A, A369S	192
332	332K	HM147823.1	DakArMg979	2	*Culex quinquefasciatus* (mosquito)	Madagascar	1988	L312A, A369S	191
332	332K	HM147822.1	SA AN 2842	2	*Syvlietta refescens* (bird)	South Africa	1958	L312V, A369S, V371I, L375I	191
332	332K	AY688948.1	Sarafend	2	?	?	?	L312A,G313R, A369S	?
332	332K+366A	EU249803.1	68856	1	*Rousettus leschenaultii* (fuit bat)	India	1968	H398Y	193
332	332M	GQ502394.1	152E-10149MO07StL	1	Human	USA	2007	P377X, S402X	194
332	332S	GQ507480.1	WG132	1	Human	USA	2005	None	195
332	332S	HM488220.1	BID-V4586	1	(mosquito)	USA	2003	None	196
366	332K+366A	EU249803.1	68856	1	*Rousettus leschenaultii* (fuit bat)	Inia	1968	H398Y	193
368	368D	GQ502373.1	078E-45078CA04SB	1	Human	USA	2004	None	194
368	368D	DQ431709.1	04-240CA	1	Human	USA	2004	None	197

Summary of Antigenic of WNV EIII Residues and Functional and Contributions Surface Loop

Residues 305-308 have no naturally occurring variation (Table 2). In the case of residue C305 this is expected due to its involvement in a cysteine bridge with residue 336.(199) The two central residues in the loop, 306 and 307, are known antigenic determinants, but their neighbors (305 and 308) are not. Residue 306 was selected as part of a yeast display library,

so is impact on the structure and function of EIII is unknown.(137) Residue K307, on the other hand, must be able to tolerate at least some diversity despite its strict conservation in nature. At least three changes (K307E/N/R) have been selected for and/or successfully engineered into WNV for their resistance to neutralization by E16, 5H10, 5C5, 3A3, and to a lesser extent 7H2.(138, 142, 144) None of the changes were attenuating in mice.(138, 144) The functional and antigenic role of residue 308 is unknown, as it has no naturally occurring variation and has not been selected as antigenically important.

The role of individual residues in the BC loop is better defined than the role of residues in the neighboring N-terminal and DE loops. At residue T332, T332A, T332K, and T332M have been identified as antigenically important using naturally occurring and engineered variants.(139, 140, 144) Changes at residue 332 result in varying degrees of escape from neutralization by 5H10, 5C5, 7H2, and E16, with T332K resulting in by far the most dramatic escape. T332V is known to cause escape from antibody binding, but was discovered in a yeast display library and so its viability in the context of an actual WNV virion is unknown.(137) Of the three variants known to be viable and antigenically important (T332A, T332K, and T332M), none are attenuating in mice or inhibitory in Vero cells.(140, 144) A third variant, T332S, is known to be viable but is not characterized. Similarly to 332, residue 330 is a known antigenic determinant. T330I results in escape from neutralization by 3A3, 5H10, and 7H2, but T330A had a less dramatic antigenic impact.(138, 140, 142) Despite its lack of naturally occurring diversity, residue 330 tolerated substitution with minimal impact on virulence or replication in Vero cells.(140) In sharp contrast to residues 330 and 332, changes at residues 331 and 333 were not well tolerated. There is no naturally occurring diversity at these residues and the engineered changes (G331A, D333E, and D33N) are highly attenuated in mice and restricted in Vero cells. The D333A mutation is completely non-

viable. Changes at residues 331 and 333 resulted in moderate to weak escape from antibody neutralization.(140)

Interestingly, in the DE loop, residue 367 has been selected as antigenically important despite its lack of naturally occurring diversity.(143) Its neighboring residues, on the other hand, do have at least some minor natural variation but were not selected as being important to antibody binding or neutralization.

	Residue										
	N-Terminal Loop				**BC Loop**				**DE Loop**		
	305	**306**	**307**	**308**	**330**	**331**	**332**	**333**	**366**	**367**	**368**
Known Antigenic Variant?	No	S306L	K307E K307N K307R	No	T330A T330I	No	T332A T332K T332M T332V	No	No	A367V	No
Naturally Occurring Variation?	None	None	None	None	None	None	T332A T332K T332M T332S	None	T366A	None	N368D

Table 2: Comparison of Surface Loop Residues with Known Antigenic Importance and Naturally Occurring Variation

Summary of current knowledge regarding naturally occurring variation and antigenic importance of individual residues in the WNV EIII surface loops.(137, 138, 142, 144)

Chapter 2: Methods

PROPAGATION OF EUKARYOTIC CELL LINES

T-150 flasks of ATCC Vero cells were grown to confluency in Vero growth media (see Appendix A for details) at 37°C with 5% CO_2. The spent media was then decanted from the flask, and the monolayer was rinsed with approximately 10ml Dulbecco's phosphate buffered saline (DPBS). Cells were detached by adding 1.5ml trypsin (Cellgro, Manassas, VA) and incubating at 37°C with 5% CO_2 for approximately 3 minutes. The reaction was stopped by adding 10ml Vero growth media. Cells were gently pipetted several times to break up any clumps. One confluent T-150 could be split 1:2 if cells were needed the following day, or up to 1:10 if cells were not needed until 3 days post-split. Alternately, one T-150 flask could be used to seed up to ten 6-well or 12-well plates for the following day. T-150 flasks contained 30ml Vero growth media, 6-well plates contained 4ml Vero growth media per well, and 12-well plates contained 2ml Vero growth media per well. Vero cells were not used past passage 30, as they become unreliable for generating WNV plaques past that point.

Duck embryo fibroblast (DEF) cells were propagated essentially the same as Vero cells, but using DEF growth media (see Appendix A for details). DEF cells were required only for two growth curve experiments in this dissertation and were used at passage 15 or lower.

C6/36 cells were propagated similarly to Vero cells, except that trypsin was only left on the cells for 1 minute and the cells were grown in a 28°C ungassed incubator. Details of the C6/36 media components are in Appendix A. These cells were only used for two growth curves, and their passage history is unknown.

WNV STRAINS

The two Arizona WNV strains (AZ10-75 and AZ10-581) were originally obtained from Dr. John-Paul Mutebi at the Centers for Disease Control and Protection, Division of Vector-Borne Diseases and deposited with Dr. Robert Tesh in the World Reference Center for Emerging Viruses and Arboviruses. They were then passaged twice in Vero cells to generate a working stock. Both strains were originally collected from mosquito pools in Gilbert, Arizona during August of 2010.The WNV SA58 virus (also known as H-442) was also obtained from Dr. Tesh and was passaged three times in Vero cells. The NY99ic wild type and mutant viruses were obtained as described in the 'Recovery of Wild-Type and Mutant NY99ic Virus' section of this chapter. Wild-type NY99ic was always obtained directly from an electroporation (passage 0), typically at three days post-electroporation. The passage history of individual mutants is described in the results.

GENERATION OF WNV EIII RECOMBINANT PROTEIN

The EIII sequence of WNV NY99 and WNV SA58 encoding the M292-K406 region was previously ligated into pET-15 vector between the NcoI and BamHI restriction sites, and the resulting plasmid was transformed into *E. coli* ER2566 bacteria. The general process used for expression and purification of EIII for WNV and other flaviviruses using a reverse ion-exchange affinity column has been previously described by Volk et al.(200) An overnight culture was diluted 1:100 in 200ml of Luria broth (LB)/Amp (see Appendix A for details), and the culture was allowed to grow at 37°C with 230rpm shaking for approximately 2 hours until the culture was mid-log phase (OD_{600}=0.5-1.0). At this point isopropylthio-β-galactoside (IPTG) (Fisher, Fair Lawn, NJ) was added to the culture to a final concentration of 1mM. The culture was allowed to grow for a further 2 hours at 37°C to allow the EIII protein to be expressed. Cells were then transferred to 50ml conical tubes and centrifuged at 1,800xg for 30 minutes at 4°C. Media was decanted and cell pellets were stored at -70°C overnight or until needed.

After thawing on ice, cells were resuspended in 30ml of denaturing buffer (20mM Tris, 200mM NaCl, 8M urea, pH 8.0, 0.45µm filtered) and lysed using a French press. The lysate was transferred into 7,000 MWCO SnakeSkin Pleated Dialysis Tubing (Pierce, Rockford, IL) and dialyzed into native buffer (20mM Tris, 200mM NaCl, pH 8.0, 0.45µm filtered). Three buffer changes with volumes of 500ml, 500ml, and 1L, were completed in the presence of a protease inhibitor cocktail (Roche, Mannheim, Germany).

Following dialysis, the sample was passed through a 0.45µm filter and stored on ice. The ÄKTAprime plus LP Chromatography System (GE Healthcare, Uppsala, Sweden) with an attached 5ml HiTrap Q FF column (GE Healthcare, Uppsala, Sweden) was flushed with 50ml of high salt buffer (20mM Tris, 1M NaCl, pH 8.0, 0.45µm filtered), then with 30ml of native buffer. The sample was then loaded into the machine, and the machine was programmed to flush the column with another 25ml of native buffer before loading the sample onto the column. The first 24ml to be eluted following each run contained the EIII protein. After the last sample had run through the system, the column was flushed with 50ml of high salt buffer followed by 30ml of native buffer to remove the bound bacterial proteins, and then stored in 20% ethanol. The eluted sample was centrifuged through a 30kD VivaSpin 20 Filter Column (Sartorius, Goettingen, Germany) at 1,800xg and 4°C until all of the sample had gone through the filter to remove any remaining bacterial contaminants. The flow-through containing the EIII protein was centrifuged through a 5kD VivaSpin 20 Filter Column at 1,800xg and 4°C until approximately 1ml remained above the filter. The size, concentration, and purity of the final product was assessed using the Protein 80 or Protein 230 kit (Agilent, Santa Clara, CA)

GENERATION OF MUTANT NY99IC PLASMIDS BY QUIKCHANGE MUTAGENESIS

Two separate methods of mutagenesis were used to generate mutant plasmids for use in the NY99ic system. All mutagenesis work was done on the pWN-AB plasmid,

which encodes the structural proteins of WNV. The QuikChange mutagenesis kit, described first, was used to generate mutants for residues L312 and T332, as well as the S66R plasmid used to evaluate the impact of a compensating mutation.

Mutants generated with the QuikChange Multi Site-Directed Mutagenesis Kit (Stratagene, Cedar Creek, TX) were obtained according to the manufacturer's instructions. Primers for the L312 and T332 mutants were designed so that four mutagenesis reactions would generate all possible amino acid substitutions by holding the first nucleotide of the codon constant and allowing the second and third nucleotides to vary. Later, some individual plasmids were generated for L312 and T332 mutants that were not easily obtained by plasmid or plaque purification. Mutagenesis primer sequences are listed in Table 3. All primers were designed using the Stratagene website (currently owned and operated by Agilent Technologies at www.genomics.agilent.com/primerDesignProgram/jsp) and synthesized by Sigma (Woodlands, TX).

Residue	Mutants Encoded	Sequence (5'-3')
L312	I/K/M/N/R/S/T	GGCGTCTGTTCAAAGGCTTTCAAGTTT**ANS**GGGACTCCCGCAGA
L312	H/P/Q	TGTTCAAAGGCTTTCAAGTTT**CMS**GGGACTCCCGCAGAC
L312	A/D/E/G/V	CGTCTGTTCAAAGGCTTTCAAGTTT**GNS**GGGACTCCCGCAG
L312	C/F/L/W/Y	GGCGTCTGTTCAAAGGCTTTCAAGTTT**TDS**GGGACTCCCGCAGA
L312	F	CTGTTCAAAGGCTTTCAAGTTT**TTT**GGGACTCCCG
L312	R	TTCAAAGGCTTCAAGTTT**CGT**GGGACTCCCGCAG
T332	I/K/M/N	GGAATTGCAGTACACTGGC**AWK**GATGGACCTTGCAA
T332	H/P/Q/R	GGAATTGCAGTACACTGGC**CVK**GATGGACCTTGCAAAGTT
T332	A/D/E/G/V	GAATTGCAGTACACTGGC**GNK**GATGGACCTTGCAAAGT
T332	C/F/L/S/W/Y	GAATTGCAGTACACTGGC**TNK**GATGGACCTTGCAAAGTT
T332	C	GGAATTGCAGTACACTGGC**TGC**GATGGACCTTGCAAAGTTC
T332	D	TTGGAATTGCAGTACACTGGC**GAT**GATGGACCTTGCAAAGTTCCT
T332	F	TGGAATTGCAGTACACTGGC**TTC**GATGGACCTTGCAAAGTTC
T332	G	GAATTGCAGTACACTGGC**GGG**GATGGACCTTGCAAAGT
T332	P	TGCAGTACACTGGC**CCG**GATGGACCTTGC
T332	V	GGAATTGCAGTACACTGGC**GTG**GATGGACCTTGCAAAGT
T332	W	GAATTGCAGTACACTGGC**TGG**GATGGACCTTGCAAAGT
T332	Y	TTGGAATTGCAGTACACTGGC**TAT**GATGGACCTTGCAAAGTTCCT
S66	R	ATTTGGCTACCGTC**AGG**GATCTCTCCACCAAAG

Table 3: Primers Used in QuikChange Mutagenesis of pWN-AB

List of primers used to generate pWN-AB plasmids with mutations at residue L312, T332, or S66 using the QuikChange mutagenesis kit. Mutated codons are designated with bolded and underlined text. D=G/A/T, M=A/C, N=A/C/G/T, V=G/A/C, W=A/T.

For each reaction, the following components were added to a 0.2ml PCR tube one at a time on ice in the order listed:

2.5µl QuikChange Multi reaction buffer (10x)

18.75-Xµl H2O

0.75µl QuikSolution

Xµl pWN-AB plasmid (100ng)

1µl primer (100ng/µl)

1µl dNTP mix (10mM each) (Roche, Mannheim, Germany)

1µl QuikChange Multi enzyme blend

Once the individual reaction components were combined, mutant plasmids were amplified by a Mastercycler gradient machine (Eppendorf, Westbury, NY), using the parameters described in Figure 3:

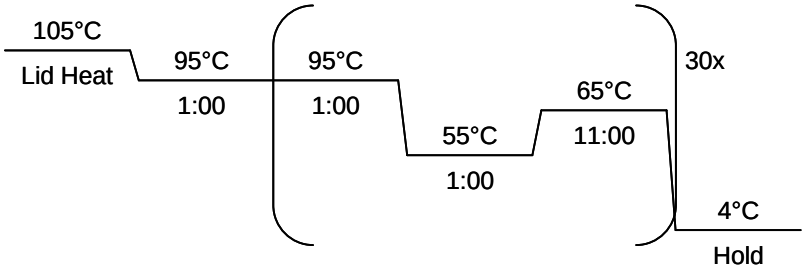

Figure 3: Cycle Parameters for QuikChange Mutagenesis of pWN-AB

Cycle parameters used to amplify mutant pWN-AB plasmids using the QuikChange Multi Kit.

Following amplification, 10 units of DpnI was added to the reaction and was allowed to incubate for 1 hour at 37°C. After the DpnI digest was complete, 5µl of DNA was added to 50µl of chemically competent *E. coli* DH5α cells. The cells and plasmid were incubated on ice for 30 minutes to allow for plasmid adsorption to the cell membrane, at 42°C for 50 seconds to permeablize the membrane and allow the plasmid to enter the cell, and then held on ice for 2 minutes to allow the membrane pores to close. Finally, 500µl of 2% LB media with no antibiotic was added to the cells, and they were grown at 37°C with 230rpm shaking for 1 hour. For reactions intended to yield plasmid pools, all 500µl of transformed bacteria were used to inoculate an overnight liquid culture of 5ml LB/Amp. For individual mutant plasmids, 100µl of transformed bacteria were grown on LB/Amp plates (see Appendix A for details). Both types of culture were grown for 15-17 hours at 37°C, either in a stationary incubator for plates or a 230rpm shaking incubator for liquid media. After this, the liquid cultures of plasmid pools were ready for immediate processing, while the plates of single mutants required the further step of picking two to three individual colonies for 16-18 hours of growth in liquid culture of 2% LB containing 100µg/ml ampicillin. Once liquid cultures were ready, 1ml of bacteria

was set aside and combined with 1ml of 1% LB, 50% glycerol to make a permanent freezer stock. Plasmid DNA was harvested from the remaining liquid culture using the GenElute Plasmid Miniprep Kit (Sigma, St. Louis, MO) according to the manufacturer's protocol. The presence of the desired mutation(s) was confirmed by submitting the plasmids to the UTMB Molecular Genomics Core for sequencing with ABI Prism 3100 Avant and 3130XL DNA sequencers. Sequences were analyzed using the Lasergene suite (DNASTAR, Madison, WI).

GENERATION OF MUTANT NY99IC PLASMIDS BY FUSION PCR

Phusion site-directed mutagenesis was used to generate all remaining mutant pWN-AB plasmids for residues C305, S306, K307, A308, T330, G331, D333, T366, A367, and N368. First, two overlapping segments were generated using a set of outer and inner primers. The outer primers were the same for all EIII mutants, and the inner primers contained the desired mutation. Similarly to the L312 and T332 mutants, degenerate primers were designed to generate multiple mutants per reaction, although in the fusion groups only amino acids within one nucleotide of the wild type codon were included (as opposed to all 19 possibilities as was the case with the QuikChange reactions). For viruses that were not easily selected by plaque purification, individual primers were designed. Mutagenesis primers are listed in Table 4. All primers were designed by hand and synthesized by IDT (Coralville, IA).

Residue	Mutants Encoded	Sense	Sequence (5'-3')
C305	F/S/Y	+	AAGAAACTTGAAAGCCTTTGA**GDA**GACGCCATAGGTTGTTCCCTTCA
C305	F/S/Y	-	TGAAGGGAACAACCTATGGCGTC**THC**TCAAAGGCTTTCAAGTTTCTT
C305	G/R/W	+	AAGAAACTTGAAAGCCTTTGA**CCD**GACGCCATAGGTTGTTCCCTTCA
C305	G/R/W	-	TGAAGGGAACAACCTATGGCGTC**BGG**TCAAAGGCTTTCAAGTTTCTT
S306	A/P/T	+	AGTCCCAAGAAACTTGAAAGCCTT**GGB**ACAGACGCCATAGGTTGTTCCCT
S306	A/P/T	-	AGGGAACAACCTATGGCGTCTGT**VCC**AAGGCTTTCAAGTTTCTTGGGACT
S306	L	+	AGTCCCAAGAAACTTGAAAGCCTT**CAA**ACAGACGCCATAGGTTGTTCCCT
S306	L	-	AGGGAACAACCTATGGCGTCTGT**TTG**AAGGCTTTCAAGTTTCTTGGGACT
K307	E/Q	+	AGTCCCAAGAAACTTGAAAGC**TTS**TGAACAGACGCCATAGGTTGTTCCCT
K307	E/Q	-	AACAACCTATGGCGTCTGTTCA**SAA**GCTTTCAAGTTTCTTGGGACT
K307	M/R/T	+	AGTCCCAAGAAACTTGAAAGC**CVT**TGAACAGACGCCATAGGTTGTTCCCT
K307	M/R/T	-	AACAACCTATGGCGTCTGTTCA**ABG**GCTTTCAAGTTTCTTGGGACT
K307	N	+	AGTCCCAAGAAACTTGAAAGC**ATT**TGAACAGACGCCATAGGTTGTT
K307	N	-	AACAACCTATGGCGTCTGTTCA**AAT**GCTTTCAAGTTTCTTGGGACT
A308	D/G/V	+	TGCGGGAGTCCCAAGAAACTTGAA**GHC**CTTTGAACAGACGCCATAGGTT
A308	D/G/V	-	AACCTATGGCGTCTGTTCAAAG**GDC**TTCAAGTTTCTTGGGACTCCCGCA
A308	P/S/T	+	TGCGGGAGTCCCAAGAAACTTGAA**GGD**CTTTGAACAGACGCCATAGGTT
A308	P/S/T	-	AACCTATGGCGTCTGTTCAAAG**HCC**TTCAAGTTTCTTGGGACTCCCGCA
A308	T	+	TGCGGGAGTCCCAAGAAACTTGAA**TGT**CTTTGAACAGACGCCATAGGTT
A308	T	-	AACCTATGGCGTCTGTTCAAAG**ACA**TTCAAGTTTCTTGGGACTCCCGCA
A308	V	+	TGCGGGAGTCCCAAGAAACTTGAA**TAC**CTTTGAACAGACGCCATAGGTT
A308	V	-	AACCTATGGCGTCTGTTCAAAG**GTA**TTCAAGTTTCTTGGGACTCCCGCA
T330	A/P/S	+	ACTTTGCAAGGTCCATCCGTGCC**GGV**GTACTGCAATTCCAACACCACAGT
T330	A/P/S	-	ACTGTGGTGTTGGAATTGCAGTAC**BCC**GGCACGGATGGACCTTGCAAAGT
T330	I/N	+	ACTTTGCAAGGTCCATCCGTGCC**GWT**GTACTGCAATTCCAACACCACAGT
T330	I/N	-	ACTGTGGTGTTGGAATTGCAGTAC**AWC**GGCACGGATGGACCTTGCAAAGT
T330	S	+	ACTTTGCAAGGTCCATCCGTGCC**CGA**GTACTGCAATTCCAACACCACA

T330	S	-	TGTGGTGTTGGAATTGCAGTAC**TCG**GGCACGGATGGACCTTGCAAAGT
G331	A/D/V	+	AGGAACTTTGCAAGGTCCATCCGT**ADC**AGTGTACTGCAATTCCAACACCA
G331	A/D/V	-	TGGTGTTGGAATTGCAGTACACT**GHT**ACGGATGGACCTTGCAAAGTTCCT
G331	C/R/S	+	AGGAACTTTGCAAGGTCCATCCGT**ACD**AGTGTACTGCAATTCCAACACCA
G331	C/R/S	-	TGGTGTTGGAATTGCAGTACACT**HGT**ACGGATGGACCTTGCAAAGTTCCT
D333	A/E/G/V	+	AGATAGGAACTTTGCAAGGTCC**TNC**CGTGCCAGTGTACTGCAATTCCAA
D333	A/E/G/V	-	TTGGAATTGCAGTACACTGGCACG**GNA**GGACCTTGCAAAGTTCCTATCT
D333	H/N/Y	+	AGATAGGAACTTTGCAAGGTCC**GTD**CGTGCCAGTGTACTGCAATTCCAA
D333	H/N/Y	-	TTGGAATTGCAGTACACTGGCACG**HAC**GGACCTTGCAAAGTTCCTATCT
T366	A/P/S	+	TCAATCAGGACCTTAGCGTTGGC**AGV**GGCCACTGAAACAAAAGGGTTGA
T366	A/P/S	-	TCAACCCTTTTGTTTCAGTGGCC**BCT**GCCAACGCTAAGGTCCTGATTGA
T366	K/M/R	+	TCAATCAGGACCTTAGCGTTGGC**CHT**GGCCACTGAAACAAAAGGGTTGA
T366	K/M/R	-	TCAACCCTTTTGTTTCAGTGGCC**ADG**GCCAACGCTAAGGTCCTGATTGA
A367	D/G/V	+	AATTCAATCAGGACCTTAGCGTT**AHC**CGTGGCCACTGAAACAAAAGGGT
A367	D/G/V	-	ACCCTTTTGTTTCAGTGGCCACG**GDT**AACGCTAAGGTCCTGATTGAATT
A367	P/S/T	+	AATTCAATCAGGACCTTAGCGTT**TGD**CGTGGCCACTGAAACAAAAGGGT
A367	P/S/T	-	ACCCTTTTGTTTCAGTGGCCACG**HCA**AACGCTAAGGTCCTGATTGAATT
N368	D/H/Y	+	TCCAATTCAATCAGGACCTTAGC**ATV**GGCCGTGGCCACTGAAACAAAA
N368	D/H/Y	-	TTTTGTTTCAGTGGCCACGGCC**BAT**GCTAAGGTCCTGATTGAATTGGA
N368	I/S/T	+	TCCAATTCAATCAGGACCTTAGC**AVT**GGCCGTGGCCACTGAAACAAAA
N368	I/S/T	-	TTTTGTTTCAGTGGCCACGGCC**ABT**GCTAAGGTCCTGATTGAATTGGA
N368	K	+	TCCAATTCAATCAGGACCTTAGC**TTT**GGCCGTGGCCACTGAAACAAAA
N368	K	-	TTTTGTTTCAGTGGCCACGGCC**AAA**GCTAAGGTCCTGATTGAATTGGA

Table 4: Primers Used in Fusion PCR Mutagenesis of pWN-AB

List of primers used to generate pWN-AB plasmids with mutations at residue C305, S306, K307, A308, T330, G331, D333, T366, A367, or N368 using fusion PCR mutagenesis. Mutated codons are designated with bolded and underlined text. B=G/T/C, D=G/A/T, H=A/T/C, N=A/C/G/T, S=G/C, V=G/A/C, W=A/T.

For segment 1, the outer forward primer (CCCAAATACAGTGTCACAATGCCGGCTGATGTCTATGGCACACCCA) was used with the inner reverse primer. For segment 2, the inner forward primer was used with the outer reverse primer (GATTCAGCATCACTCCTGCGGCGCCTTCATACACACTAAAGCTTGGA). All reaction components were added individually on ice in the order listed:

31.2-XµL H_2O

10µL Phusion HF Reaction Buffer (5x) (Finnzymes, Espoo, Finland)

1µL PCR Nucleotide Mix (10mM each)(Roche, Mannheim, Germany)

3.65µL Forward Primer (100ng/µL)

3.65µL Reverse Primer (100ng/µL)

XµL pWN-AB (20ng DNA)

0.5µL Phusion Hot Start DNA Polymerase (2U/µL)(Finnzymes, Espoo, Finland)

Segments 1 and 2 were amplified by a Mastercycler gradient machine (Eppendorf, Westbury, NY) using the parameters described in Figure 4:

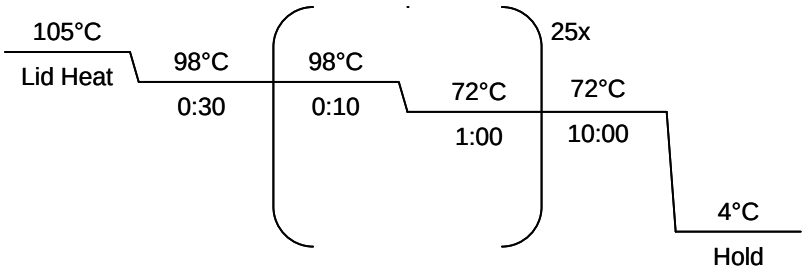

Figure 4: Cycle Parameters for the Generation of Segments 1 and 2 with Fusion PCR
Cycle parameters used to amplify overlapping segments of the pWN-AB plasmid using fusion PCR.

After checking this initial amplification on a gel, segments 1 and 2 were used as the template for a second round of amplification using the outer primers pWNAB_NgoMIV_F and pWNAB_NarI_R. Again, all reaction components were added individually in the order listed:

29.2µL H_2O

10µL Phusion HF Reaction Buffer (5x)

1µL PCR Nucleotide Mix (10mM each)

3.65µL pWNAB_NgoMIV_F (100ng/µL)

3.65µL pWNAB_NarI_R (100ng/µL)

1µL Segment 1 PCR Product

1µL Segment 2 PCR Product

0.5µL Phusion Hot Start DNA Polymerase (2U/µL)

The fusion product was amplified by a Mastercycler gradent machine using parameters similar to those described in Figure 2, except that the 72°C extension was increased from 1 minute to 1 minute 15 seconds.

The entire fusion product was then loaded onto a 1.2% agarose (BioExpress, Kaysville, UT), 1xTAE gel with 0.2x GelRed stain (BioTium, Hayward, CA), run at 120-180V, and visualized with on a UV light box. The PCR product was excised from the gel and purified using the QIAquick Gel Extraction Kit (Qiagen, Germantown, MD) according to the manufacturer's instructions and its concentration was determined with a Nanodrop 1000 (NanoDrop, Wilmington, DE).

Once the fusion PCR product was available, both the PCR insert and the pWN-AB backbone were digested with 5 units NgoMIV and 5 units NarI in buffer 4 (NEB, Ipswich, MA). The pWN-AB backbone also had 0.5 units of CIP (NEB, Ipswich, MA) added to it at that time to prevent it from self-annealing during the subsequent ligation. The amount of PCR insert and pWN-AB backbone digested was such that the subsequent ligation contained 1µg of DNA with a 3:1 insert:vector molar ratio. The reaction was allowed to proceed at 37°C for 2 hours, followed by a 20 minute incubation at 80°C to inactivate the enzymes. The digestions were loaded onto a 13x16.5cm 1.2% agarose, 1xTAE gel with 0.2x GelRed and run at 120V until the dye front reached the end of the gel. The bands were visualized on a UV box, and the 1kb insert and 4.6kb vector bands

were excised and purified using the QIAquick Gel Extraction Kit according to the manufacturer's instructions. The insert and vector were ligated together by 400 units T4 DNA ligase (NEB, Ipswich, MA) at 16°C overnight.

After ligation, mutant pWN-AB plasmids were recovered as described in the QuikChange protocol. Briefly, the plasmids were transformed into *E. coli* DH5α bacterial cells, overnight cultures were generated, bacterial stocks were frozen down for future use, and plasmids were harvested and sent to the UTMB Molecular Genomics core for sequencing.

RECOVERY OF WILD-TYPE AND MUTANT NY99IC VIRUS

The general protocol for recovery of WNV NY99ic virus and the construction of the pWN-AB and pWN-CG plasmids have been described previously by Beasley et al.(183) Bacterial stocks of *E. coli* DH5α containing either wild-type or mutant pWN-AB or wild-type pWN-CG plasmid were used to inoculate 100ml of LB/Amp, which was grown for 16-18 hours at 37°C with 200rpm shaking. The cells were then transferred to two 50ml conical tubes and centrifuged for 20 minutes at 2,850xg and 4°C to pellet the cells. Plasmid was harvested from the cells using the Plasmid Midi Prep kit (Qiagen, Hilden, Germany) according to the manufacturer's instructions, with the final DNA pellet being resuspended in 90µl TE buffer. Concentration and purity of each purified plasmid was determined using the NanoDrop 1000 (NanoDrop, Wilmington, DE).

Once plasmids were successfully recovered, 2µg each of pWN-AB and pWN-CG were digested by 5 units of NgoMIV and 10 units of XbaI (NEB, Ipswich, MA) for 2 hours at 37°C. The digested plasmids were loaded into a 13x16.5cm 1% agarose gel in 1xTAE with a lane of 1kb ladder (NEB, Ipswich, MA) flanking both the pWN-AB and pWN-CG plasmid(s). The samples were run at 120-150V until the dye front reached the end of the gel. At this point a strip of gel containing the 1kb ladder and a small fraction of the first plasmid lane was excised from the gel and placed in a container with 1xTAE

and 0.2xGelRed for 10-15 minutes. The ladder and the sliver of plasmid were visualized on a UV light box, and the location of the desired bands (5.2kb for pWN-AB and 8kb for pWN-CG) was marked by cutting a small notch out of the excised gel strip. The strip was removed from the UV light and returned to the rest of the gel, where the notch was used as a guide to cut the desired bands from the remaining, unstained portion of the gel without having to expose it to UV light and thus avoiding the risk of cross-linking thymines. The linearized pWN-AB and pWN-CG plasmids were purified away from the agarose using the QIAquick Gel Extraction Kit (Qiagen, Germantown, MD) according to the manufacturer's directions. The digested pWN-AB and pWN-CG bands were ligated overnight at 4°C by 400 units of T4 DNA ligase (NEB, Ipswich, MA).

After the ligation was complete, the T4 DNA ligase was heat inactivated at 70°C for 10 minutes, and the sample was digested by 50 units of XbaI at 37°C for 2 hours. The restriction enzyme was then inactivated by the addition of proteinase K (Sigma, St. Louis, MO) to a final concentration 0.67mg/ml and incubated for 1 hour at 37°C. An equal volume of phenol/chloroform/isoamyl alcohol (Roche, Indianapolis, IN) was then added, and the sample was vortexed for 25 seconds, held at room temperature for 5 minutes, then centrifuged for 2 minutes at 15,700xg. The aqueous phase containing the DNA was transferred to a fresh 1.5ml tube, and the sample was phenol/chloroform/isoamyl alcohol purified one more time. Finally, an equal volume of chloroform (Fisher, Fair Lawn, NJ) was added to the sample, which was vortexed for 30 seconds and centrifuged for 1 minute at 15,700xg. The aqueous phase (approximately 500µl) was transferred to a final fresh 1.5ml tube, to which 50µl of 3M potassium acetate, pH 5.2 (Sigma, St. Louis, MO) and 1ml of 100% ethanol (Fisher, Fair Lawn, NJ) were added. The sample was left at -20°C overnight to precipitate the DNA.

On the final day of the infectious clone recovery, the tube containing the ligated, full-length-genome-equivalent DNA was centrifuged for 20 minutes at 15,300xg and 4°C. The liquid was carefully pipetted out of the tube, and the DNA pellet was allowed

to air dry before being resuspended in 10µl TE. RNA was in vitro transcribed using the T7-Flash Ampliscribe Kit (Epicentre, Madison, WI), supplemented with the m7G(5')ppp(5')A RNA cap structure analog (NEB, Ipswich, MA). For each transcription reaction, the following reagents were added to the DNA one at a time, in the order listed:

7.2µl NTP solution (2.5mM A, 25mM C/G/U)

2.5µl AmpliScribe reaction buffer (10x)

1.8µl m7G(5')ppp(5')A RNA cap structure analog (40mM)

2µl DTT (100mM)

2µl AmpliScribe T7-Flash enzyme solution

The in vitro RNA transcription was allowed to proceed for 30 minutes at 37°C, and the resulting RNA-containing sample was stored on ice until immediately prior to electroporation.

Flasks of Vero cells were rinsed with DPBS (Cellgro, Manassas, VA), detached with trypsin (Cellgro, Manassas, VA), and resuspended in Vero growth media. The cell suspensions were transferred to 50ml conical tubes and centrifuged at 1,500xg and 4°C for 5 minutes. The media was discarded, and the cells were resuspended in 20ml chilled DPBS, then stored on ice. A further 1:10 dilution of cells in DPBS was made and used to determine the total number of cells using a hemocytometer. After counting, cells were centrifuged again at 1,500xg and 4°C for 5 minutes, then resuspended in the appropriate amount of DPBS to give a final concentration of $0.6\text{-}1.2 \times 10^7$ cells/ml. Pre-chilled 2mm gap sterile electroporation cuvettes (Fisher, Fair Lawn, NJ) were loaded with 500µl of cells and the previously transcribed RNA. Samples received two pulses of electricity in quick succession from a GenePulser Electroporation System (BioRad, Hercules, CA) at a setting of 1.50V, 25µFD, and 400Ω. After a 10 minute rest at room temperature, the cells were transferred to a T-75 flask containing 20ml of Vero growth media and transferred to the 37°C, 5%CO_2 incubator in the BSL-3 laboratory. Virus was typically ready for

harvest 2-4 days post-electroporation. Aliquots of virus were stored at -70°C until needed.

NUCLEOTIDE SEQUENCING OF WNV

WNV RNA was extracted from virus stocks using the QIAamp Viral RNA Mini Kit (Qiagen, Germantown, MD). Once the RNA was obtained from WNV stocks, the prM/E coding region between nucleotides 401 and 2504 was amplified by RT-PCR using either the Titan One Tube RT-PCR kit (Roche, Indianapolis, IN) or a two step RT-PCR. (201) In case of a two step reaction, the cDNA was generated using AMV reverse transcriptase (Roche, Mannheim, Germany), and PCR was done using the High Fidelity PCR Master Mix (Roche, Mannheim, Germany).

RNA was amplified with the Titan kit by combining the following components:

25.2µl H_2O

1µl dNTP Mix (10mM each)

2.5µl DTT (100mM)

1µl RNase Inhibitor (5U/µl)

10µl RT-PCR Buffer (5x)

1µl Titan Enzyme Mix

2.13µl WN-401 (100ng/µl)

2.13µl WN-2504A (100ng/µl)

5µl RNA

Typically, a master mix containing all reaction components except the RNA template was used. An H_2O negative control was always included to ensure that the sequences obtained were not the result of contamination. Amplicons were generated by a Mastercycler gradient machine (Eppendorf, Westbury, NY) using the parameters described in Figure 5:

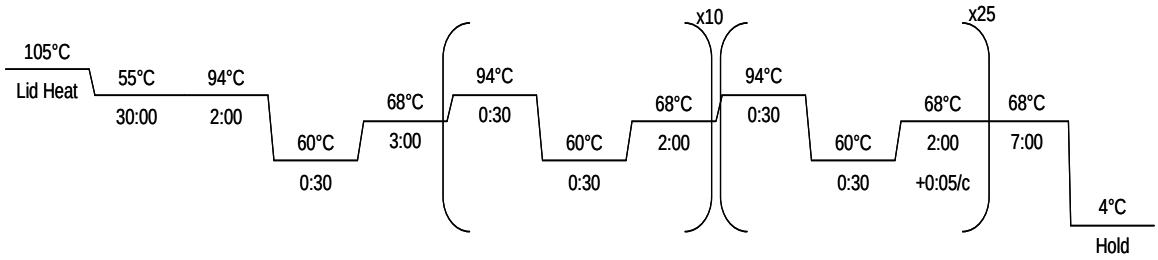

Figure 5: Cycle Parameters for Amplification of WNV prM/E Region Using Titan Kit

Cycle parameters used to amplify the prM/E region of WNV using the WN401/WN2504A primer pair with the Titan One Tube RT-PCR kit.

When the two-step RT-PCR was used, 2µl of RNA was combined with 5.4µl WN-2504A (100ng/µl), and the mix was heated to 95°C for 5 minutes before being cooled on ice for 2 minutes. After the primer and template had cooled, 2.6µl of a mix containing 2µl RT buffer (5x), 0.4µl dNTP mix (10mM each), and 0.2µl AMV RT were added to each sample. The cDNA was generated by a Mastercycler gradient machine (Eppendorf, Westbury, NY) using the parameters described in Figure 6:

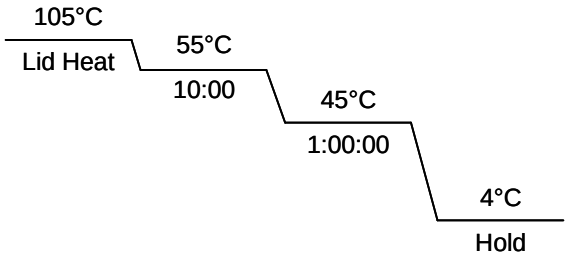

Figure 6: Cycle Parameters for Generation of WNV cDNA Using AMV RT

Cycle parameters used to generate WNV cDNA using the WN2504A primer with AMV RT enzyme.

After cDNA synthesis, 45µl of a master mix containing the equivalent of the following reaction components was added to 5µl cDNA:

19.1µl H_2O

0.47µl WN-401 (100ng/µl)

0.46µl WN-2504A (100ng/µl)

25µl High Fidelity PCR Master Mix

An H_2O negative control was always included to ensure that the sequences obtained were not the result of contamination. Amplicons covering the 401 to 2504 nucleotide region were generated by a Mastercycler gradient machine using the parameters described in Figure 7:

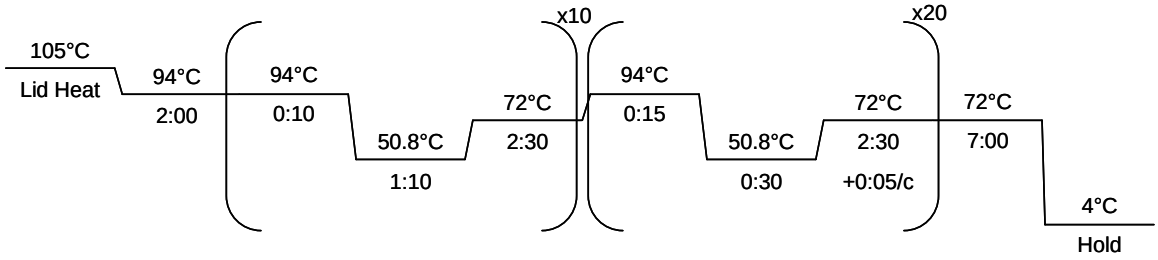

Figure 7: Cycle Parameters for Amplification of WNV prM/E Region Using High Fidelity PCR Master Mix

Cycle parameters used to amplify the prM/E region of WNV using the WN401/WN2504A primer pair with High Fidelity PCR Master Mix.

Once the amplicons were generated, either by one step or two step RT-PCR, they were loaded onto a 1.2% agarose, 1xTAE gel with 0.2x GelRed stain, run at 120-180V, and visualized on a UV light box. The PCR product was excised from the gel and purified using the QIAquick Gel Extraction Kit (Qiagen, Germantown, MD) according to the manufacturer's instructions. Purified PCR amplicons were send to the UTMB Molecular Genomics Core for sequencing using the WN-401, WN-1219A, WN-1101, WN-1816A, WN-1751, WNSA58-1751, WN-2504A, and WNSA58-2504A primers described in Table 5.(201)

Primer	Sequence (5'-3')
WN-401	AAAAGAAAAGAGGAGGAAAG
WN-1219A	GTTTGTCATTGTGAGCTTCT
WN-1101	GATGAATATGGAGGCGGTCA
WN-1816A	TGCATCAAGCTTTGGCTGGA
WN-1751	CCGACGTCAACTTGACAGTG
WNSA58-1751	TGCACCAAGCTTTGGCTGGG
WN-2504A	TCTTGCCGGCTGATGTCTAT
WNSA58-2504A	TCTTGCCTACCAATGTCAAT

Table 5: Primers for Sequencing the prM/E region of WNV

Set of primers used to sequence the prM/E region of WNV. Primers were previously designed by Beasley *et al.*(201)

WNV PLAQUE ASSAYS

Media was discarded from a 12-well plate of nearly confluent Vero cells, and the monolayer was rinsed with DPBS. Virus was serially 10-fold diluted in DPBS, typically covering a range of $1:10^1$-$1:10^6$, and 100µl of diluted virus was added to individual wells of a 12-well plate. The plates were incubated for 1 hour at room temperature before 2ml of overlay was added to each well. Overlay consists of an equal mix of 2% agar (Sigma, Portugal) and 2x Vero maintenance media (see Appendix A for details). The plates were incubated at 37°C with 5% CO_2 for 2 days. As this point, 1ml of stain overlay was added to each well. The stain overlay is the same as the original overlay with the addition of neutral red solution (Sigma, St. Louis, MO) to a final concentration of 160mg/L. The plates were covered with foil to protect them from light and returned to the 37°C, 5% CO_2 incubator. Plaques were read with the aid of a light box at days 3 and 4 post-infection.

WNV NEUTRALIZATION INDEX ASSAYS

WNV neutralization index assays were performed to compare the ability of monoclonal antibodies and polyclonal sera to neutralize wild-type and mutant WNV. Virus was serially 10-fold diluted in Vero maintenance media (see Appendix A for details) in 96-well plates. Antibody was also diluted in Vero maintenance media. Anti-WNV monoclonal antibodies 5H10 and 7H2 (BioReliance, Rockville, MD) were diluted to 2.5ng/µl and anti-WNV EIII rabbit serum (Harlan Bioproducts for Science, Indianapolis, IN) was diluted 1:50. After their subsequent 1:2 dilution these concentrations were equivalent to 80 times the 5H10 $PRNT_{50}$, 420 times the 7H2 $PRNT_{50}$, and 100 times the anti-WNV EIII serum $PRNT_{50}$.(202) A no-antibody control was also included for the calculation of neutralization indices. Equal volumes of diluted virus and antibody were combined and allowed to bind to each other for 1 hour at room temperature. After the 1 hour incubation period, 100µl of diluted virus was added to individual wells of a 12-well plate of Vero cells. The virus:antibody mixture was allowed to infect the monolayer for 1 hour, and was then overlaid, stained, and visualized as described in the WNV plaque assay method. Assays were conducted in duplicate. Neutralization indices were defined as the $\log_{10}$ reduction in antibody titer caused by each antibody in comparison with the no-antibody control. Neutralization index averages and standard deviations were calculated in Excel 2003 (Microsoft, Redmond, WA). When all neutralization index data had been gathered, clustering analysis was performed to identify significant differences in neutralization activity for the various virus/antibody combinations that had been evaluated. First, the appropriate number of clusters was determined using k-means analysis performed with the 'stats' package in R 3.0.2 (R Foundation for Statistical Computing, Vienna, Austria). The data for all antibodies and all mutants was combined to ensure that the full range of possible values, from strong neutralization to strong escape, was adequately represented when determining groups.

Individual mutant/antibody combinations were assigned to a particular cluster by the average method of hierarchical clustering, also using R 3.0.2 (R Foundation for Statistical Computing, Vienna, Austria).

WNV PLAQUE REDUCTION NEUTRALIZATION TESTS

WNV PRNTs were performed to compare the ability of anti-EIII mouse sera to neutralize homologous and heterologous strains of WNV. Virus was diluted to approximately 400pfu/ml in Vero maintenance media. Sera was serially 2-fold diluted from 1:20-1:320. A no-antibody control was also included for the calculation of PRNT value. Equal volumes of virus and antibody were combined and allowed to bind to each other for 1 hour at room temperature. After the 1 hour incubation period, 100µl of diluted virus was added to individual wells of a 12-well plate of Vero cells. The virus:antibody mixture was allowed to infect the monolayer for 1 hour, and was then overlaid, stained, and visualized as described in the WNV plaque assay method. $PRNT_{50}$ values were defined as the highest dilution capable of reducing the number of plaques by at least 50% in comparison with the no-antibody control. $PRNT_{50}$ values, averages, and standard deviations were calculated and the results for mutants were compared to wild-type using an unpaired, 2-tailed student's t-test in Excel 2003 (Microsoft, Redmond, WA). Graphs were also generated in Excel 2003.

PREPARATION OF INFECTED CELL LYSATES

To make cell lysates for Western blotting, T-25 flasks of Vero cells were rinsed with DPBS and infected with 100µl virus for 30-60 minutes, then filled with 6ml Vero maintenance media and placed in a 37°C incubator with 5% CO2. When early cytopathic effect (CPE) was visible, typically 2-3 days post-infection, the media was poured out of the flask and the flask was stored at -70°C overnight. The cells were then thawed at room temperature and the monolayer was resuspended in 1ml of 10% w/v sodium dodecyl

sulfate (Sigma, Japan). The lysate was incubated at room temperature for 10 minutes before being transferred to a cryovial and heat inactivated at 56°C for 30 minutes.

POLYACRYLAMIDE GEL ELECTROPHORESIS (PAGE) AND WESTERN BLOTTING

Binding of monoclonal antibodies and polyclonal sera to wild-type and mutant WNV E proteins was assessed by Western blotting. To separate the cell lysates, a 8x10x0.75cm SDS-polyacrylamide gel was poured with a 12% acrylamide (Sigma, St. Louis, MO) body and a 4% polyacrylamide stack. Once the gel solidified, 2.5µl of lysate was run against the Full Range Rainbow Recombinant Protein Molecular Weight Marker (GE Healthcare, Piscataway, NJ). The samples were run at 120V in a Mini-PROTEAN Tetra cell (Bio-Rad Hercules, CA) until the loading dye reached the bottom of the body of the gel. The gel was then gently removed from its glass plates and placed flush against a Trans-Blot transfer medium nitrocellulose membrane (BioRad, Hercules, CA). The gel and membrane were sandwiched between one fiber pad and two pieces of filter paper on either side, and the proteins were transferred to the membrane for 2 hours at 200mA in a Mini Trans-Blot cell (Bio-Rad, Hercules, CA). The locations of the protein weight markers were marked on the membrane with a pencil, and the membrane was placed in a container of 1xTBS with 3%BSA (Sigma, St. Louis, MO) at 4°C overnight to block non-specific binding.

After the overnight blocking step, the membrane was placed in a container with approximately 30ml wash buffer (1xTBS with 0.2% Tween-20) on a rocker for 5 minutes at room temperature. A piece of parafilm was then secured to the rocker, and the membrane was placed on the parafilm. Appropriately diluted primary antibody was pipetted onto the membrane and was allowed to wash over the membrane for 1 hour at room temperature with gentle rocking. More diluted antibody was added as necessary to prevent the membrane from drying. Primary antibodies included anti-WNV mouse

immune ascitic fluid (MIAF) at 1:500, anti-WNV EIII rabbit serum at 1:500, 5H10 at 0.5ng/µl, and 7H2 at 0.25ng/µl. All antibodies were diluted in wash buffer.

After the primary antibody incubation, the membrane was washed three times for five minutes each in a container with approximately 30ml wash buffer with gentle rocking. Secondary antibody, either goat anti-mouse IgG with horseradish peroxidase (HRP) or goat anti-rabbit IgG with HRP (Sigma, St. Louis, MO), was diluted 1:5,000. The membrane was incubated with the diluted secondary antibody for 1 hour at room temperature with gentle rocking, followed by another three washes. The membranes were developed using the ECL Western Blotting Detection Reagents (GE Healthcare, Buckinghamshire, UK) and then exposed to ECL Hyperfilm (GE Healthcare, Buckinghamshire, UK) for visualization.

ELISA

ELISAs were performed to compare the ability of anti-EIII mouse sera to bind to EIII proteins from homologous and heterologous strains of WNV. Proteins were diluted to 2ng/µl in borate saline (0.12M NaCl, 0.024M NaOH, 0.05M H3BO3, pH 9.0), and 50µl of diluted protein or a borate saline-only negative control was added to the wells of a MaxiSorp U-bottom plate (Nunc, Roskilde, Denmark). The plate was covered and left at 4°C overnight. The plate was then washed one time by hand by filling all wells with wash buffer (1xPBS with 0.05% Tween-20) and then removing the buffer by inverting the plate and vigorously blotting on a stack of paper towels. The wells were blocked with 65µl blocking buffer (wash buffer with 3% BSA to prevent non-specific antibody binding), covered, and left at room temperature for 1 hour. After blocking the plates were washed twice as described above. Primary antibodies were serially 2-fold diluted in wash buffer from 1:250-1:32,000, and 50µl of each diluted sample were added to the wells of the ELISA plate. The primary antibodies were allowed to bind for 1 hour at room temperature before the plates were washed three times. Secondary antibody, in this

case goat anti-mouse IgG with HRP (Sigma, St. Louis, MO), was diluted 1:5,000 in wash buffer and 50µl were added to each well. The secondary antibody was allowed to bind for 1 hour at room temperature, before the plates were washed with four times. For visualization, 50µl of 3,3',5,5'-tetramethylbenzidine (TMB) liquid substrate system for ELISA (Sigma, S. Louis, MO) was added to each well. After 10 minutes, the reaction was stopped by the addition of 50µl 3M HCl to each well. Absorbances were read on a Sunrise plate reader (Tecan, San Jose, CA) at 450nm, with a reference reading at 650nm. The reference reading was subtracted from the absorbance at 450nm, and the resulting number was used in downstream analysis. Averages and standard deviations were calculated and the results were compared using an unpaired, 2-tailed Student's t-test in Excel 2003 (Microsoft, Redmond, WA). Graphs were also generated in Excel 2003.

WNV *IN VITRO* REPLICATION KINETICS

To measure in vitro replication kinetics, Vero, DEF, and C6/36 cells were grown to confluency in 6-well plates. Media was decanted from the plates and the monolayers were rinsed once with DPBS, then $9.5x10^3$pfu of virus in 200µl DPBS was added to each well for an approximate multiplicity of infection (MOI) of 0.01. Infections were conducted in duplicate. The virus was allowed to infect the monolayer for one hour at room temperature, then the monolayers were rinsed three times with DPBS to remove any unbound virus and cells were overlaid with 6ml of the appropriate maintenance media (see Appendix A for details).

Vero and DEF plates were incubated at 37°C with 5% CO_2, and C6/36 cells were incubated at 28°C in an ungassed incubator. Samples for L312 and T332 mutants were collected at 0, 0.5, 1, 1.5, 2, 3, 4, and 5 days post-infection. Samples for all other mutants were collected at 0, 1, 3, and 5 days post-infection. During collections, two 250µl samples were collected from each well and the volume was replaced with 500µl of fresh maintenance media. Aliquots were stored at -70°C until needed for analysis. Viral titers

at each timepoint were determined via WNV plaque assay as described above. Variation at each timepoint was assessed using a one-way ANOVA analysis of the log_{10} titers in PASW Statistics 18 (SPSS, Quarry Bay, Hong Kong) with a significance threshold of $p<0.05$. Log_{10} titers were used instead of raw titers to allow for the detection of significance for strains with higher and lower titers than wild type. For those timepoints with significant variation, the individual strains that differed significantly from the wild type control were determined using a post-hoc Bonferroni test with a significant threshold of 0.05 (comparing 6 and 8 to 7 gives equal weight to the 10-fold changes from wild type in either direction, whereas raw numbers would give a difference of 9,000,000 for the decrease and 99,000,000 for the increase, making increased titers much more likely to reach statistical significance then decreased titers). Graphs were generated in Excel 2003 (Microsoft, Redmond, WA) using the average log_{10} values, with error bars representing standard deviation of the log_{10} values.

WNV MOUSE VIRULENCE STUDIES

Groups of 3-4-week-old female Swiss Webster mice (Harlan Laboratories, Houston, TX) were injected with virus diluted in 100µl PBS via the IP route. For virulence screening studies, the virus dose was 100pfu and the cohort sizes were 8-10 mice. For 50% lethal dose (LD_{50}) studies, the doses included 10-fold serial dilutions ranging from 1,000-0.1pfu and each dose had a cohort size of 5 mice. Mice were monitored for 21 days post-infection. Animals were counted as deceased on a given day if they were either found dead during the health check or were euthanized due to severity of symptoms (paralysis or hunching with immobility). Average survival times with standard deviations were determined using Excel 2003 (Microsoft, Redmond, WA). Survival analysis was conducted using the Kaplan-Meir test in SPSS Statistics 17.0 (IBM, Armonk, NY).

WNV MOUSE PROTECTION STUDIES

Groups of 3-4-week-old female Swiss Webster mice received two doses of either NY99 EIII or SA58 EIII protein before being challenged with either homologous or heterologous virus. Cohort sizes were as follows:

1. NY99 EIII vaccination vs. NY99ic challenge, n=10
2. SA58 EIII vaccination vs. NY99ic challenge, n=10
3. PBS vaccination vs. NY99ic challenge, n=5
4. NY99 EIII vaccination vs. SA58 challenge, n=9
5. SA58 EIII vaccination vs. SA58 challenge, n=10
6. PBS vaccination vs. SA58 challenge, n=4

On day 0 the mice were given 8µg of protein in DPBS (or plain PBS for as a control) emulsified in an equal volume of Freund's incomplete adjuvant (Thermo, Rockford, IL) in a final volume of 80µl per mouse. On day 16 the mice were given 25µg of protein in DPBS (or plain PBS for a control) emulsified in an equal volume of Freund's incomplete adjuvant in a final volume of 100µl per mouse. Both vaccinations were delivered via the IP route. On day 28, mice were ear punctured to allow for individual identification, and blood was collected from each animal via a retro-orbital bleed. On day 30 the mice were challenged with 500pfu of either NY99ic or SA58 virus diluted in DPBS to a final volume of 100µl and delivered via the IP route. Mice were monitored for 30 days post-infection. Animals were counted as deceased on a given day if they were either found dead during the health check or were euthanized due to severity of symptoms (paralysis or hunching with immobility). Average survival times with standard deviations were determined and difference between homologous and heterologous protection were assessed via unpaired, 2-tailed Student's t-test using Excel 2003 (Microsoft, Redmond, WA). Survival analysis was conducted using the Kaplan-Meir test in SPSS Statistics 17.0 (IBM, Armonk, NY).

Chapter 3: Impact of Variation at Residue L312

RATIONALE AND APPROACH

In 2010 there were 167 cases of human West Nile disease in Arizona, a large increase from the 20 cases recorded in 2009.(203) To investigate entomological characteristics of this outbreak, mosquitoes were collected from Gilbert, Arizona, where there was a significant amount of WNV activity, and from Phoenix, Arizona, where there was relatively little disease.(204) Behavioral and environmental differences between humans with WNV disease and uninfected humans were also examined.(205) Gross physical examination and PCR analysis of bloodmeal type and WNV infection status revealed that *Culex quinquefasciatus* were likely the main vector responsible for spreading WNV between birds and to humans during the 2010 Arizona outbtreak.(204) *Culex quinuefasciatus* mosquitoes from Gilbert fed on birds (77%) and humans (13%), while mosquitoes from Phoenix fed exclusively on birds. *Culex quinquefasciatus* mosquitoes collected from Phoenix were slightly more likely to be infected with WNV, but the overall number of mosquitoes in Gilbert was so much higher, and they were so much more likely to have fed on a human prior to capture in Gilbert, that the overall chances of a human encountering a WNV-infected *Culex quinquefasciatus* mosquito were much higher in the outbreak region of Gilbert than the control region of Phoenix. Subsequent analysis of behavioral and environmental factors at the homes of infected and uninfected humans confirmed the importance of mosquito abundance to WNV risk, with the presence of standing water at the home and the proximity to the water district both significantly increasing the likelihood of human disease.(205)

To assess the potential contribution of virological changes to the outbreak, several strains of WNV were isolated from the infected mosquitoes. Of the fifteen strains for which E genes were sequenced, seven encoded an L312I mutation. These strains cluster

with the recently described SW/WN03 genotype.(206) Residue L312 is located on the surface of EIII, immediately after the C-terminus of the A strand.(63) Because it is surface exposed, it is possible that residue L312 is important to the antigenicity and/or function of EIII. Unlike lineage 1 WNV, the majority of lineage 2 WVN strains have an alanine at position 312. There is diversity at this residue within lineage 2 viruses, which have on occasion been isolated with a valine at position 312: a crombec bird from South Africa in 1958 (accession HM147822), a warbler from Cyprus in 1968 (accession GQ903680), a parrot from Madagascar in 1978 (accession DQ176636), and a human from South Africa in 2000 (accession EF429199).(192, 207, 208) In addition to the naturally occurring difference between lineage 1 and lineage 2 strains of WNV and the diversity within lineage 2 WNV, there is diversity at residue L312 within the lineage 1 WNV isolates. In addition to its detection during the 2010 Arizona outbreak, several other strains have had the L312I mutation: a crow from Illinois in 2005 (accession DQ874409), a human from South Dakota in 2005 (accession DQ666452), a human from Missouri in 2007(accession GQ502396), a human from Nevada in 2009 (accession JF957175), and a human from Arizona in 2011 (accession JQ700438).(195, 209-211) Interestingly, all of the lineage 1 strains with the L312I variant group with the SW/WN03 genotype that emerged in the United States in 2003.(206)

Because residue L312 has naturally occurring diversity both between and within lineages 1 and 2, because the L312I mutation has been detected in the United States periodically for a span of 6 years, because all of the L312I strains belong to the newly identified SW/WN03 genotype, and because L312I was detected in multiple isolates from a significant outbreak of human disease in Arizona during 2010, the functional and antigenic impact of L312 was investigated. All amino acid substitutions that could be obtained with a single nucleotide substitution to the wild-type NY99 codon were generated in the NY99ic. An exception was L312V, which was not characterized due to valine being the dominant codon in lineage 2 strains and therefore being assumed to be

well tolerated. The viable L312 mutants, along with two strains from the Arizona 2010 outbreak encoding natural L312I substitutions, were characterized. Antibody neutralization was determined for two monoclonal antibodies known to bind EIII (5H10 and 7H2) and for polyclonal serum against WNV EIII meant to simulate the immune response to a potential EIII-based vaccine. The impact of residue L312 on viral fitness was determined by examining replication kinetics in three cell types: Vero, DEF, and C6/36. Finally, the LD_{50} value in a Swiss Webster mouse model was determined to examine any potential attenuation.

RESULTS

Mutant Recovery

All of the desired L312 mutants (L312F, L312H, L312I, L212P, and L312R) were viable. No compensating mutations in the prM/E coding region of the working stocks were detected, and the L312 substitutions were stable during three passages in Vero cells.

Antibody-Mediated Neutralization

Changes at residue 312 had only minor impacts on antibody neutralization (Table 6). One issue of note is that even the NY99ic wild-type control groups with the moderate neutralization cluster for the monoclonal antibodies 5H10 and 7H2. This is likely due to the use of an older aliquot of antibody than was utilized in other experiments. Of all the NY99ic L312 mutants and Arizona strains, only AZ10-75 clustered apart from the wild-type, and it did so with both monoclonal antibodies and with the polyclonal anti-EIII serum. Although there was significant variation within each antibody group, none of the NY99ic L312 mutants or the Arizona strains significantly differed from wild-type. The only strain-antibody combination to approach significance compared to wild-type was L312P with 7H2, which had a Bonferroni-corrected p-value of 0.053 when compared to NY99ic wild-type with 7H2.

WNV NY99ic Strain	Antibody		
	5H10	7H2	Anti-EIII Serum
Wild-type	1.5±0.2	1.5±0.2	2.4±0.3
L312F	1.5±0.4	1.5±0.4	2.5±0.4
L312H	2.0±0.1	1.7±0.3	2.9±0.0
L312I	1.4±0.3	1.8±0.4	2.5±0.4
AZ10-75 (312I)	1.1±0.1	1.1±0.2	2.1±0.3
AZ10-581 (312I)	1.5±0.2	1.4±0.4	2.5±0.2
L312P	2.2±0.1	2.0±0.1	2.6±0.2
L312R	1.8±0.2	1.7±0.1	2.7±0.0

Table 6: Neutralization Indices of WNV L312 Mutants and Naturally Occurring Variants

Neutralization indices of WNV NY99ic wild-type and L3312 mutants and naturally occurring variants by the 5H10 and 7H2 monoclonal antibodies and by rabbit anti-EIII polyclonal serum. Values given as Avg±SD. Green = strongly neutralized, yellow = moderately neutralized, and red = weakly neutralized. * indicates statistically significant difference ($p<0.05$) from wild-type using the Bonferroni post-hoc test following one-way ANOVA.

In vitro Replication Kinetics

All of the WVN NY99ic L312 mutants and naturally occurring AZ10 variants were able to replicate in Vero cells (Figure 9). When the NY99ic wild-type reached its peak at 3 days post-infection, all other strains were within 0.1 $\log_{10}$ pfu/ml of the NY99ic wild-type titer except for L312P, L312R, and AZ10-581, which were 0.7-1.0 $\log_{10}$pfu/ml lower than that of wild-type. Several L312 mutants lagged behind the NY99ic wild-type by at least 1.0 $\log_{10}$ pfu/ml at 1 day post infection: L312H, L312I, and L312P. The L312H mutant, in particular, was 3.2 $\log_{10}$ pfu/ml below the NY99ic wild-type titer at 1 day post infection, and it remained 1.1 $\log_{10}$ pfu/ml below the NY99ic wild-type at 1.5 days post infection before recovering to wild-type-level titers. The only other strains to differ from NY99ic wild-type by at least 1.0 $\log_{10}$ pfu/ml were L312R, which was 1.0 $\log_{10}$ pfu/ml below NY99ic wild-type at 3 days post-infection, and AZ10-581, which was 1.1 $\log_{10}$ pfu/ml below NY99ic wild-type at 4 days post-infection.

There was significant variation between the strains at all timepoints except the very early timepoints (0 and 0.5 days post-infection) when the majority of strains are below the limit of detection and the 2 days post-infection timepoint (Table 7). In addition to those strains that differed from NY99ic wild-type by at least 1.0$\log_{10}$ pfu/ml at some

point, there were eight strain/timepoint combinations that were statistically different from NY99ic wild-type: AZ10-75 and AZ10-581 at 1 day post-infection, AZ10-581 and L312P at 3 days post-infection, AZ10-75 and L312P at 4 days post-infection, and AZ10-75 and L312P at 5 days post-infection. In all cases, the strains that were significantly different from NY99ic wild-type were at lower titers than NY99ic wild-type.

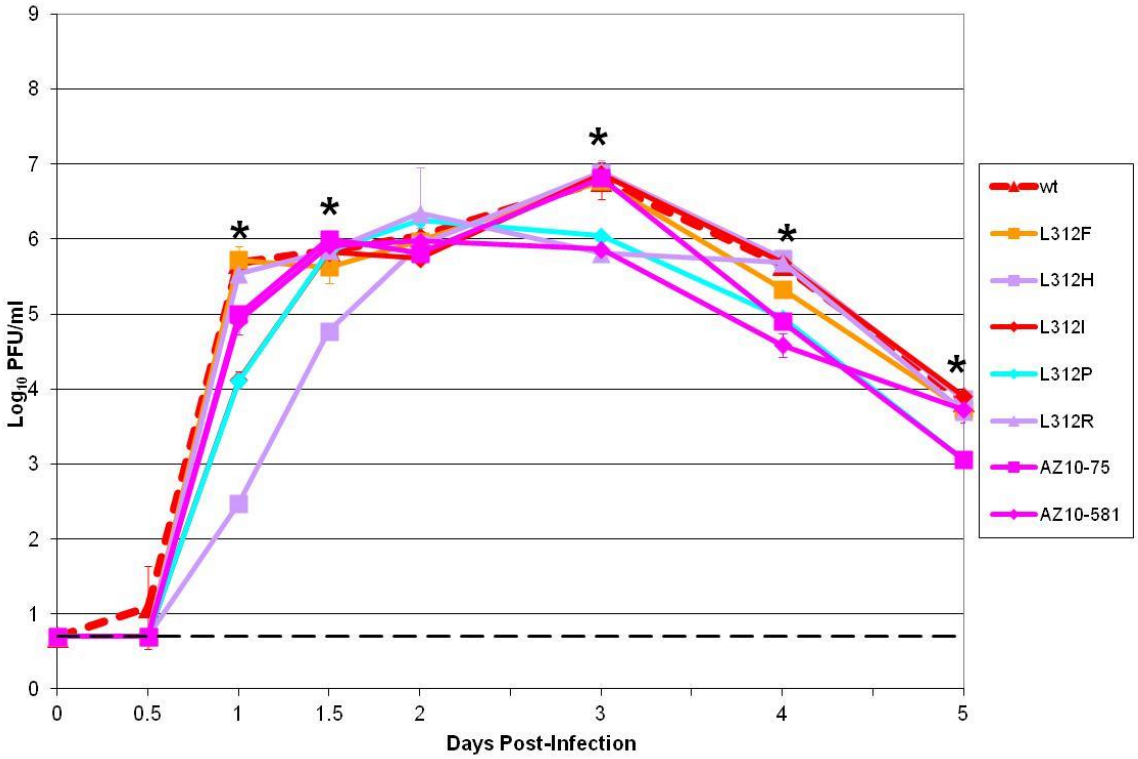

Figure 9: Replication of WNV L312 Mutants and Naturally Occurring Variants in Vero Cells

Growth kinetics of WNV wild-type and L312 mutants and naturally occurring variants in Vero cells. Dashed black line = limit of detection. Error bars = standard deviation. Dark blue = neutral polar. Red = hydrophobic aliphatic. Orange = hydrophobic aromatic. Purple = Basic. Light blue = unique. Pink = naturally occurring variant. * = statistically significant variation between strains using one-way ANOVA analysis with a significance threshold of 0.05.

	Days Post-Infection							
	0	**0.5**	**1**	**1.5**	**2**	**3**	**4**	**5**
ANOVA	N/A	0.493	0.000	0.000	0.318	0.000	0.000	0.000
WNV NY99ic Strain								
L312F	N/A	1.000	1.000	1.000	1.000	1.000	0.351	1.000
L312H	N/A	1.000	0.000	0.001	1.000	1.000	1.000	1.000
L312I	N/A	1.000	0.000	1.000	1.000	1.000	1.000	1.000
AZ10-75	N/A	1.000	0.011	1.000	1.000	1.000	0.002	0.002
AZ10-581	N/A	1.000	0.005	1.000	1.000	0.003	0.000	1.000
L312P	N/A	1.000	0.000	1.000	1.000	0.013	0.003	0.002
L312R	N/A	1.000	1.000	1.000	1.000	0.002	1.000	1.000

Table 7: Statistical Analysis of WNV L312 Mutant and Naturally Occurring Variant Replication in Vero Cells

Significance values obtained by one-way ANOVA with Bonferroni post-hoc analysis comparing each strain to the wild-type control. N/A = not applicable. Green = mutant is significantly higher than the wild-type control. Red = mutant is significantly lower than the wild-type control. White = mutant is not significantly different than the wild-type control. Threshold for significance = 0.05.

All of the WVN NY99ic L312 mutants and naturally occurring AZ10 variants were also able to replicate in DEF cells (Figure 10). When N99ic wild-type was at its peak at 3 days post-infection all L312 mutants and naturally occurring AZ10 variants were within 0.6 $\log_{10}$ pfu/ml of the wild-type titer except for AZ10-581, which was1.1 $\log_{10}$ pfu/ml below the wild-type. Other than AZ10-581 at the peak, only two strains differed from NY99ic wild-type by at least 1.0 $\log_{10}$ pfu/ml at any measured timepoint: L312P was 1.5 $\log_{10}$ pfu/ml below NY99ic wild-type at 1 day post-infection and L312R was 1.0 $\log_{10}$ pfu/ml above NY99ic wild-type at 5 days post-infection.

When statistical analysis was performed, however, there were several other strain/timepoint combinations that differed significantly from NY99ic wild-type and there was statistically significant variation between strains at all timepoints with measurable titers (Table 8). At 1 day post-infection, the earliest timepoint with measurable titers, every strain except for L312F is significantly lower than the NY99ic wild-type titer. By day 1.5 post-infection, however, all of the strains have recovered to wild-type-level titers. The L312P mutant is also statistically lower than NY99ic wild-type at 2 and 4 days post infection, and the AZ10-581 strain is statistically lower than NY99ic wild-type at 3 and 4 days post-infection. By 5 days post-infection only L312H

and L312R are statistically higher than NY99ic wild-type, and they are both at higher titers than NY99ic wild-type.

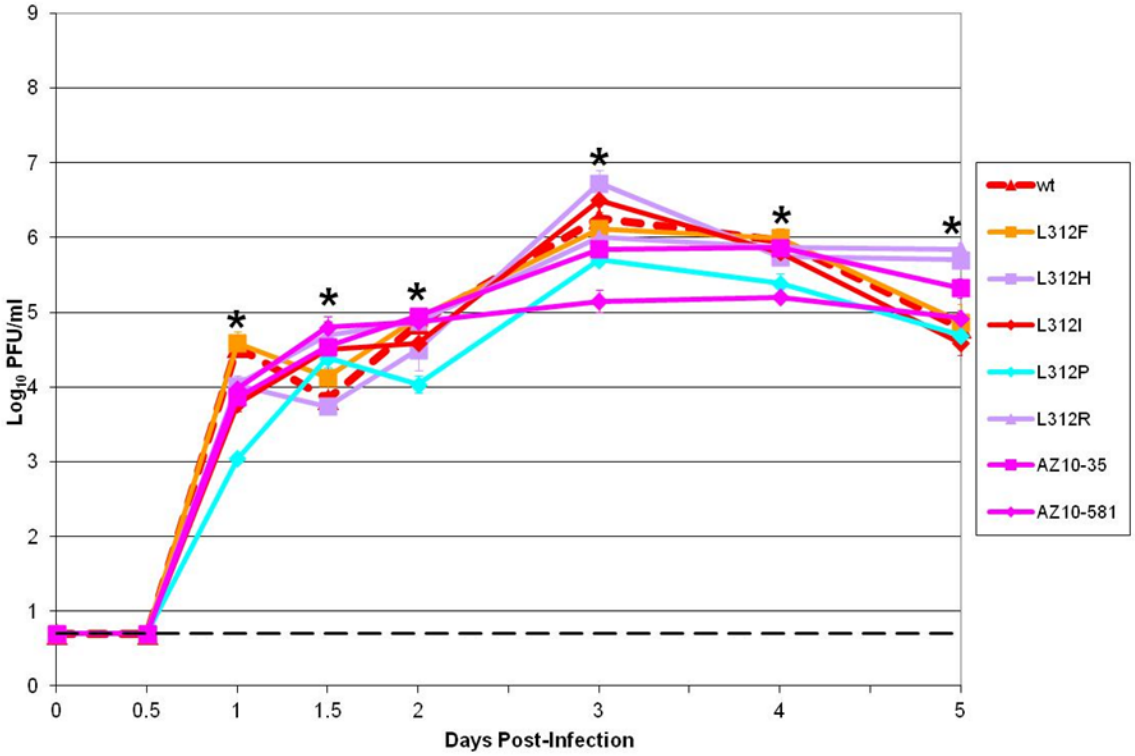

Figure 10: Replication of WNV L312 Mutants and Naturally Occurring Variants in DEF Cells

Growth kinetics of WNV wild-type and L312 mutants and naturally occurring variants in DEF cells. Dashed black line = limit of detection. Error bars = standard deviation. Dark blue = neutral polar. Red = hydrophobic aliphatic. Orange = hydrophobic aromatic. Purple = Basic. Light blue = unique. Pink = naturally occurring variant. * = statistically significant variation between strains using one-way ANOVA analysis with a significance threshold of 0.05.

	Days Post-Infection							
	0	**0.5**	**1**	**1.5**	**2**	**3**	**4**	**5**
ANOVA	N/A	N/A	0.000	0.021	0.001	0.000	0.000	0.000
WNV NY99ic Strain								
L312F	N/A	N/A	1.000	1.000	1.000	1.000	1.000	1.000
L312H	N/A	N/A	0.016	1.000	0.774	0.512	1.000	0.005
L312I	N/A	N/A	0.001	0.842	1.000	1.000	1.000	1.000
AZ10-75	N/A	N/A	0.003	0.658	1.000	0.873	1.000	0.155
AZ10-581	N/A	N/A	0.009	0.141	1.000	0.003	0.002	1.000
L312P	N/A	N/A	0.000	1.000	0.007	0.230	0.013	1.000
L312R	N/A	N/A	0.019	0.266	1.000	1.000	1.000	0.002

Table 8: Statistical Analysis of WNV L312 Mutant and Naturally Occurring Variant Replication in DEF Cells

Significance values obtained by one-way ANOVA with Bonferroni post-hoc analysis comparing each strain to the wild-type control. N/A = not applicable. Green = mutant is significantly higher than the wild-type control. Red = mutant is significantly lower than the wild-type control. White = mutant is not significantly different than the wild-type control. Threshold for significance = 0.05.

All NY99ic L312 mutants and naturally occurring AZ10 variants were also able to replicate in C6/36 cells (Figure 11). At 5 days post-infection, all of the L312 mutants on the NY99ic backbone were within 0.6 $\log_{10}$ pfu/ml, and the two naturally occurring variants (AZ10-75 and AZ10-581) were 0.9 $\log_{10}$ pfu/ml below the wild-type titer. The two naturally occurring variants were also the only two strains to differ from NY99ic wild-type by at least 1.0 $\log_{10}$ pfu/ml at any measured timepoint. AZ10-75 was 1.1 $\log_{10}$ pfu/ml below NY99ic wild-type at 1.5 days post infection and is 1.8 $\log_{10}$ pfu/ml below NY99ic wild-type at 4 days post-infection. AZ10-581 was 1.4 $\log_{10}$ pfu/ml below NY99ic wild-type at 1.5 days post-infection, 1.0 $\log_{10}$ pfu/ml below NY99ic wild-type at 3 days post-infection, and 1.8 $\log_{10}$ pfu/ml below NY99ic wild-type at 4 days post-infection.

There was statistically significant variation between the strains at all timepoints measured between 1.5 and 5 days post-infection (Table 9). AZ10-581 was the only strain to differ significantly from NY99ic wild-type at 1.5 days post-infection, and no strains differed significantly from NY99ic wild-type at 2 days post infection. The later timepoints (days 3-5 post-infection), however, had more widespread significant variation from NY99ic wild-type. L312H and L312R differed from NY99ic wild-type at only a

one timepoint each (4 and 5 days post-infection, respectively). L312I and L312P both differed significantly from NY99ic wild-type at two timepoints (days 3-4 and 4-5 post-infection, respectively). Finally, the two naturally occurring variants from Arizona, AZ10-75 and AZ10-581, differed significantly from NY99ic wild-type at 3, 4, and 5 days post-infection. All strains that differed significantly from NY99ic wild-type were significantly lower than NY99ic wild-type at the relevant timepoint.

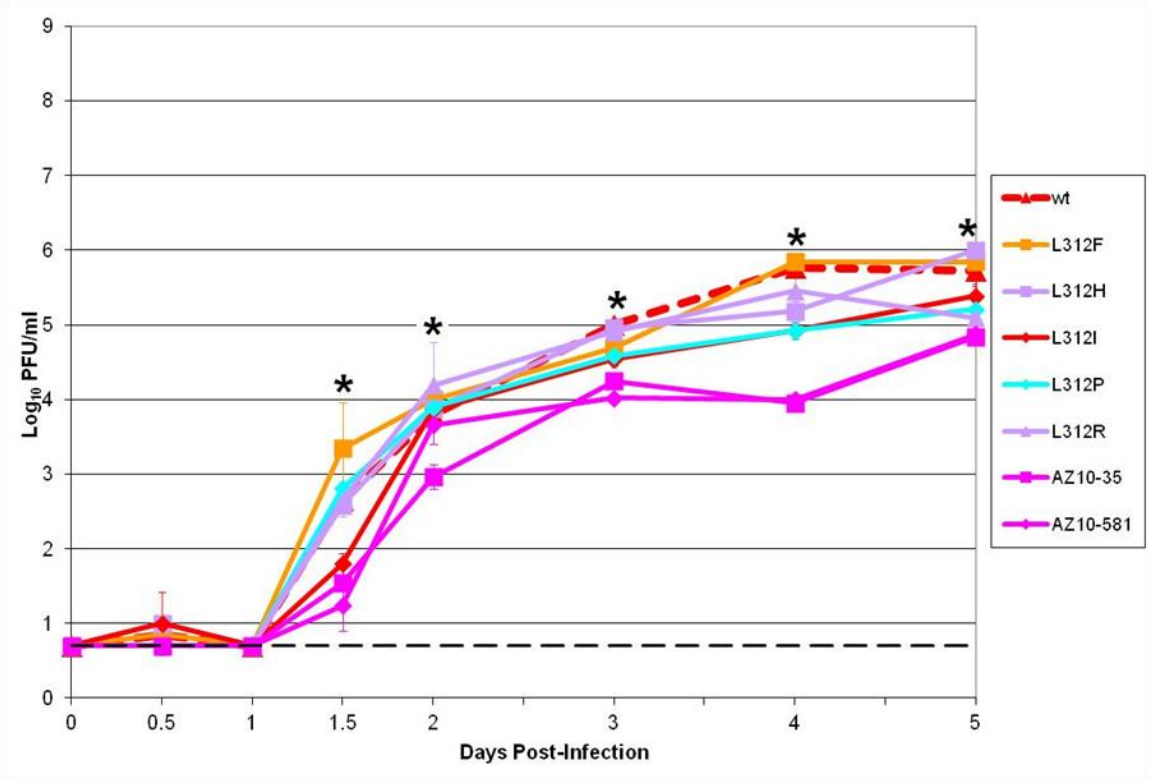

Figure 11: Replication of WNV L312 Mutants and Naturally Occurring Variants in C6/36 Cells

Growth kinetics of WNV wild-type and L312 mutants and naturally occurring variants in C6/36 cells. Dashed black line = limit of detection. Error bars = standard deviation. Dark blue = neutral polar. Red = hydrophobic aliphatic. Orange = hydrophobic aromatic. Purple = Basic. Light blue = unique. Pink = naturally occurring variant. * = statistically significant variation between strains using one-way ANOVA analysis with a significance threshold of 0.05.

	Days Post-Infection							
	0	0.5	1	1.5	2	3	4	5
ANOVA	N/A	0.469	N/A	0.001	0.027	0.000	0.000	0.000
WNV NY99ic Strain								
L312F	N/A	1.000	N/A	0.894	1.000	0.385	1.000	1.000
L312H	N/A	1.000	N/A	1.000	1.000	1.000	0.028	0.840
L312I	N/A	1.000	N/A	0.356	1.000	0.036	0.003	0.349
AZ10-75	N/A	1.000	N/A	0.087	0.253	0.001	0.000	0.001
AZ10-581	N/A	1.000	N/A	0.020	1.000	0.000	0.000	0.001
L312P	N/A	1.000	N/A	1.000	1.000	0.072	0.003	0.030
L312R	N/A	1.000	N/A	1.000	1.000	1.000	0.691	0.009

Table 9: Statistical Analysis of WNV L312 Mutant and Naturally Occurring Variant Replication in C6/36 Cells

Significance values obtained by one-way ANOVA with Bonferroni post-hoc analysis comparing each strain to the wild-type control. N/A = not applicable. Green = mutant is significantly higher than the wild-type control. Red = mutant is significantly lower than the wild-type control. White = mutant is not significantly different than the wild-type control. Threshold for significance = 0.05.

Mouse Virulence

Variation at residue L312 generally had no significant impact on mouse virulence, with LD_{50} values ranging from 0.3-2.0 pfu (Table 10). The exception was the L312P mutant, was highly attenuated in mice, resulting in 100% survival at the 100 pfu screening dose and having a LD_{50} value above 250 pfu. There was no statistically significant variation in the AST.

WNV Strain	LD_{50} (pfu)	AST±SD (days)
NY99ic Wild-type	0.3	8.4±1.1
NY99ic L312F	1.3	10.8±2.5
NY99ic L312H	0.8	8.8±1.8
NY99ic L312I	1.3	8.6±1.5
AZ10-75 (312I)	0.5	7.8±1.3
AZ10-581 (312I)	0.8	9.4±2.1
NY99ic L312P	>250	N/A
NY99ic L312R	2.0	8.0±2.0

Table 10: Virulence of WNV L312 Mutants and Naturally Occurring Variants in a Swiss Webster Mouse Model

Survival data for WNV wild-type and L312 mutants and naturally occurring variants in 3-4-week-old Swiss Webster mice. AST includes data for the 100pfu cohort.* = p-value <0.05compared to wild type values using the Kaplan Meier log rank test (% Survival column) or the Bonferroni post-hoc test following one-way ANOVA (AST±SD column).

DISCUSSION

In general, mutations of residue L312 seemed to have very little impact on the antigenicity or function of WNV EIII. Only AZ10-75 grouped apart from the NY99ic wild-type cluster regarding strength of antibody-mediated neutralization. The reason for the different neutralization of AZ10-75 compared to the L312 mutants and AZ10-581 is unknown; although AZ10-75 has no additional mutations in E at the consensus level, it is possible that there are subpopulations within AZ10-75 that are responsible for escape from neutralization. Previous studies of antibody-mediated neutralization using strains with variable amino acids at residue 312 had also hinted that L312 is unlikely to have a strong antigenic role.(139) This is consistent the residue's location away from the cluster of surface loop residues in the N-terminal, BC, and DE loops that have previously been identified as antigenic determinants and have had at least some impact on viability and fitness.(63, 65, 137-140, 142-144, 189) All attempted amino acid substitutions at residue 312 were tolerated, but they did have some statistically significant impacts on *in vitro* replication. Changes at 312 tended to cause decreased titers at early and late timepoints in Vero cells, at early timepoints in DEF cells, and at late timepoints in C6/36 cells. These differences in cell culture did not, however, translate to differences in mouse virulence (except in the case of L312P, which significantly lower than NY99ic wild-type at 4 of 8 timepoints in Vero cells, 3 of 8 timepoints in DEF cells, and 2 of 8 timepoints in C6/36 cells, and was highly attenuated in mice). Although these experiments did not demonstrate a clear role for L312 in either antigenicity or function, selection analysis has suggested that L312 may be under positive selective pressure.(192) It is possible that L312 plays some role that was not detected in cell culture or a mouse model but might be identifiable though *in vivo* studies of the avian or mosquito hosts that more closely mimic the natural transmission cycle of WNV. Of these two possibilities (bird and mosquito), the *in vitro* replication data suggests that the mosquito might be more likely to

demonstrate a difference *in vivo*; the main source of variation in DEF cells was early in the timecourse when technical issues such as the exact amount of virus input is likely to have more influence, whereas the main source of variation in C6/36 was later in the timecourse when the titers were at their highest measured points. However, the Arizona strains tested were isolated from mosquitoes, so perhaps the *in vitro* late-timepoint lag was a function of C6/36 cells being derived from *Aedes albopictus* as opposed to the *Culex* spp. primarily responsible for WNV transmission.

Chapter 4: Impact of Variation at Residue T332

RATIONALE AND APPROACH

Residue T332 is a known major antigenic determinant for WNV, with three possible mutations (T332A, T332K, and T332M) already documented in the literature. A study similar to this one used a single virus pool containing all possible T332 mutants to demonstrate that many substitutions (15 of 19) result in some degree of resistance to antibody-mediated neutralization, but that that resistant pool can be quickly purified to only one or two mutants that are both extremely resistant to neutralization and viable (in this case it was T332K and T332R mutants resisting neutralization by E16).(212) Mutants at residue T332 have been selected both *in vitro* and *in vivo* for resistance to neutralization by the monoclonal antibodies E16 and 5H10.(138, 144) In addition, it has been shown *in vitro* that naturally occurring lineage 1 and lineage 2 T332 variants are resistant to neutralization by polyclonal serum raised against recombinant WNV EIII protein (although neutralization by polyclonal serum raised against whole virus is retained).(139) There are several naturally occurring strains that have amino acids other than threonine at residue T332. None of the engineered, selected, or naturally occurring WNV T332 variants result in major changes in mouse virulence or growth in Vero cells.(138, 140) For these reasons, the full range of tolerated T332 mutants and their impact on antigenicity, growth, and virulence was assessed.

To accomplish this, pools of mutant NY99ic virus covering all possible substitutions were generated. Individual mutants were purified either from these pools of mutant NY99ic virus or from individual electroporations using individual mutant plasmids. Antigenicity of successfully recovered mutants was assessed by determining a neutralization index for the monoclonal antibodies 5H10 and 7H2 and for polyclonal serum raised against WNV EIII. Western blots with infected cell lysates were run to

determine whether any observed loss in neutralization was necessarily associated with a complete or partial loss of binding. Replication kinetics were assessed in Vero, DEF, and C6/36 cells. These cell lines were selected to represent a mammalian, avian, and mosquito host. Samples were collected daily for five days, with half day timepoints collected at 0.5 and 1.5 days post-infection. The five day range was chosen because it covers the time of initial infection through the time at which a WNV-infected Vero monolayer dies. Half-day samples were collected early in the growth curve to reveal any changes in early replication efficiency which may have impacted fitness in a host or vector. Virulence was assessed using a lethal Swiss Webster mouse model as a proxy for the potential of WNV to cause neuroinvasive disease and death in infected humans. A subset of viruses underwent LD_{50} characterization in Swiss Webster mice. The mutants were selected to represent the full range of amino acid categories (acidic, aromatic, basic, etc.) and to represent any mutants with non-wild-type phenotypes discovered during the antigenicity and/or replication kinetics screening.

RESULTS

Mutant Recovery

All of the WNV T332 mutants were viable. A summary of how each mutant was obtained (individual electroporation vs. plaque purification) and which passage(s) were used for characterization experiments can be found in Table 11. Viruses obtained from individual electroporations were available as passage 0 and passage 1 stocks representing the original electroporation (passage 0) and a stock obtained by passaging the original electroporated virus one time in Vero cells (passage 1). Plaque purified viruses were available as passage three stocks because they were obtained from an electroporated pool (passage 0), titered in a 6-well plate on a Vero monolayer to allow for selection of individual plaques (passage 1), and those individual plaques were then grown in a T-25 of Vero cells and 2-3 aliquots were frozen in advance of identification by nucleotide

sequencing (passage 2). Once the identities of each plaque purified stock were known, individual stocks were selected to be amplified in a T-75 of Vero cells to make a large working stock (passage 3). Sequencing of the prM/E coding region revealed that both the T332P and T332W mutants had an additional S66R mutation. These mutants were both plaque purified from separate virus pools, and in each case the S66R mutation was present in the earliest possible sample for a plaque purified virus (passage 2). The closest distance between residue T332 and S66 is 55.1 angstrom, measuring between the T332 residue about a 3-fold axis of symmetry and a S66 residue about a neighboring 5-fold axis of symmetry (the distance between T332 and S66 within an E monomer is 83.3 angstrom). Both residues T332 and S66 are surface exposed to at least some extent (Figure 12). To assess the impact of the S66R mutation and its potential role as an adaptive mutation, individual T332P, T332W, and S66R mutants were recovered from individual electroporations. The single and double 332/66 mutants were evaluated in Vero cells and in mice.

WNV NY99ic Mutant	Source	Passage(s) Used
T332A	Electroporation	0, 1
T332C	Electroporation	0, 1
T332D	Electroporation	0, 1
T332E	Plaque Purification	3
T332F	Electroporation	0, 1
T332G	Electroporation	0, 1
T332H	Plaque Purification	3
T332I	Plaque Purification	3
T332K	Electroporation	0, 1
T332L	Plaque Purification	3
T332M	Electroporation	0, 1
T332N	Plaque Purification	3
T332P	Electroporation	0
T332P+S66R	Plaque Purification	3
T332Q	Plaque Purification	3
T332R	Plaque Purification	3
T332S	Plaque Purification	3
T332V	Electroporation	0, 1
T332W	Electroporation	0
T332W+S66R	Plaque Purification	3
T332Y	Electroporation	0, 1
S66R	Electroporation	0

Table 11: Generation of WNV T332 Mutant Stocks

Summary of how each WNV T332 mutant stock was obtained.

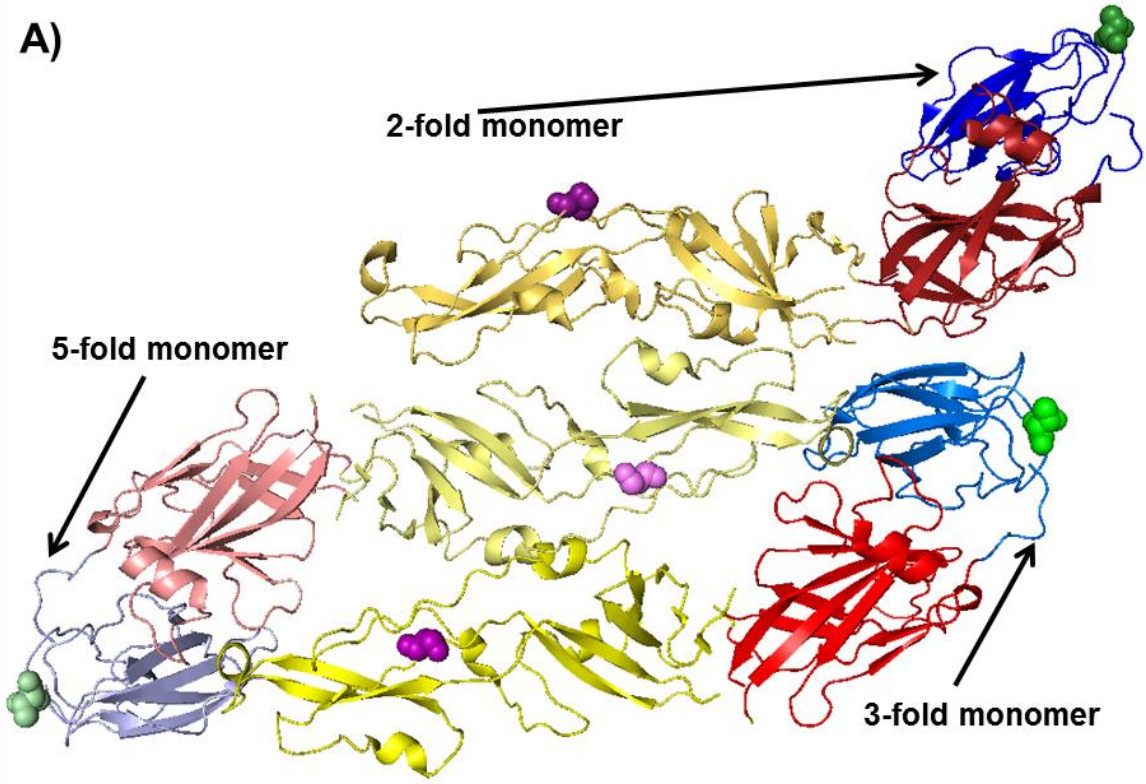
A)
2-fold monomer
5-fold monomer
3-fold monomer

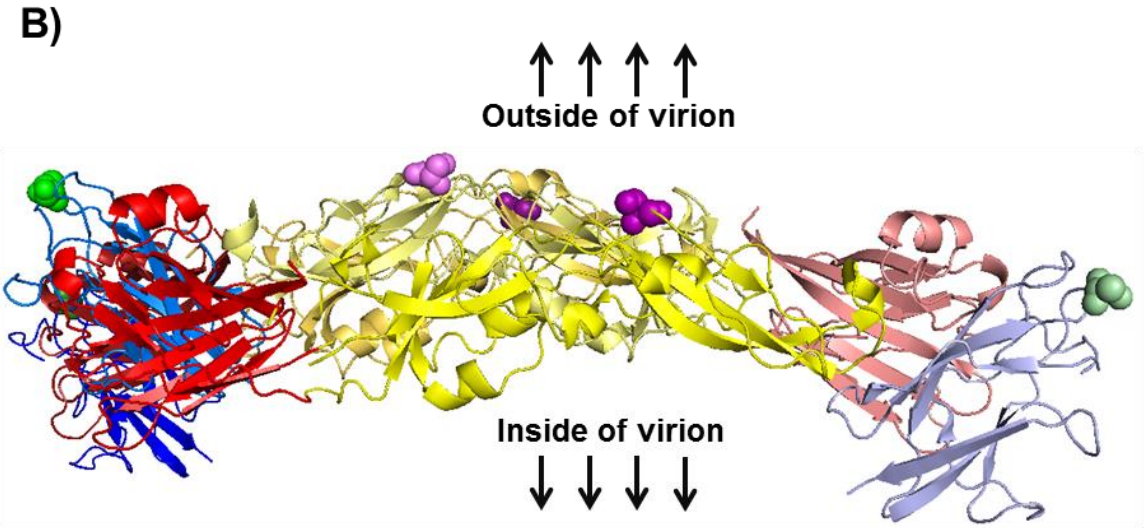
B)
Outside of virion
Inside of virion

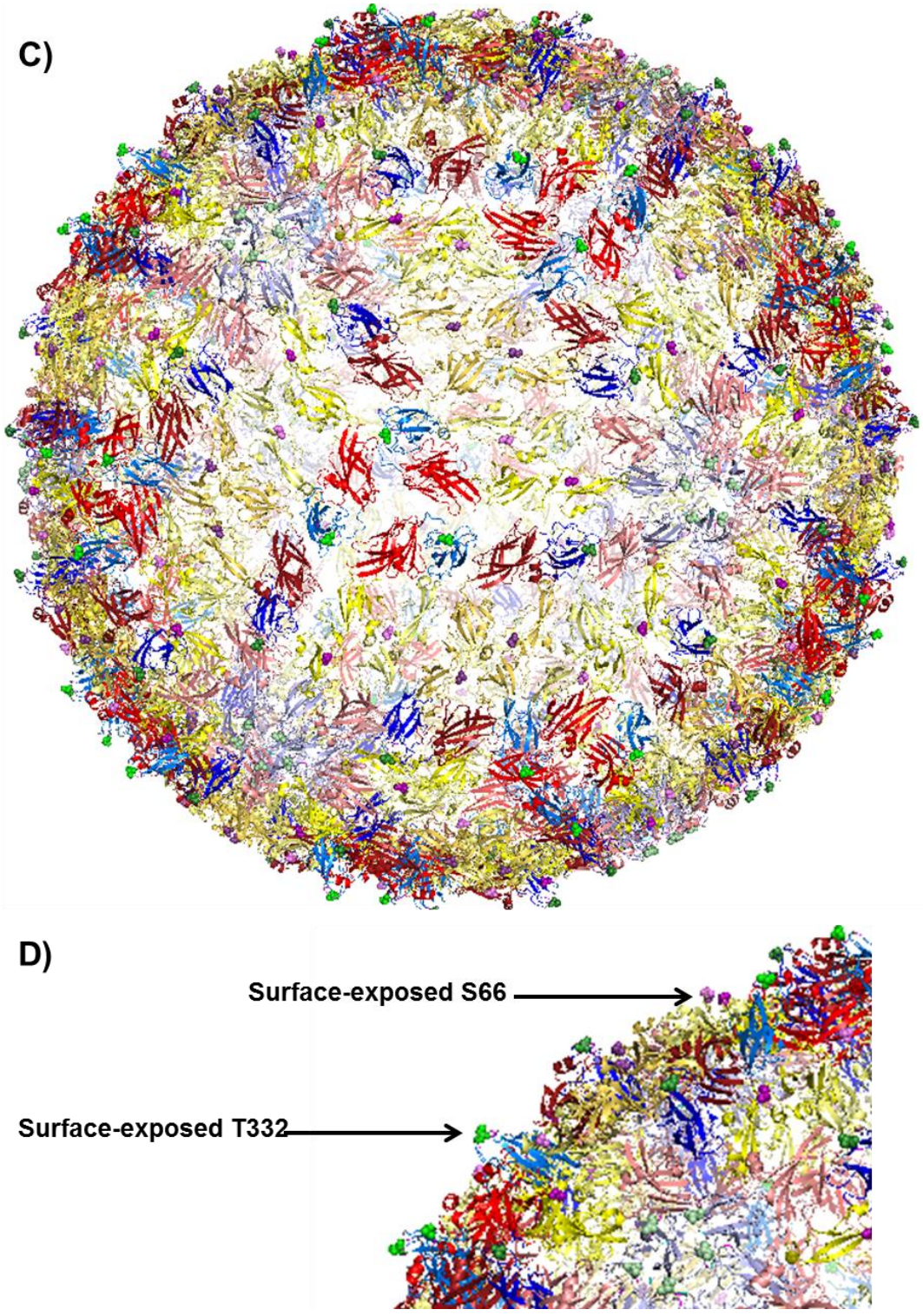

Figure 12: Location of Residues T332 and S66

(A) Top view and (B) side view of E trimers. (C) Whole virus and (D) enlarged section of whole virus. Monomers shaded such that light = 5-fold axis of symmetry, bright = 3-fold axis of symmetry, and dark = 2-fold axis of symmetry. Red = EI, yellow = EII, blue = EIII, green = T332, and purple = S66. Images generated using the PyMol Graphics System, Version 1.3, Schrödinger, LLC with PDB ID 3IYW.

Antigenicity

The vast majority of substitutions at residue T332 had moderate or severe impacts on antibody neutralization (Table 12). None of the 19 possible substitutions retained strong neutralization by either 5H10 or 7H2. Even the polyclonal anti-WNV EIII serum was only able to strongly neutralize three of the 19 possible substitutions (T332A, T332P+S66R, and T332S). The non-conservative acidic, basic, and aromatic substitutions were not strongly neutralized by any of the monoclonal or polyclonal antibodies tested. Only two of the 19 possible substitutions, T332A and T332P+S66R, retained moderate neutralization by the monoclonal antibodies and strong neutralization by the polyclonal antibody.

	Antibody		
WNV NY99ic Strain	**5H10**	**7H2**	**Anti-EIII Serum**
Wild-type	2.5±0.0	3.3±0.3	2.6±0.2
T332A	1.4±0.1*	1.5±0.0*	2.4±0.1
T332C	0.9±0.0*	0.1±0.1*	0.9±0.0*
T332D	0.1±0.1*	0.1±0.2*	0.7±0.0*
T332E	0.1±0.1*	0.1±0.0*	0.8±0.1*
T332F	0.3±0.1*	0.7±0.0*	0.6±0.2*
T332G	1.3±0.1*	1.0±0.1*	1.8±0.1*
T332H	0.2±0.0*	0.1±0.0*	0.1±0.0*
T332I	0.8±0.1*	1.0±0.1*	0.8±0.3*
T332K	0.2±0.4*	0.1±0.2*	0.5±0.2*
T332L	0.5±0.1*	1.5±0.0*	0.4±0.1*
T332M	1.0±0.0*	1.7±0.0*	1.0±0.1*
T332N	0.9±0.3*	1.2±0.1*	0.9±0.0*
T332P+S66R	0.7±0.0*	1.1±0.1*	3.1±0.0
T332Q	0.6±0.1*	0.6±0.0*	0.6±0.0*
T332R	0.7±0.0*	0.1±0.2*	0.8±0.2*
T332S	2.2±0.0	1.9±0.1*	3.0±0.1
T332V	1.0±0.1*	1.8±0.2*	1.6±0.1*
T332W+S66R	-0.1±0.1*	0.3±0.0*	0.3±0.2*
T332Y	0.0±0.1*	0.3±0.1*	0.3±0.1*

Table 12: Neutralization Indices of WNV T332 Mutants

Neutralization indices of WNV NY99ic wild-type and T332 mutants by the 5H10 and 7H2 monoclonal antibodies and by rabbit anti-EIII polyclonal serum. Values given as Avg±SD. Green = strongly neutralized, yellow = moderately neutralized, and red = weakly neutralized. * indicates statistically significant difference ($p<0.05$) from wild-type using the Bonferroni post-hoc test following one-way ANOVA.

Western blotting demonstrated that most mutations of residue T332 affected the strength of monoclonal but not polyclonal antibody binding (Figure 13). 5H10 strongly bound the T332A, T332E, T332G, T332L, T332M, T332S, and T332V mutants. These strongly 5H10-bound mutants had neutralization indices of at least 1.0 except for T332E and T332L, which had neutralization indices of 0.1 and 0.5, respectively (Table 13). 7H2 strongly bound T332A, T332E, T332I, T332L, T332S, and T332V. The strongly 7H2-bound mutants again generally had neutralization indices of at least 1.0, but there were a few more exceptions than was the case for 5H10. The T332M, T332N, and T332P+S66R mutants were weakly bound by 7H2 despite having neutralization indices of 1.7, 1.2, and 1.1, respectively. Conversely, the T332E mutant was again strongly bound despite having a neutralization index of 0.1. Binding by anti-WNV EIII serum was roughly equal for all mutants, despite differences in neutralization. This may be due to the antibody response to EIII recombinant protein generating a population of antibodies that bind epitopes exposed in this infected cell lysate but hidden in the context of an assembled virion. Coomassie staining and WNV MIAF controls were approximately even across all mutants as was expected.

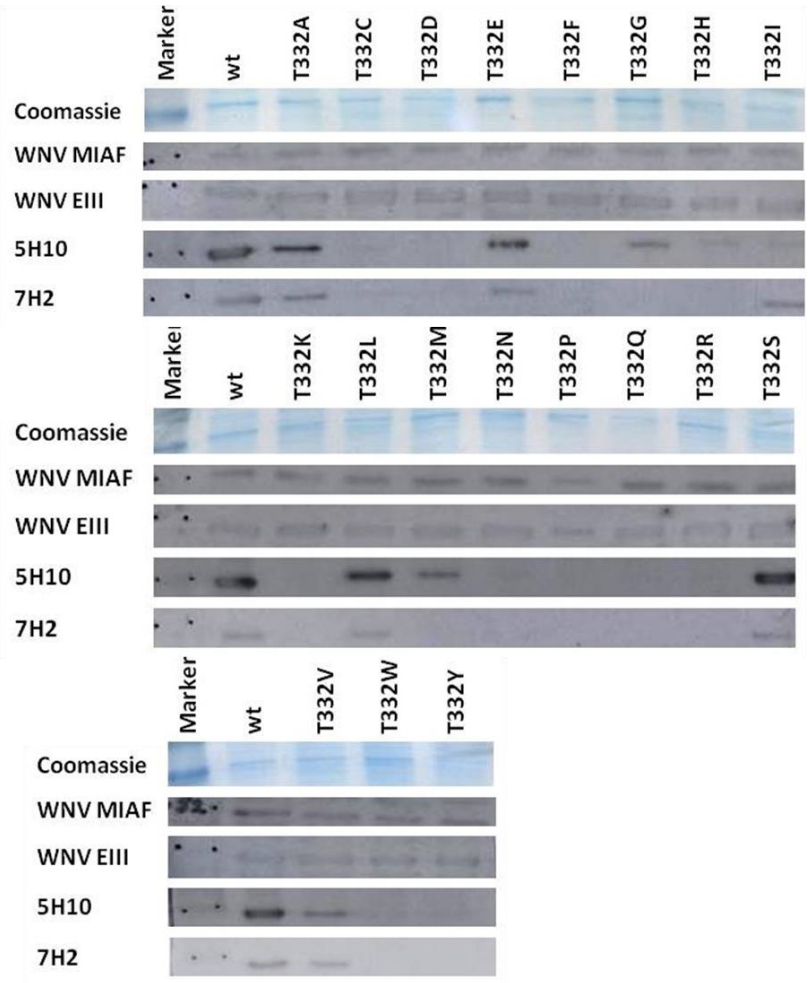

Figure 13: Binding of Monoclonal and Polyclonal Antibodies to WNV T332 Mutants

Western blot of WNV T332 mutant cell lysates. Images have been cropped to show only the ~50kDa region of the gels and films corresponding to the size of whole E. White lanes separate individual gels.

	5H10	
Strain	**Neut**	**Binding**
Wild-type	2.5±0.0	Strong
T332S	2.2±0.0	Strong
T332A	1.4±0.1*	Strong
T332G	1.3±0.1*	Strong
T332M	1.0±0.0*	Strong
T332V	1.0±0.1*	Strong
T332N	0.9±0.3*	Weak
T332C	0.9±0.0*	Weak
T332I	0.8±0.1*	Weak
T332R	0.7±0.0*	Weak
T332P	0.7±0.0*	Weak
T332Q	0.6±0.1*	Weak
T332L	0.5±0.1*	Strong
T332F	0.3±0.1*	Weak
T332H	0.2±0.0*	Weak
T332K	0.2±0.4*	Weak
T332D	0.1±0.1*	Weak
T332E	0.1±0.1*	Strong
T332W	-0.1±0.1*	Weak
T332Y	0.0±0.1*	Weak

	7H2	
Strain	**Neut**	**Binding**
Wild-type	3.3±0.3	Strong
T332S	1.9±0.1*	Strong
T332V	1.8±0.2*	Strong
T332M	1.7±0.0*	Weak
T332A	1.5±0.0*	Strong
T332L	1.5±0.0*	Strong
T332N	1.2±0.1*	Weak
T332P	1.1±0.1*	Weak
T332I	1.0±0.1*	Strong
T332G	1.0±0.1*	Weak
T332F	0.7±0.0*	Weak
T332Q	0.6±0.0*	Weak
T332W	0.3±0.0*	Weak
T332Y	0.3±0.1*	Weak
T332K	0.1±0.2*	Weak
T332E	0.1±0.0*	Strong
T332H	0.1±0.0*	Weak
T332C	0.1±0.1*	Weak
T332R	0.1±0.2*	Weak
T332D	0.1±0.2*	Weak

	α-EIII	
Strain	**Neut**	**Binding**
T332P	3.1±0.0	Strong
T332S	3.0±0.1	Strong
Wild-type	2.6±0.2	Strong
T332A	2.4±0.1	Strong
T332G	1.8±0.1*	Strong
T332V	1.6±0.1*	Strong
T332M	1.0±0.1*	Strong
T332N	0.9±0.0*	Strong
T332C	0.9±0.0*	Strong
T332I	0.8±0.3*	Strong
T332E	0.8±0.1*	Strong
T332R	0.8±0.2*	Strong
T332D	0.7±0.0*	Strong
T332F	0.6±0.2*	Strong
T332Q	0.6±0.0*	Strong
T332K	0.5±0.2*	Strong
T332L	0.4±0.1*	Strong
T332W	0.3±0.2*	Strong
T332Y	0.3±0.1*	Strong
T332H	0.1±0.0*	Strong

Table 13: Correlation Between Antibody Neutralization and Antibody Binding for WNV T332 Mutants

Summary of neutralization indices and binding strength for each virus:antibody combination using WNV T332 mutants. For each antibody, mutants are ordered with the most strongly neutralized at the top and the most weakly neutralized at the bottom. For neutralization indices, values given as Avg±SD. Green = strongly neutralized, yellow = moderately neutralized, and red = weakly neutralized. * indicates statistically significant difference ($p<0.05$) from wild-type using the Bonferroni post-hoc test following one-way ANOVA. Binding strengths were qualitatively described, see figure 13 for images.

In vitro Replication Kinetics

All WNV T332 mutants replicated in Vero cells (Figure14). Twelve of the 19 NY99ic mutants differed from NY99ic wild-type by at least 1.0log10 pfu/ml at at least one timepoint, with the majority of that variation occurring before 2 days post-infection. Mutants T332I, T332Q, T332S, and T332V differed from NY99ic wild-type at only one timepoint between 0 and 1 days post-infection, and their titers were only higher than NY99ic wild-type by 1.0-1.1$\log_{10}$ pfu/ml. Mutants T332E, T332L, T332N, and T332R reached titers higher than those of NY99ic wild-type at both 1 and 1.5 days post-infection; these mutants were within 1.1-1.4$\log_{10}$ pfu/ml of NY99ic wild-type, except for T332L, which was 2.0-2.1$\log_{10}$ pfu/ml different than NY99ic wild-type. Similarly, T332H was 1.1$\log_{10}$ pfu/ml higher than NY99ic wild-type at 0.5 days post-infection and 1.6$\log_{10}$ pfu/ml higher than wild-type at 1.5 days post-infection. Only three strains were below NY99ic wild-type by at least 1.0$\log_{10}$ pfu/ml at any timepoint: T332P+S66R, T332W+S66R, and T332Y. T332P+S66R was 1.7$\log_{10}$ pfu/ml below NY99ic wild-type at both 3 and 4 days post-infection. Interestingly, both T332W+S66R were higher than NY99ic wild-type early in the timecourse and lower than NY99ic wild-type late in the timecourse. T332Y was 1.1$\log_{10}$ pfu/ml above NY99ic wild-type at 1.5 days post-infection, but it was 1.0-1.4$\log_{10}$ pfu/ml below NY99ic wild-type at 4 and 5 days post-infection. T332W+S66R was 1.1$\log_{10}$ pfu/ml above NY99ic wild-type at 0 days post-infection and was 1.1-1.6$\log_{10}$ pfu/ml above NY99ic wild-type at 1, 1.5, and 2 days post-infection. By days 4 and 5 post-infection, though, T332W+S66R was 1.4-1.9$\log_{10}$ pfu/ml below NY99ic wild-type.

According to the results of the one-way ANOVA, there was statistically significant variation between the strains at all timepoints except for 0 days post-infection (Table 14). In general, mutants that differed from NY99ic wild-type by at least 1.0log10 pfu/ml were also statistically different than NY99ic wild-type at that timepoint according

to Bonferroni post-hoc analysis. Exceptions include T332V at 0 days post-infection, T332E,T332I, and T332S at 1 day post-infection, T332W+S66R at days 0 and 2 post-infection, and T332Y at 4 days post-infection, which all differed from NY99ic wild-type by 1.0-1.1$\log_{10}$ pfu/ml but were not statistically different. T332N at 1 day post-infection was on the border of significant (p=0.050) and was 1.2$\log_{10}$ pfu/ml higher than NY99ic wild-type. There were also two instances of mutant titers being classified as statistically different from NY99ic wild-type despite differing by less than 1.0$\log_{10}$ pfu/ml: T332H, which was 0.5$\log_{10}$ pfu/ml higher than NY99ic wild-type at 5 days post-infection, and T332P+S66R, which was 0.7$\log_{10}$ pfu/ml lower than NY99ic wild-type at 5 days post-infection.

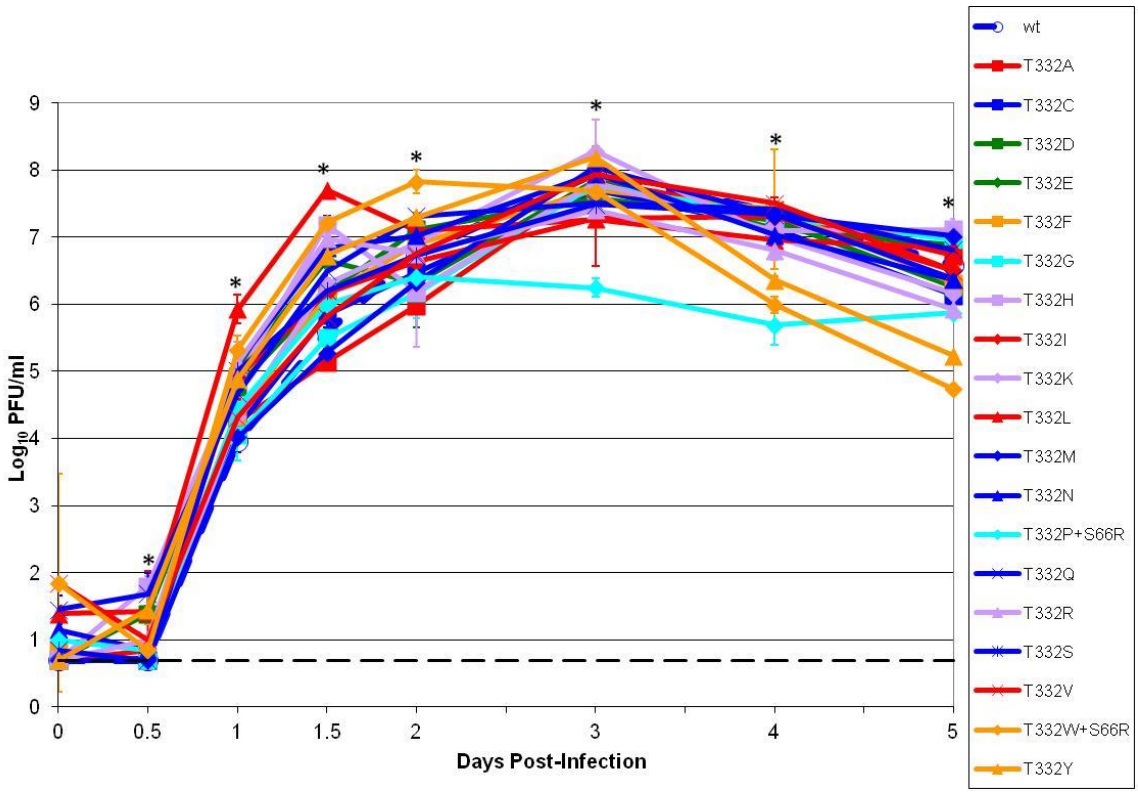

Figure14: Replication of WNV T332 Mutants in Vero Cells

Growth kinetics of WNV wild-type and T332 mutants in Vero cells. Dashed black line = limit of detection. Error bars = standard deviation. Dark blue = neutral polar. Red = hydrophobic aliphatic. Green = acidic. Orange = hydrophobic aromatic. Purple = Basic. Light blue = unique. * = statistically significant variation between strains using one-way ANOVA analysis with a significance threshold of 0.05.

	Days Post-Infection							
	0	**0.5**	**1**	**1.5**	**2**	**3**	**4**	**5**
ANOVA	0.442	0.000	0.000	0.000	0.001	0.000	0.000	0.000
WNV NY99ic Strain								
T332A	N/A	1.000	1.000	1.000	1.000	1.000	1.000	1.000
T332C	N/A	1.000	1.000	1.000	1.000	1.000	1.000	0.159
T332D	N/A	0.295	1.000	1.000	1.000	1.000	1.000	1.000
T332E	N/A	1.000	0.094	0.019	1.000	1.000	1.000	1.000
T332F	N/A	1.000	1.000	1.000	1.000	1.000	1.000	1.000
T332G	N/A	1.000	1.000	1.000	1.000	1.000	1.000	0.852
T332H	N/A	0.002	0.428	0.000	1.000	1.000	1.000	0.043
T332I	N/A	1.000	0.287	1.000	1.000	1.000	1.000	1.000
T332K	N/A	1.000	1.000	0.828	1.000	1.000	1.000	0.261
T332L	N/A	0.192	0.000	0.000	1.000	0.865	1.000	1.000
T332M	N/A	1.000	1.000	1.000	1.000	1.000	1.000	0.318
T332N	N/A	1.000	0.050	0.003	1.000	1.000	1.000	1.000
T332P+S66R	N/A	1.000	1.000	1.000	1.000	0.000	0.000	0.001
T332Q	N/A	0.007	1.000	0.105	1.000	1.000	1.000	1.000
T332R	N/A	1.000	0.044	0.001	1.000	1.000	1.000	0.003
T332S	N/A	1.000	0.141	1.000	1.000	1.000	1.000	1.000
T332V	N/A	1.000	1.000	1.000	1.000	1.000	1.000	1.000
T332W+S66R	N/A	1.000	0.008	0.000	0.339	1.000	0.004	0.000
T332Y	N/A	0.140	0.392	0.009	1.000	1.000	1.000	0.000

Table 14: Statistical Analysis of WNV T332 Mutant Replication Kinetics in Vero Cells

Significance values obtained by one-way ANOVA with Bonferroni post-hoc analysis comparing each strain to the wild-type control. N/A = not applicable. Green = mutant is significantly higher than the wild-type control. Red = mutant is significantly lower than the wild-type control. White = mutant is not significantly different than the wild-type control. Threshold for significance = 0.05.

To elucidate a possible compensating role of the S66R compensating mutation on WNV replication in Vero cells, the T332P, T332W, and S66R single and double mutants underwent an additional growth comparison experiment in Vero cells (Figure 15). The S66R mutation alone did not impact growth in any significant way. The T332W and T332W+S66R mutants replicated very similarly to each other and to wild-type, despite the early high and later low titers for T332W+S66R seen in the previous growth curve in Vero cells (Figure 14). It may be worth noting that the increased post-peak decline of T332Y and T332W+S66R seen in Figure 14 and the lack of increased decline of T332W+S66R seen in Figure 15 may be due to the physical handling of the infected plates during the timecourse. During the timecourse conducted for Figure 14, the plate containing the T332W+S66R and T332Y duplicates was on the bottom of the stack of infected plates. Such plate stacking was not necessary during the timecourse evaluating

the impact of S66R. Thus, it is possible that restricted gas circulation may have accelerated the onset of CPE between days 3 and 4 post-infection, thus causing the increased decline of T332W+S66R and T332Y titers seen in Figure 14.

The T332P and T332P+S66R mutants both replicated to lower titers compared to wild-type, with deficits of 1.3$\log_{10}$pfu/ml and 1.6$\log_{10}$pfu/ml, respectively. The results for T332P+S66R are comparable to those seen in the previous growth curve in Vero cells (Figure 14).

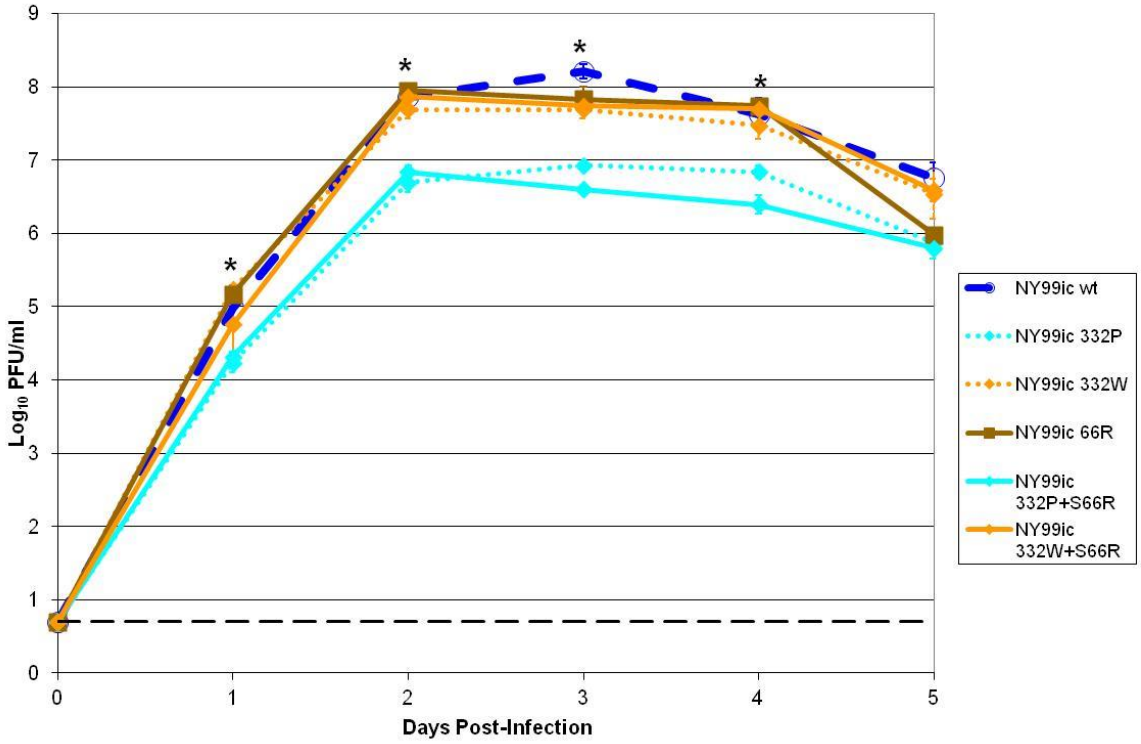

Figure15: Role of S66R Compensating Mutation in WNV Replication in Vero Cells

Growth kinetics of WNV wild-type, T332+S66 combined mutants, and T332 and S66 individual mutants in Vero cells. Dashed black line = limit of detection. Error bars = standard deviation. Dark blue = neutral polar. Orange = hydrophobic aromatic. Light blue = unique. Brown = S66R .

All of the WNV T332 mutants replicated in DEF cells, and there was generally very little deviation from NY99ic wild-type (Figure 16). In fact, only T332M differed from NY99ic wild-type by at least 1.0$\log_{10}$ pfu/ml at more than one timepoint (days 1 and 1.5 post-infection). At 1 day post-infection, T332I was 1.0$\log_{10}$ pfu/ml below NY99ic wild-type and T332M was 1.0$\log_{10}$ pfu/ml higher than NY99ic wild-type. At 1.5 days post-infection, when the highest number of mutants differed from NY99ic wild-type, T332F, T332K, T332M, T332R, and T332Y were 1.0-1.5$\log_{10}$ pfu/ml higher than NY99ic wild-type. Finally, at 4 days post-infection, T332G and T332V were 1.0$\log_{10}$ and 1.2$\log_{10}$ pfu/ml higher than NY99ic wild-type, respectively.

Unlike the WNV T332 mutant replication in Vero cells, there was statistically significant diversity at all timepoints measured (Table 15). All of the mutant/timepoint combinations that differed from NY99ic wild-type by at least 1.0$\log_{10}$ pfu/ml were also statistically different from NY99ic wild-type. There were also six mutant/timepoint combinations that were less than 1.0$\log_{10}$ pfu/ml higher than NY99ic wild-type but were statistically higher than NY99ic wild-type. T332F and T332K were 0.6$\log_{10}$ and 0.7$\log_{10}$ pfu/ml higher than NY99ic wild-type at 1 day post-infection, respectively. T332C and T332G were 0.8$\log_{10}$ pfu/ml and 0.9$\log_{10}$ pfu/ml higher than NY99ic wild-type at 1.5 days post-infection, respectively. Finally, at 2 days post infection T332D was 0.8$\log_{10}$ pfu/ml lower than and T332R was 0.9$\log_{10}$ pfu higher than NY99ic wild-type, respectively.

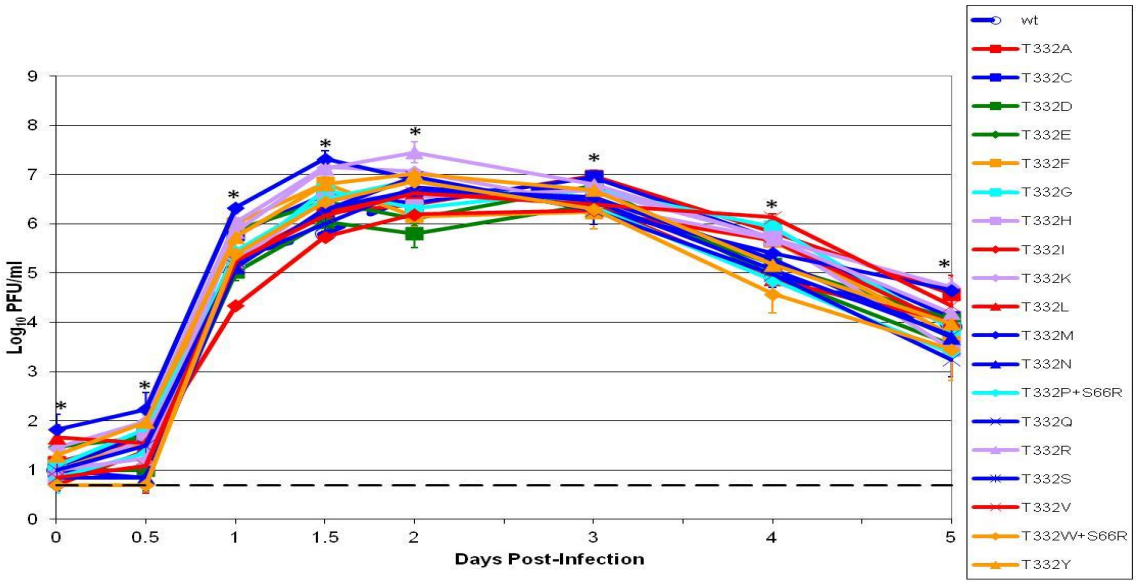

Figure 16: Replication of WNV T332 Mutants in DEF Cells

Growth kinetics of WNV wild-type and T332 mutants in DEF cells. Dashed black line = limit of detection. Error bars = standard deviation. Dark blue = neutral polar. Red = hydrophobic aliphatic. Green = acidic. Orange = hydrophobic aromatic. Purple = Basic. Light blue = unique. * = statistically significant variation between strains using one-way ANOVA analysis with a significance threshold of 0.05.

	Days Post-Infection							
	0	**0.5**	**1**	**1.5**	**2**	**3**	**4**	**5**
ANOVA	0.021	0.001	0.000	0.000	0.000	0.000	0.000	0.000
WNV NY99ic Strain								
T332A	1.000	1.000	1.000	1.000	1.000	1.000	0.100	1.000
T332C	1.000	1.000	1.000	0.027	1.000	1.000	0.453	1.000
T332D	1.000	1.000	1.000	1.000	0.019	1.000	1.000	1.000
T332E	1.000	1.000	0.270	0.185	1.000	1.000	1.000	1.000
T332F	1.000	1.000	0.025	0.000	1.000	0.264	0.597	1.000
T332G	1.000	1.000	1.000	0.006	1.000	1.000	0.026	1.000
T332H	1.000	1.000	1.000	0.091	1.000	1.000	0.307	1.000
T332I	1.000	1.000	0.000	1.000	1.000	0.525	0.597	1.000
T332K	1.000	1.000	0.021	0.000	1.000	1.000	0.453	0.310
T332L	1.000	1.000	1.000	1.000	1.000	1.000	1.000	1.000
T332M	1.000	1.000	0.000	0.000	1.000	0.738	1.000	0.682
T332N	1.000	1.000	1.000	1.000	1.000	1.000	1.000	1.000
T332P+S66R	1.000	1.000	1.000	0.091	1.000	1.000	1.000	1.000
T332Q	1.000	1.000	1.000	1.000	1.000	0.525	1.000	1.000
T332R	1.000	1.000	0.489	0.000	0.009	1.000	0.453	1.000
T332S	1.000	1.000	1.000	1.000	1.000	1.000	1.000	1.000
T332V	1.000	1.000	1.000	1.000	1.000	1.000	0.003	1.000
T332W+S66R	1.000	1.000	1.000	0.199	1.000	0.738	1.000	1.000
T332Y	1.000	1.000	1.000	0.001	1.000	1.000	1.000	1.000

Table 15: Statistical Analysis of WNV T332 Mutant Replication Kinetics in DEF Cells

Significance values obtained by one-way ANOVA with Bonferroni post-hoc analysis comparing each strain to the wild-type control. N/A = not applicable. Green = mutant is significantly higher than the wild-type control. Red = mutant is significantly lower than the wild-type control. White = mutant is not significantly different than the wild-type control. Threshold for significance = 0.05.

As with the Vero and DEF cells, all WNV T332 mutants are able replicate in C6/36 cells (Figure 17). Nine of 19 mutants differed from NY99ic wild-type by at least 1.0$\log_{10}$ pfu/ml at at least one timepoint. Six of those mutants differed by 1.0-1.1log10 pfu/ml lower than NY99ic wild-type at a single timepoint: T332P+S66R at 2 days post-infection, T332A, T332E, T332F, and T332I at 3 days post-infection, and T332N at 4 days post-infection. T332K was 1.0-1.3$\log_{10}$ pfu/ml lower than NY99ic wild-type at 1, 3, and 4 days post-infection. T332W+S66R was 1.1-1.6$\log_{10}$ pfu/ml lower than NY99ic wild-type at 1, 3, 4, and 5 days post infection. Finally, T332Y was 1.0-1.1$\log_{10}$ pfu/ml lower than NY99ic wild-type at days 3 and 5 post-infection.

There was statistically significant variation between strains at all measured timepoints between 1 and 5 days post-infection (Table 16). The strain/timepoint combinations that differed from NY99ic wild-type by at least 1.0$\log_{10}$ pfu/ml were all statistically significant except for T332W+S66R at 1 day post-infection, which was 1.1$\log_{10}$ pfu/ml lower than NY99ic wild-type but had a p-value of 0.139. There were also 19 strain/timepoint combinations that were statistically different than NY99ic wild-type despite being less than 1.0$\log_{10}$ pfu/ml different. T332C was 0.8$\log_{10}$ and 0.5$\log_{10}$ pfu/ml lower than NY99ic at days 3 and 5 post-infection, respectively. T332D was 0.4$\log_{10}$ pfu/ml higher than NY99ic wild-type, the only strain/timepoint combination to be significantly higher than NY99ic wild-type in C6/36 cells. T332F, in addition to the previously described differences at day 3 post-infection, was 0.9$\log_{10}$ and 0.5$\log_{10}$ pfu/ml lower than NY99ic wild-type at days 4 and 5 post-infection. T332I, in addition to its differences at day 3, was 0.5$\log_{10}$ pfu/ml lower than NY99ic wild-type at 5 days post-infection. T332K, in addition to its differences at 1, 3, and 4 days post-infection, was 0.9$\log_{10}$ and 0.7$\log_{10}$ pfu/ml lower than NY99ic wild-type at 2 and 5 days post-infection, respectively. T332N, in addition to its previously noted differences, is 0.9$\log_{10}$ and 0.4$\log_{10}$ pfu/ml lower than NY99ic wild-type at 3 and 5 days post-infection, respectively. T332P+S66R, in addition to being below NY99ic wild-type at 2 days post-infection, was

0.8$\log_{10}$ and 0.7$\log_{10}$ pfu/ml lower than NY99ic wild-type at 3 and 4 days post-infection, respectively. T332R, which did not differ from NY99ic wild-type by 1.0$\log_{10}$ or greater pfu/ml at any timepoint, was 0.8-0.9$\log_{10}$ pfu/ml lower than NY99ic wild-type at days 3-5 post-infection. Similarly, T332S, which also didn't differ from NY99ic wild-type by 1.0$\log_{10}$ pfu/ml or greater at any timepoint, was 0.9$\log_{10}$ and 0.4$\log_{10}$ pfu/ml lower than NY99ic wild-type at 3 and 5 days post-infection, respectively. T332W+S66R, which was previously mentioned as being lower than NY99ic wild-type at 1, 3, 4, and 5 days post-infection, was 0.9$\log_{10}$ pfu/ml lower than NY99ic wild-type at 1.5 days post-infection. Finally, T332Y, previously mentioned as differing from wild-type at 3 and 5 days post-infection, was 0.9$\log_{10}$ pfu/ml lower than NY99ic wild-type at 4 days post-infection.

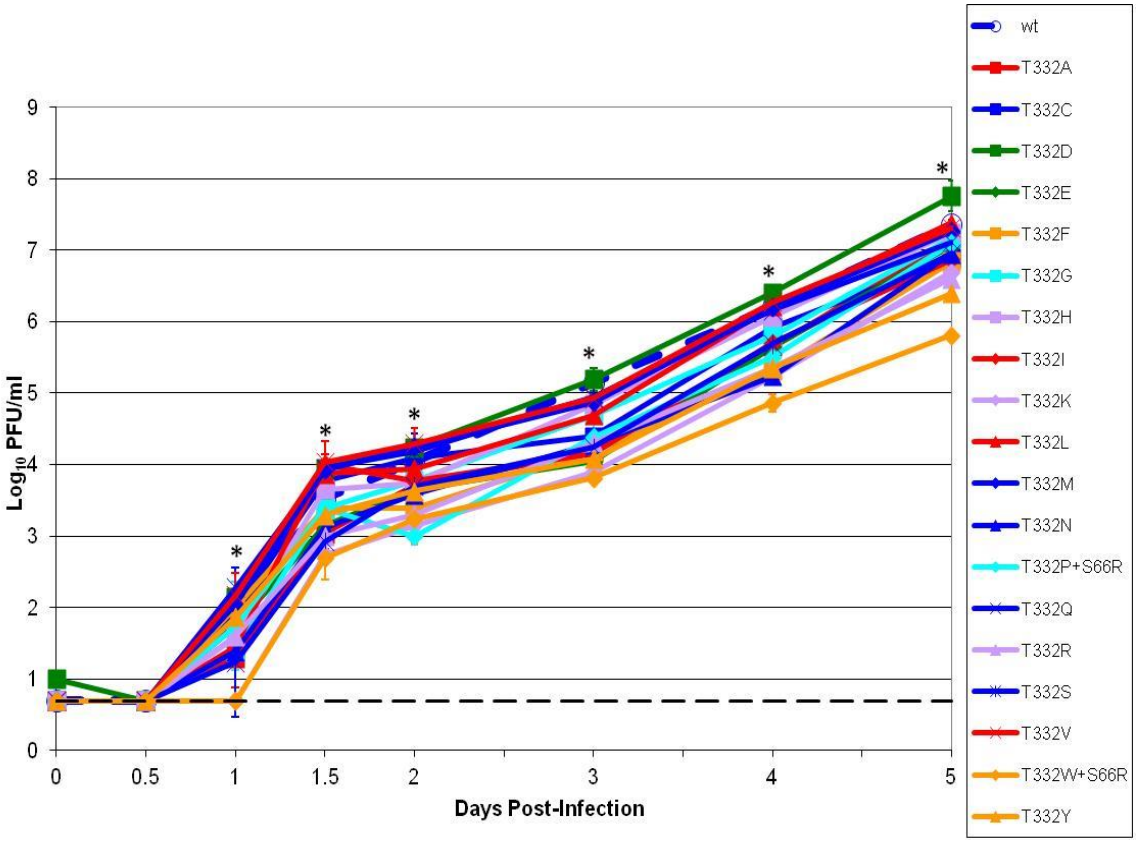

Figure 17: Replication of WNV T332 Mutants in C6/36 Cells

Growth kinetics of WNV wild-type and T332 mutants in C6/36 cells. Dashed black line = limit of detection. Error bars = standard deviation. Dark blue = neutral polar. Red = hydrophobic aliphatic. Green = acidic. Orange = hydrophobic aromatic. Purple = Basic. Light blue = unique. * = statistically significant variation between strains using one-way ANOVA analysis with a significance threshold of 0.05.

	Days Post-Infection							
	0	**0.5**	**1**	**1.5**	**2**	**3**	**4**	**5**
ANOVA	N/A	N/A	0.000	0.000	0.000	0.000	0.000	0.000
WNV NY99ic Strain								
T332A	N/A	N/A	1.000	1.000	1.000	0.000	0.097	1.000
T332C	N/A	N/A	1.000	1.000	1.000	0.000	1.000	0.001
T332D	N/A	N/A	1.000	1.000	1.000	1.000	1.000	0.007
T332E	N/A	N/A	1.000	1.000	1.000	0.000	0.097	0.118
T332F	N/A	N/A	1.000	1.000	0.394	0.000	0.000	0.000
T332G	N/A	N/A	1.000	1.000	1.000	0.141	1.000	1.000
T332H	N/A	N/A	1.000	1.000	1.000	1.000	1.000	1.000
T332I	N/A	N/A	1.000	1.000	1.000	0.000	0.256	0.000
T332K	N/A	N/A	0.139	0.008	0.019	0.000	0.000	0.000
T332L	N/A	N/A	1.000	1.000	1.000	0.141	1.000	1.000
T332M	N/A	N/A	1.000	1.000	1.000	1.000	1.000	1.000
T332N	N/A	N/A	1.000	1.000	1.000	0.000	0.000	0.004
T332P+S66R	N/A	N/A	1.000	1.000	0.003	0.000	0.008	0.356
T332Q	N/A	N/A	1.000	1.000	1.000	1.000	1.000	0.569
T332R	N/A	N/A	1.000	0.390	0.126	0.000	0.001	0.000
T332S	N/A	N/A	1.000	0.135	1.000	0.000	0.197	0.004
T332V	N/A	N/A	1.000	0.887	1.000	1.000	1.000	1.000
T332W+S66R	N/A	N/A	0.139	0.004	0.059	0.000	0.000	0.000
T332Y	N/A	N/A	1.000	1.000	1.000	0.000	0.001	0.000

Table 16: Statistical Analysis of WNV T332 Mutant Replication Kinetics in C6/36 Cells

Significance values obtained by one-way ANOVA with Bonferroni post-hoc analysis comparing each strain to the wild-type control. N/A = not applicable. Green = mutant is significantly higher than the wild-type control. Red = mutant is significantly lower than the wild-type control. White = mutant is not significantly different than the wild-type control. Threshold for significance = 0.05.

Mouse Virulence

In general, mutations at residue T332 did not strongly impact virulence in mice (Table 17). This was true regardless of whether the change was conservative or non-conservative. The only substitution that caused major attenuation was T332P and this was true whether the additional S66R mutation was present or absent. Of the mutants encoding conservative neutral polar substitutions, T332C came the closest to attenuation, with 40% survival compared to 7% survival for the wild-type. The mutants encoding hydrophobic aliphatic substitutions were also quite similar to wild-type, with the exception of T332I, which had a significantly higher % survival. The mutants encoding acidic, basic, and hydrophobic aromatic substitutions were all virulent in mice, although T332R had a slightly higher LD_{50} value of 12.6pfu compared to 0.5pfu for wild-type. Of

note, both the T332W and T332W+S66R mutants were virulent in mice as measured by LD_{50}, % survival, and AST. Both the T332P and the T332P+S66R mutants were highly attenuated in mice. The LD_{50} values of the T332P mutants were over 2,000-fold increased compared to wild-type, and over half of the mice survived the 100pfu dose. The AST values for T332P and T332P+S336, while not significantly different than wild-type, were 1.8-4.3 days longer.

WNV NY99ic Strain	LD_{50} (pfu)	Survival		AST±SD (days)
		%	Alive/Total	
Wild-type	0.5	7	1/15	8.7±2.3
S66R	0.1	0	0/10	9.7±1.9
T332A	ND	10	1/10	8.3±1.3
T332C	ND	40	4/10	8.7±1.9
T332D	0.8	0	0/10	8.2±1.2
T332E	ND	0	0/10	7.6±1.1
T332F	ND	0	0/10	8.0±1.5
T332G	ND	0	0/10	8.6±1.6
T332H	0.3	10	1/10	8.7±2.2
T332I	ND	30*	3/10	10.9±2.7
T332K	ND	0	0/10	8.5±1.0
T332L	ND	20	2/10	8.5±0.8
T332M	ND	20	2/10	8.8±2.1
T332N	ND	0	0/10	8.3±1.4
T332P	>1,000	70*	7/10	11.3±2.1
T332P + S66R	>1,000	87*	12/15	13.0±7.1
T332Q	ND	0	0/10	9.3±1.5
T332R	12.6	20	2/10	9.4±2.3
T332S	ND	10	1/10	7.4±1.0
T332V	ND	0	0/10	8.2±0.9
T332W	0.2	30	3/10	9.4±1.9
T332W + S66R	1.3	20	3/15	8.8±2.1
T332Y	0.1	0	0/10	9.4±1.3

Table 17: Virulence of WNV T332 Mutants in a Swiss Webster Mouse Model

Survival data for WNV wild-type and T332 mutants in 3-4-week-old Swiss Webster mice. ND = no data. AST includes data for the 100pfu cohort.* = p-value <0.05compared to wild type values using the Kaplan Meier log rank test (% Survival column) or the Bonferroni post-hoc test following one-way ANOVA (AST±SD column).

DISCUSSION

Residue T332 of WNV NY99ic E tolerated a wide range of amino acid substitutions. In fact, all possible amino acids at residue 332 yielded viable virus. The T332P mutant was the only one with markedly different *in vitro* growth and mouse virulence phenotypes. In addition to its lower peak titer compared to wild-type in Vero cells, T332P was highly attenuated in mice. Interestingly, lower post-peak titers in Vero cells (as was seen for T332W+S66R and T332Y) did not seem to correlate with *in vivo* attenuation, perhaps because after day 3 the monolayer had degraded enough that titers did not reflect a replication phenotype so much as a stability phenotype. Also, between the collection of the 3 days post-infection and 4 days post-infection timepoints, the infected plates sat for 24 hours without observation, so it is possible that the rate of inactivation in culture media at 37°C is the same for T332W+S66R/T332Y and the wild-type, but that the degradation of the monolayers in T332W+S66R/T332Y-infected wells began earlier than the degradation of the wild-type infected wells. Furthermore, the more rapid post-peak decrease of T332W+S66R was not replicated in the subsequent growth curve designed to elucidate the role of S66R. Whatever defect caused T332P to reach lower peak titers in the mammalian Vero cell line may have had an impact *in vivo* in the mammalian Swiss Webster mouse model. Because residue T332 so readily tolerated all other amino acids, it is possible that the introduction of a proline at this site was attenuating, not because it disrupted the functional role of residue 332, but because it introduced a kink in the BC loop of EIII and therefore disrupted some other, more functionally critical residue. The previously documented functional importance of neighboring residues G331 and D333 supports this hypothesis.(140)

Of note, the decrease in peak titer seen for WNV T332P in Vero cells was not duplicated in the DEF or the C6/36 cells. Because the main functional role of EIII is thought to be receptor binding, this may indicate that WNV utilizes different receptor(s)

in these different cell lines even though soluble WNV EIII is antagonistic to infection of both Vero and C6/36 cells.(81, 191, 213) In fact, previous studies have described two possible mammalian receptors, DC-SIGN and $\alpha_v\beta_3$ integrin, with molecular weights of 45kDaand 105kDa, respectively, and the possible C6/36 receptors identified thus far are 70kDa and 95kDa.(74, 79, 80, 214) The 70kDa protein may be heat shock cognate 70. Initial discovery of the 70kDa protein's involvement in WNV infection also demonstrated its importance to DENV-2 and JEV infection, and both of these flaviviruses use heat shock cognate 70 (a 72kDa protein) during entry into mosquito cells.(214-216) However, although WNV T332P replicated to wild-type level titers in DEF and C6/36 cells, it is the only mutant obtainable within one nucleotide of the wild-type codon that has not yet been found in any natural isolates. This may indicate critical differences between WNV receptor binding and replication *in vitro* (which was performed without obvious defect in the growth curves) and *in vivo* (as would be required of a naturally occurring isolate) in birds and mosquitoes. The reason for the relative scarcity of naturally occurring variation at residue T332 was not clearly defined by these experiments, however the results of the C6/36 growth curve hint that T332 mutants may face at least a subtle disadvantage regarding replication in mosquito cells. To investigate this possibility with any kind of certainty further studies would be needed, including growth curves using a *Culex* spp. cell line and ideally a higher number of replicates. It would also be useful to examine the impact of changes to T332 on the level of viremia needed to infect mosquitoes, the kinetics of spread throughout the mosquito, and the concentration of virus reached in the various parts of the mosquito, especially the saliva.

Two of the nineteen WNV T332 mutants had a S66R mutation. Both were obtained via plaque purification (as opposed to individual electroporations). There is no naturally occurring variation at residue S66, and the S66R mutation did not impact WNV replication kinetics in Vero cells or WNV virulence in mice. One possible explanation for the acquisition of this mutation is an adaptation to growth in Vero cells. Although

WNV does not typically use heparan sulfate as a receptor, gain-of-charge mutations do allow other viruses to acquire a heparan sulfate-binding phenotype. However, these mutations are often associated with *in vivo* attenuation, which was not the case with the S66R mutation.(80, 81, 213, 217-219)

In contrast to its apparently minor functional role, residue T332 had a substantial impact on antigenicity. This is consistent with previous studies indicating that changes at residue T332 have impacts on neutralization by monoclonal and polyclonal antibodies.(65, 137, 139, 140, 144) Every single mutation at residue T332 resulted in moderate or strong escape from neutralization by 7H2, and all but T332S gained moderate or strong escape from 5H10 neutralization. Perhaps more alarmingly, 16 of the 19 possible T332 mutants gained moderate or strong escape from neutralization by the polyclonal anti-WNV EIII serum. The strongest escape from both the monoclonal and polyclonal antibodies tended to be from the acidic, basic, and aromatic substitutions (see Appendix B). The apparent ease with which WNV can tolerate mutation at residue T332, combined with the likelihood that a change at 332 will result in resistance to neutralization by monoclonal and/or polyclonal antibodies, is a potential issue for the development of vaccines and therapeutics that target only EIII. Although the dead end host status of humans means that any such acquired resistance is unlikely to become widespread, it could complicate prevention and treatment efforts for individual patients.

Chapter 5: Impact of Variation in WNV EIII Surface Loop Residues

RATIONALE AND APPROACH

Residues S306, K307, T330, T332, and A367 in WNV EIII have all been identified as critical antigenic determinants through selection of neutralization or binding resistant mutants. However, neighboring residues (C305, A308, G331, D333, T366, and N368) have not been selected, despite their close physical proximity (Figure 17). Little is known about whether this is due to the relative antigenic irrelevance of the neighboring residues, or whether it is due to structural or functional constraints. On the one hand, residue C305 is part of a critical disulfide bond, and engineered changes at residues G331 and D333 are attenuating .(140, 142) On the other hand, residues T366 and N368 both have naturally occurring variation but have not been selected in antigenic studies, while A367 has no natural variation but has been selected in antigenic studies.(143)

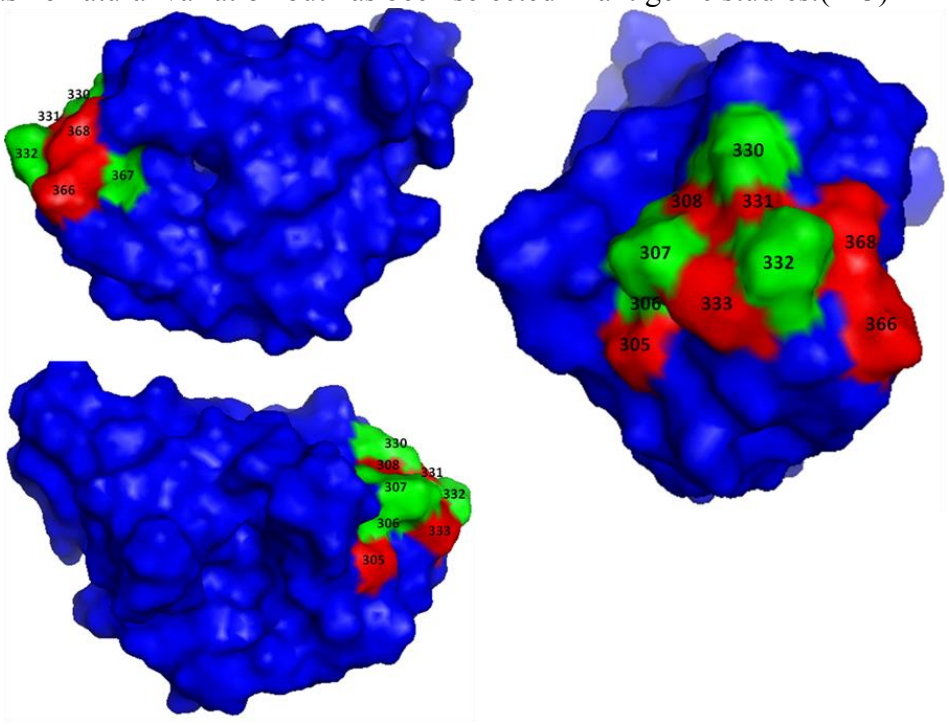

Figure 17: Location of Antigenic Determinants in WNV EIII

Green = Known antigenic determinants. Red = Neighboring residues. Blue = Other EIII residues. Image generated using the PyMol Graphics System, Version 1.3, Schrödinger, LLC with PDB ID 1S6N.

To determine the extent of variation tolerated in residues of the N-terminal (C305, S306, K307, and A308), BC (T330, G333, and D333) and DE (T366, A367, and N368) loops, and to assess how those residues contribute to the antigenic and functional phenotype of EIII, a panel of surface loop mutants was generated using the NY99ic system. This panel was designed to include all possible mutants that could be obtained with a single nucleotide substitution to the wild type NY99ic backbone, for a total of 59 possible mutants. Viable mutants were obtained from both plaque purification of virus pools and individual electroporations.

Antigenicity was assessed using neutralization index assays with the monoclonal antibodies 5H10 and 7H2 and with polyclonal serum against WNV EIII. Western blots were not included because Zhang *et al*. and the assessment of residue T332 described in Chapter 4 of this dissertation already demonstrated that binding by monoclonal antibodies correlates extremely well with neutralization and that binding by polyclonal serum against EIII is not affected by surface loop mutations even if they result in neutralization deficits.(140)

In vitro growth kinetics were assessed in Vero cells, with samples collected at 1, 3, and 5 days post-infection. These timepoints were selected to give a snapshot of early titers, peak titers, and post-monolayer death titers. The other intermediate timepoints were not included in this work because they were not especially informative in previous experiments. Vero cells were chosen both because they were the only cell line to show any major difference in the T332 mutants (see Chapter 4). Virulence was determined using a Swiss Webster mouse model of fatal neuroinvasive disease.

Several mutants which would otherwise have been included in the 59-virus panel had been previously recovered and characterized, and so were not used extensively in this work (Table 18). A K307E neutralization escape mutant of WNV NY99 was previously characterized by Zhang *et al*. (144) They found that, antigenically, K307E is quite an important change and that its $PRNT_{50}$ value for the potently neutralizing antibody E16 is

over 10μg/ml, compared to wild type which was 50% neutralized at approximately 0.1μg/ml. Also, K307E is virulent in mice. Both T330A and T330I mutants of NY99ic were previously recovered and characterized.(140) T330A is strongly neutralized by both 5H10 and 7H2, grows to high titer in Vero cells, and is virulent in mice. In contrast, the T330I mutation causes moderate escape from 5H10 and 7H2 neutralization, but is also able to grow to high titers in Vero cells and is virulence in mice. G331A results in borderline strong/moderate neutralization escape from both 5H10 and 7H2, but reaches a low peak titer in Vero cells and is highly attenuated in mice, suggesting a functional or structural role for G331.(140) Finally, D333E and D333N mutants of NY99ic were also generated and characterized by Zhang *et al*.(140) A D333A mutant was not successfully recovered. The D333E mutant is fully neutralized by 5H10 but demonstrates moderate escape from 7H2 neutralization. D333N, on the other hand, is fully neutralized by 7H2 but demonstrates moderate escape from 5H10. Both D333E and D333N grow to low peak titers in Vero cells. D333E is moderately attenuated in mice, with an LD_{50} approximately 60-fold higher than that of wild-type, and D333N is strongly attenuated with an LD_{50} over 770-fold higher than that of wild-type. These results suggest that 333 may also have a functional or structural role.

	Category of Data		
WNV NY99ic Strain	**Antigenicity**	**Vero Growth**	**Virulence**
K307E	Yes (escape)	No	Yes (virulent)
T330A	Yes (neutralized)	Yes (high)	Yes (virulent)
T330I	Yes (escape)	Yes (high)	Yes (virulent)
G331A	Yes (escape)	Yes (low)	Yes (attenuated)
D333E	Yes (mixed)	Yes (low)	Yes (mildly attenuated)
D333N	Yes (mixed)	Yes (low)	Yes (attenuated)

Table 18: Previously Characterized WNV EIII Surface Mutants

Summary of previously characterized WNV EIII surface loop mutants. In the antigenicity category, mutants were either well neutralized by all antibodies tested (neutralized), escaped from neutralization by all antibodies tested (escape), or displayed a combination of escape from some antibodies and neutralization by others (mixed). In the Vero Growth category, mutants either reach high peak titers approximately equivalent to wild-type or low peak titers compared to wild-type (low = $>1\log_{10}$/pfu/ml deficit). In the Virulence category, mutants can either be virulent, mildly attenuated (>50-fold LD_{50} increase), or attenuated (>500-fold LD_{50} increase).(140, 144)

RESULTS

Mutant Recovery

Of the 59 EIII surface loop mutants originally included in this panel, six had been previously characterized and therefore were not included, 15 were not viable, and 38 were successfully recovered (Table 19). The non-viable mutants were located at either C305, G331, or D333. None of the C305 mutants in the panel were viable. At residue G331, only the G331A and G331S mutants were successfully recovered. Both were recovered via plaque purification, but G331A was not used in these experiments due to its previous characterization.(140) At residue D333, the only viable mutants in the panel were D333E and D333N, which had both been previously recovered and characterized.(140)

Full prM/E sequencing revealed several additional mutations in the panel. The K307N virus had a single nucleotide substitution in prM, but it was a non-coding change. Another K307 mutant, K307T, was found to have a T129S mutation located in domain II of E, located at the C-terminal end of the e strand, just upstream of the link between strand e of EII and strand E_0 of EI. The closest distance between K307 and T129 is 31.3 angstrom and is between neighboring E monomers about the 3-fold axis of symmetry. The G331S mutant acquired a H395Y mutation in strand G of the EIII domain. The closest distance between G331 and H395 is 20.9 angstrom within a given monomer of E. Finally, the G331D mutant was obtained as a small passage 2 stock immediately following plaque purification, but the virus reverted to its wild-type G331 residue when growing a larger passage 3 stock for experimental use. Both compensating mutations (T129S and H395Y) are at locations that are surface exposed in the context of an E monomer but are largely buried between multiple monomers in the context of a whole virion (i.e., they are in the envelope layer of the capsid, not exposed on the surface facing either the interior or the exterior of the virion) (Figure 18).

WNV NY99ic Mutant	Source	Passage(s) Used
C305F	Not Viable	Not Viable
C305G	Not Viable	Not Viable
C305R	Not Viable	Not Viable
C305S	Not Viable	Not Viable
C305W	Not Viable	Not Viable
C305Y	Not Viable	Not Viable
S306A	Electroporation	0
S306L	Electroporation	0
S306P	Plaque Purified	3
S306T	Electroporation	0
K307E	Not Included	N/A
K307M	Plaque Purified	3
K307N	Plaque Purified	3
K307Q	Plaque Purified	3
K307R	Plaque Purified	4
K307T+T129S	Plaque Purified	4
A308D	Electroporation	0
A308G	Electroporation	0
A308P	Electroporation	0
A308S	Electroporation	0
A308T	Electroporation	0
A308V	Electroporation	0
T330A	Not Included	N/A
T330I	Not Included	N/A
T330N	Electroporation	1
T330P	Plaque Purified	4
T330S	Electroporation	0
G331A	Not Included	N/A
G331C	Not Viable	Not Viable
G331D	Not Viable	Not Viable

WNV NY99ic Mutant	Source	Passage(s) Used
G331R	Not Viable	Not Viable
G331S+H395Y	Plaque Purified	4
G331V	Not Viable	Not Viable
D333A	Not Viable	Not Viable
D333E	Not Included	N/A
D333G	Not Viable	Not Viable
D333H	Not Viable	Not Viable
D333N	Not Included	N/A
D333V	Not Viable	Not Viable
D333Y	Not Viable	Not Viable
T366A	Plaque Purified	4
T366K	Plaque Purified	4
T366M	Plaque Purified	4
T366P	Plaque Purified	4
T366R	Electroporation	0
T366S	Plaque Purified	4
A367D	Electroporation	0
A367G	Electroporation	0
A67P	Electroporation	1
A367S	Electroporation	0
A367T	Electroporation	1
A367V	Plaque Purified	4
N368D	Plaque Purified	4
N368H	Electroporation	0
N368I	Plaque Purified	4
N368K	Plaque Purified	4
N368S	Electroporation	0
N368T	Plaque Purified	4
N368Y	Plaque Purified	3

Table 19: Generation of WNV EIII Surface Loop Mutant Stocks

Summary of how each WNV EIII surface loop mutant stock was obtained.

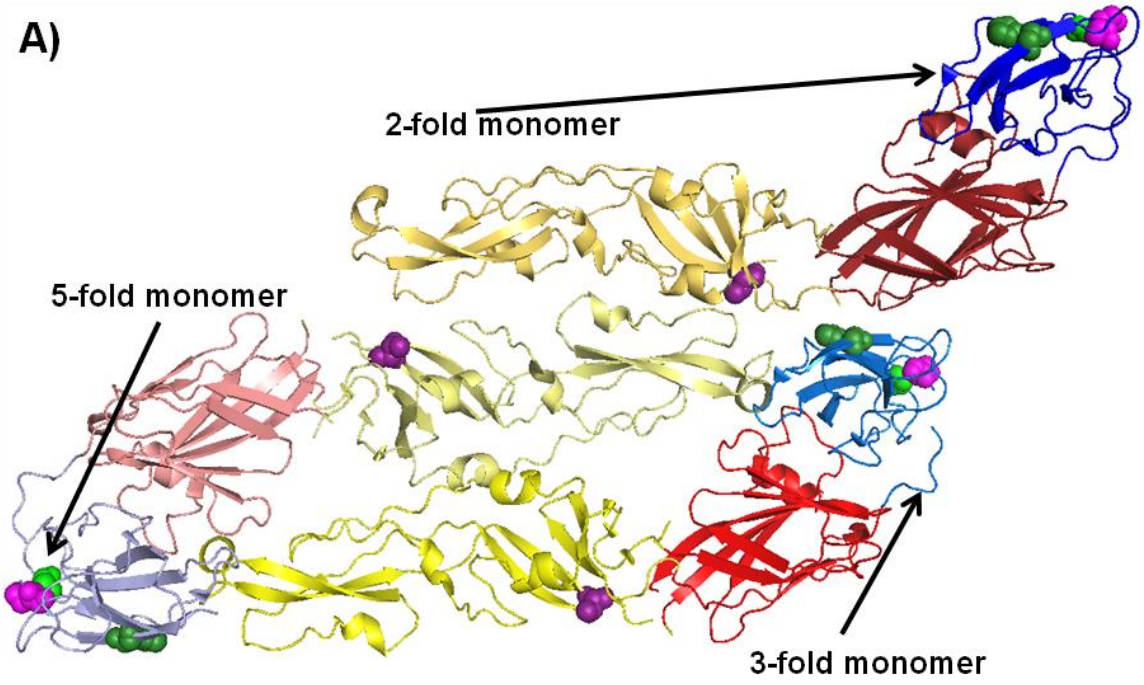
A)
2-fold monomer
5-fold monomer
3-fold monomer

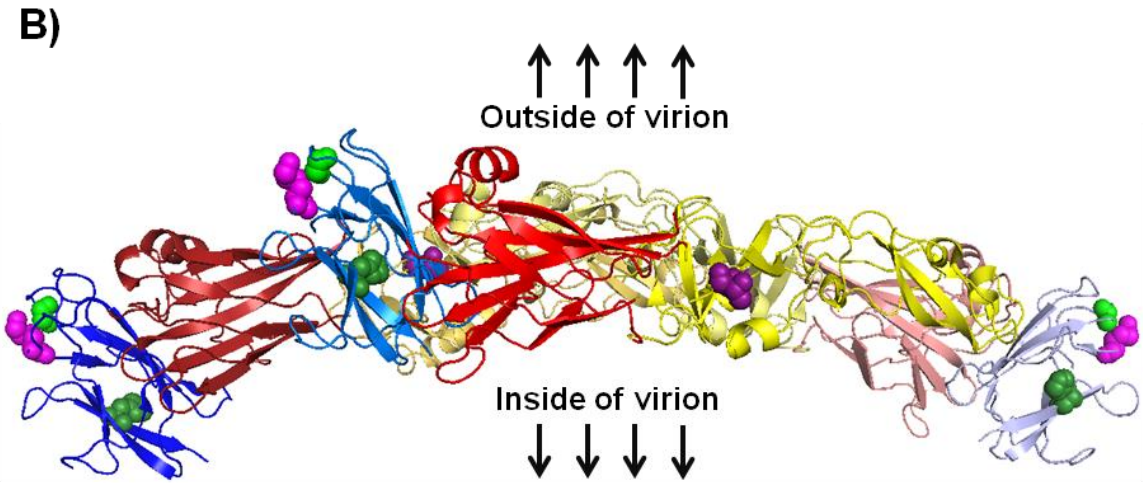
B)
Outside of virion
Inside of virion

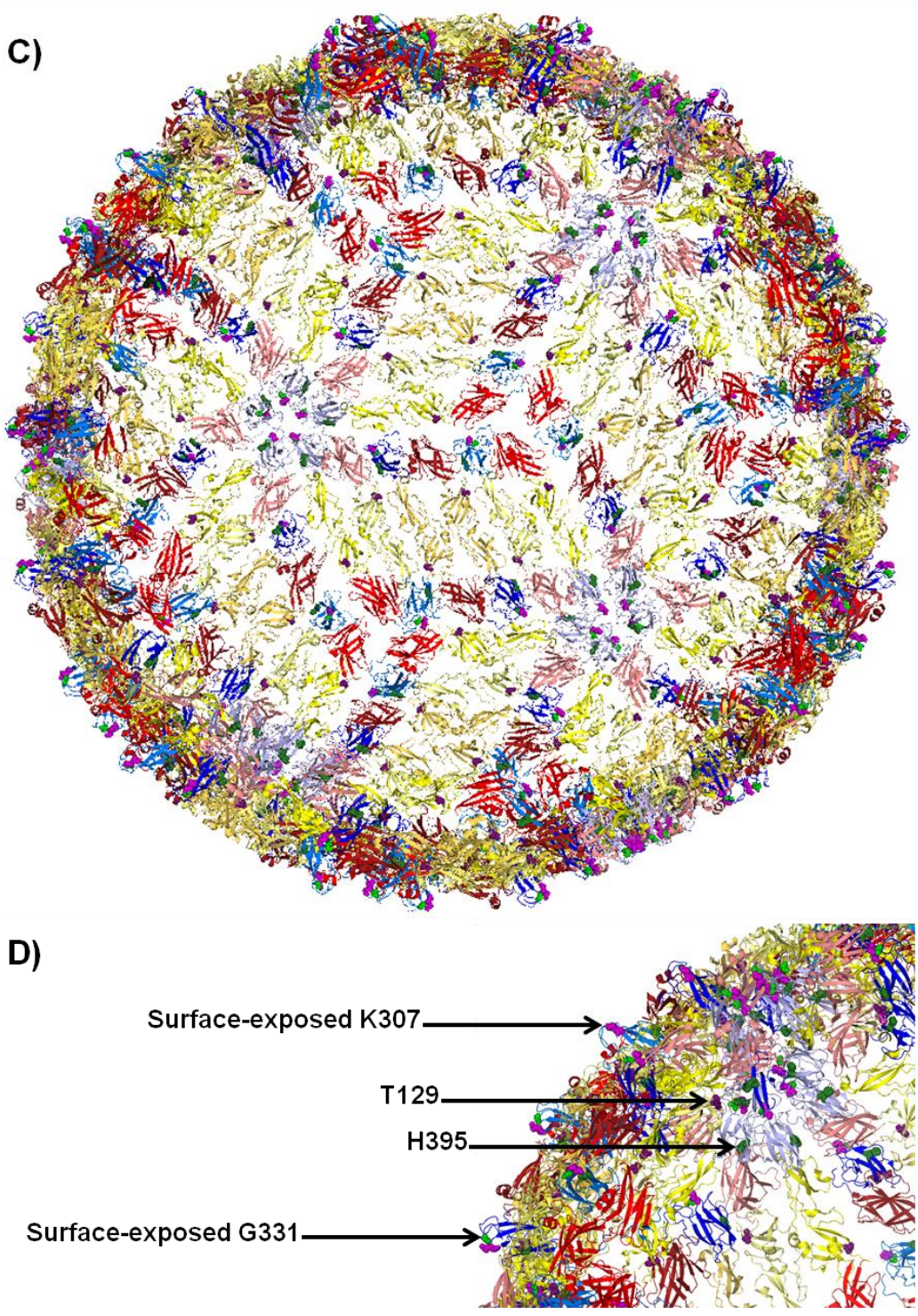

Figure 18: Location of Residues T129, K307, G331, and H395

(A) Top view and (B) side view of E trimers. (C) Whole virus and (D) enlarged section of whole virus. Monomers shaded such that light = 5-fold axis of symmetry, bright = 3-fold axis of symmetry, and dark = 2-fold axis of symmetry. Red = EI, yellow = EII, blue = EIII, bright purple = K307, dark purple = T129, bright green = G331, dark green H395. Images generated using the PyMol Graphics System, Version 1.3, Schrödinger, LLC with PDB ID 3IYW.

Antibody-Mediated Neutralization

The impact of EIII surface loop mutations to antibody-mediated neutralization varied depending on which residue was mutated (Table 20). It should be noted that the antigenicity of the N368Y mutant was not assessed due to low stock titers, and the neutralization of A308V by 5H10 and 7H2 could not be assessed due to a lack of available virus aliquots. All other viable mutants that were not previously characterized were included. Every residue had at least one substitution that resulted in weak neutralization by 5H10 or 7H2 except for N368. For 5H10, residues S306, K307, T330, and T366, were most important to neutralization, with all characterized mutants at these residues resulting in weak or moderate escape. This was compared to 50-67% of the A308, A367, and N368 mutants. For 7H2, all K307 mutants resulted in moderate or weak neutralization, but the other residues had a more limited impact with 0% of N368, 20% of A308, 25% of S306, and 33% of T330, T366, and A367 mutants resulting in moderate or weak neutralization. The G331S+H395Y mutations affected epitopes recognized by 5H10 and 7H2, but because only one G331 mutant was characterized it was impossible to deduce a pattern.

In contrast to the previous observations with NY99ic T332 mutants, neutralization by the polyclonal anti-WNV EIII serum was largely unaffected by the vast majority of these surface loop mutations. Roughly one third of the mutants tested (32%) retained strong neutralization by the anti-EIII serum, with 50% being moderately neutralized and only 18% resulting in weak neutralization. Loss of neutralization was most common in S306, K307, and T330 mutants, all of which were moderately or weakly neutralized. A367 was close, with 83% of mutants resulting in moderate or weak neutralization. Next was N368, which had no weakly neutralized mutants but was moderately neutralized 66% of the time. A308 and T366 had the least impact on neutralization by anti-EIII serum, with no weakly neutralized mutants and only 33% moderately neutralized.

WNV NY99ic Strain	Antibody		
	5H10	7H2	Anti-EIII Serum
Wild-type	2.8±0.2	>3.2	2.7±0.0
S306A	1.9±0.0*	>2.9	2.0±0.1*
S306L	1.5±0.0*	2.7±0.1*	1.1±0.1*
S306P	0.8±0.0*	>2.8	1.9±0.1*
S306T	0.1±0.1*	2.0±0.1*	1.4±0.0*
K307M	0.0±0.0*	1.0±0.0*	1.7±0.1*
K307N	-0.2±0.0*	0.8±0.1*	0.8±0.1*
K307Q	-0.1±0.1*	0.7±0.1*	0.9±0.0*
K307R	0.2±0.1*	2.1±0.1*	1.5±0.1*
K307T+T129S	-0.3±0.0*	0.8±0.2*	0.9±0.1*
A308D	0.9±0.2*	2.8±0.2	1.5±0.1*
A308G	1.2±0.1*	>3.3	1.9±0.1*
A308P	>3.0	0.2±0.0*	2.8±0.0
A308S	1.7±0.0*	>3.3	2.6±0.1
A308T	2.2±0.3	2.9±0.1	2.4±0.1
A308V	N/A	N/A	2.6±0.1
T330N	0.4±0.1*	2.2±0.1*	1.4±0.0*
T330P	1.8±0.4*	3.2±0.2	1.7±0.1*
T330S	1.4±0.2*	2.5±0.1*	2.2±0.1*
G331S+H395Y	0.0±0.0*	1.9±0.0*	1.0±0.0*
T366A	1.8±0.1*	>3.0	2.0±0.0*
T366K	1.3±0.1*	>3.0	3.0±0.1
T366M	1.4±0.0*	>2.7*	2.8±0.0
T366P	>1.9	>1.9*	1.7±0.1*
T366R	0.0±0.0*	1.5±0.5*	>3.1
T366S	1.7±0.2*	>3.0	2.5±0.2
A367D	>3.3	0.2±0.0*	0.8±0.1*
A367G	1.4±0.1*	2.1±0.1*	2.3±0.5
A367P	2.1±0.1	>3.2	1.8±0.1*
A367S	2.3±0.3	>3.0	1.0±0.1*
A367T	2.1±0.1	>3.1	1.9±0.0*
A367V	2.1±0.0	>3.1	1.9±0.1*
N368D	1.4±0.1*	3.4±0.1	2.8±0.0
N368H	2.3±0.1	>3.0	2.3±0.2
N368I	2.7±0.6	>3.1	1.2±0.2*
N368K	2.7±0.4	>3.0	2.2±0.0*
N368S	2.0±0.1	3.2±0.1	1.2±0.1*
N368T	>3.0	>3.0	2.1±0.1*

Table 20: Neutralization Indices of WNV EIII Surface Loop Mutants

Neutralization indices of WNV NY99ic wild-type and EIII surface loop mutants by the 5H10 and 7H2 monoclonal antibodies and by rabbit anti-EIII polyclonal serum. Values given as Avg±SD. Green = strongly neutralized, yellow = moderately neutralized, and red = weakly neutralized. * indicates statistically significant difference ($p<0.05$) from wild-type using the Bonferroni post-hoc test following one-way ANOVA.

In vitro Replication Kinetics

Similar to NY99ic wild-type, the viable N-terminal loop (residues 306-308) mutants were able to replicate to 7-8$\log_{10}$ pfu/ml by 3 days post-infection (Figure 19). There is, however, a fairly large amount of variation, especially at the 1 day post-infection timepoint. In fact, nine of the 16 mutants are substantially lower than NY99ic wild-type at 1 day post-infection, with the deficit ranging from 1.2-2.0$\log_{10}$ pfu/ml: S306A, S306L, S306P, K307E, K307M, K307N, K370Q, A308T, and A308V. Conversely, the S306T mutant is 2.4$\log_{10}$ pfu/ml higher than NY99ic wild-type at 1 day post-infection. In addition to their absolute differences, all of the strains that differ from NY99ic wild-type by at least 1.0log10 pfu/ml at 1 day post-infection are statistically different from NY99ic wild-type (Table 21). There are no mutants that differ from NY99ic wild-type by at least 1.0$\log_{10}$ pfu/ml at 3 or 5 days post-infection, and there are also no mutants that are statistically different from NY99ic wild-type at these timepoints.

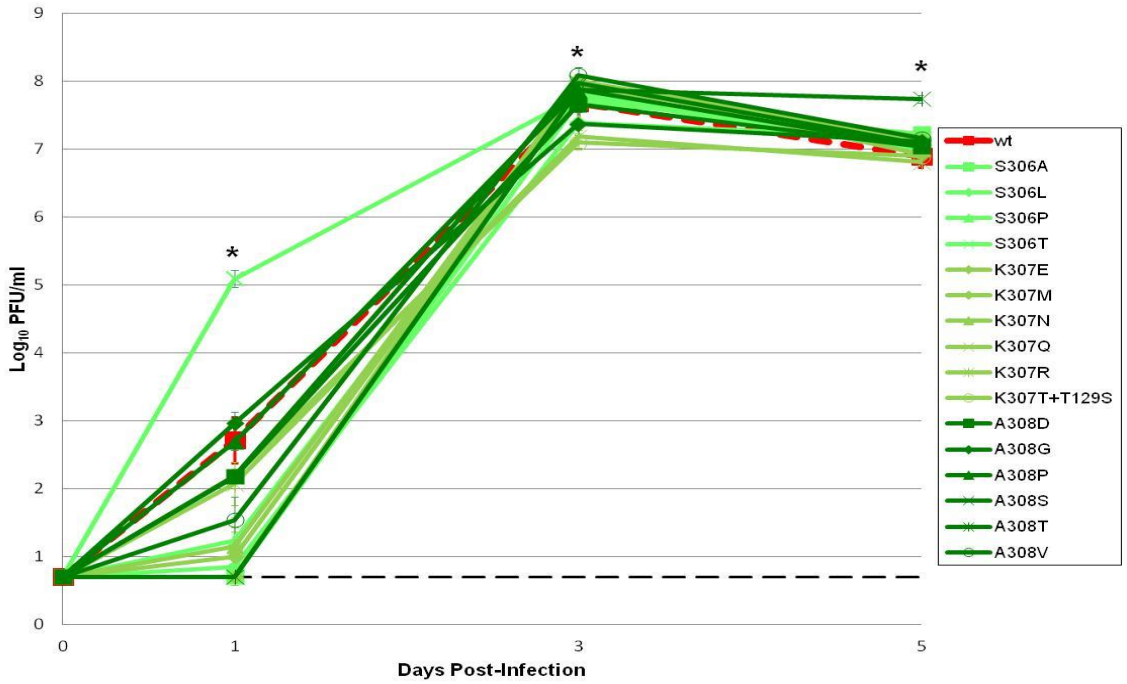

Figure 19: Replication of WNV EIII N-Terminal Loop Mutants in Vero Cells

Growth kinetics of WNV wild-type and EIII N-terminal surface loop mutants in Vero cells. Dashed black line = limit of detection. Error bars = standard deviation. * = statistically significant variation between strains using one-way ANOVA analysis with a significance threshold of 0.05.

	Days Post-Infection			
	0	**1**	**3**	**5**
ANOVA	N/A	0.000	0.000	0.000
WNV NY99ic Strain				
S306A	N/A	0.000	1.000	1.000
S306L	N/A	0.000	1.000	1.000
S306P	N/A	0.000	1.000	1.000
S306T	N/A	0.000	1.000	1.000
K307E	N/A	0.000	1.000	1.000
K307M	N/A	0.000	1.000	1.000
K307N	N/A	0.000	1.000	1.000
K307Q	N/A	0.000	1.000	1.000
K307R	N/A	1.000	0.697	1.000
K307T+T129S	N/A	1.000	0.101	1.000
A308D	N/A	1.000	1.000	1.000
A308G	N/A	1.000	1.000	1.000
A308P	N/A	1.000	1.000	1.000
A308S	N/A	1.000	1.000	1.000
A308T	N/A	0.000	1.000	0.976
A308V	N/A	0.003	1.000	1.000

Table 21: Statistical Analysis of WNV EIII N-Terminal Loop Mutant Replication Kinetics in Vero Cells

Significance values obtained by one-way ANOVA with Bonferroni post-hoc analysis comparing each strain to the wild-type control. N/A = not applicable. Green = mutant is significantly higher than the wild-type control. Red = mutant is significantly lower than the wild-type control. White = mutant is not significantly different than the wild-type control. Threshold for significance = 0.05.

Following the results of the initial *in vitro* replication results for the EIII mutants, a second, smaller growth curve was conducted to determine whether the early variation was due to actual, biological differences or simply technical differences such as different quantities of virus being used during the initial infections. To this end, three viruses were selected: NY99ic wild-type, S306A (which was 2.0$\log_{10}$ pfu/ml below NY99ic wild-type at 1 day post-infection in the initial timecourse), and S306T (which was 2.4$\log_{10}$ pfu/ml above NY99ic wild-type at 1 day post-infection in the initial timecouse). These viruses were used to infect Vero cells in 6-well plates at expected MOIs of 0.04, 0.01, and 0.001 (0.04 was the highest MOI possible for the stock with the lowest titer). The dilutions were back-titered to determine the actual MOI, and samples were collected daily for 5 days and titered on Vero cells.

The back-titers revealed that NY99ic wild-type and S306A had actual MOIs quite close to their expected MOIs (Table 22). S306T, on the other hand, had actual MOIs

approximately 10-fold higher than expected. This is consistent with the extremely elevated 1 day post-infection titer for S306T seen in Figure 19.

Virus	**NY99ic wild-type**			**NY99ic S306A**			**NY99ic S306T**		
Expected MOI	0.001	0.01	0.04	0.001	0.01	0.04	0.001	0.01	0.04
Actual MOI	0.002	0.02	0.06	0.001	0.01	0.08	0.02	0.2	0.9

Table 22: Expected and Actual MOIs in Repeat Timecourse

Expected MOIs for NY99ic wild-type, S306A, and S306T+T129S and their actual MOIs as determine by back-titer.

The results of the multi-MOI timecourse highlight the role of virus input on early timepoint titers (Figure 20A). At 1 day post-infection, the earliest post-infection timepoint measured by the full EIII surface loop mutant timecourse and the first timepoint in the multi-MOI timecourse for which all strain/MOI combinations have a measurable titer, the NY99ic wild-type samples have a range of $1.6\log_{10}$ pfu/ml, the S306A samples have a range of $1.0\log_{10}$ pfu/ml, and the S306T samples have a range of $0.9\log_{10}$ pfu/ml. These 1 day post-infection timepoints had the largest range for NY99ic wild-type and S306A, but S306T had a larger range at 0 ($2.0\log_{10}$ pfu/ml) and 0.5 ($2.8\log_{10}$ pfu/ml) days post-infection. By the time titers begin to plateau at 2 days post-infection there is considerably less range both within and between each strain.

When the growth curves with the most similar actual, back-titered MOIs are compared (expected MOI 0.01 for NY99ic wild-type and S306A, and expected MOI 0.001 for S306T), a clearer picture emerges (Figure 20B). When changes in MOI were accounted for, the differences between NY99ic wild-type and S306T became negligible. The differences between NY99ic wild-type and S306A, however, were maintained. In the initial timecourse, S306A was undetectable at 1 day post-infection, while NY99ic wild-type was at $2.7\log_{10}$ pfu/ml, giving a difference of at least $2.0\log_{10}$ pfu/ml. In the multi-MOI timecourse, S306A was undetectable at 0 and 0.5 days post-infection, while NY99ic wild-type was at $1.3\log_{10}$ pfu/ml and $1.8\log_{10}$ pfu/ml, respectively. Even at 1 day

post-infection, S306A had a deficit of 1.6log$_{10}$ pfu/ml compared to NY99ic wild-type. Thus, while the radical early difference of S306T was likely technical artifact, some of the more subtle early replication deficits of the WNV surface loop EIII mutants may be real.

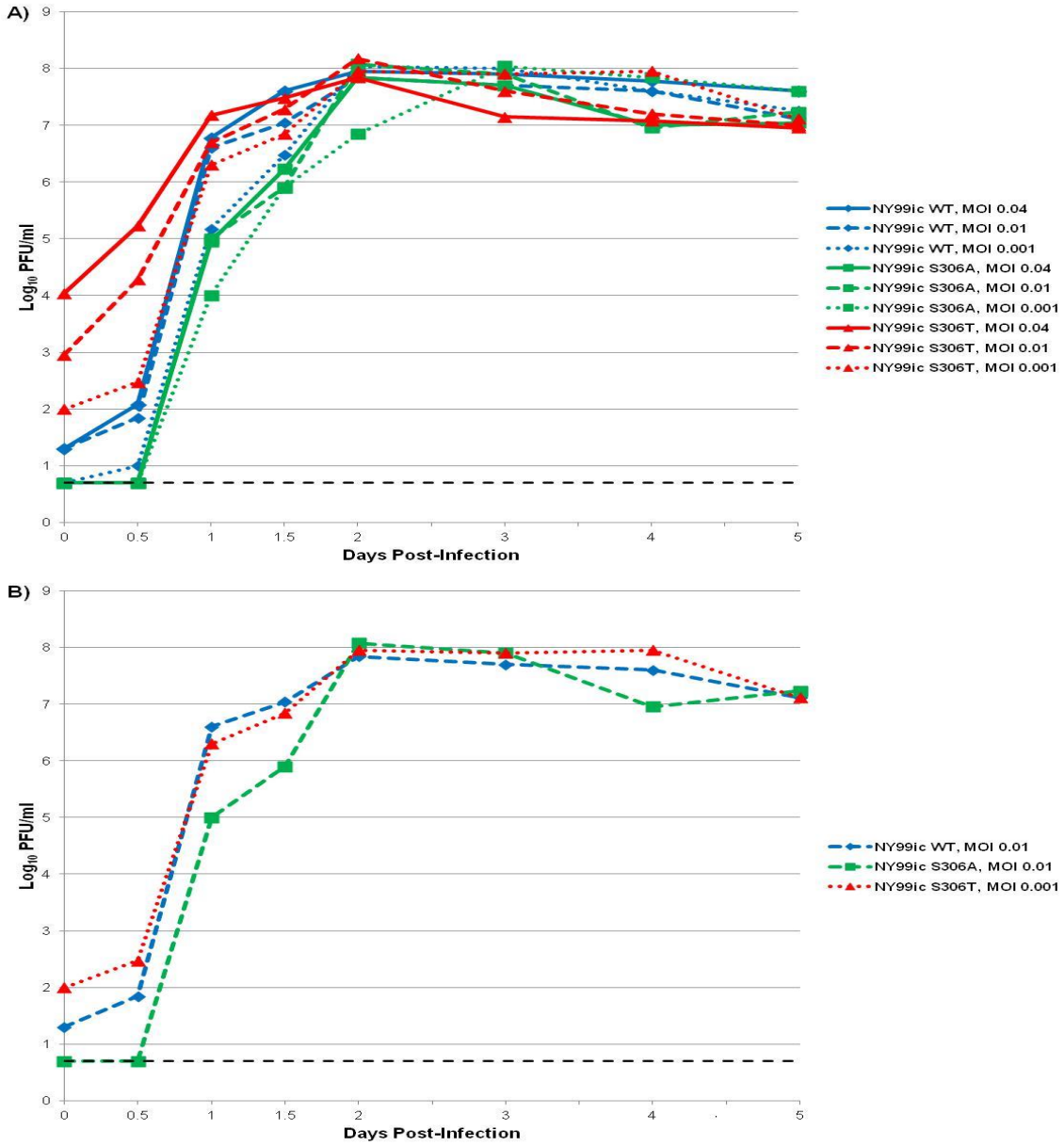

Figure 20: Replication of Selected WNV EIII Surface Loop Mutants with Multiple MOIs in Vero Cells

Replication kinetics of WNV NY99ic wild-type, S306A, and S306T in Vero cells (A) at expected MOIs of 0.04, 0.01, and 0.001, and (B) at actual, back-titered MOIs of approximately 0.01.

The BC surface loop mutants all replicated in Vero cells (Figure 21). At 1 day post-infection, G331S+H395Y is 1.4$\log_{10}$ pfu/ml higher than NY99ic wild-type and T330S is 1.0$\log_{10}$ pfu/ml lower than NY99ic wild-type. The other mutants (T330N and T330P) are both within 1.0$\log_{10}$ pfu/ml at 1 day post-infection. In addition to the mutants that differ from NY99ic wild-type by at least 1.0log10 pfu/ml, T330S is statistically different from NY99ic wild-type at 3 days post-infection, despite only being 0.7$\log_{10}$ pfu/ml higher (Table 23).

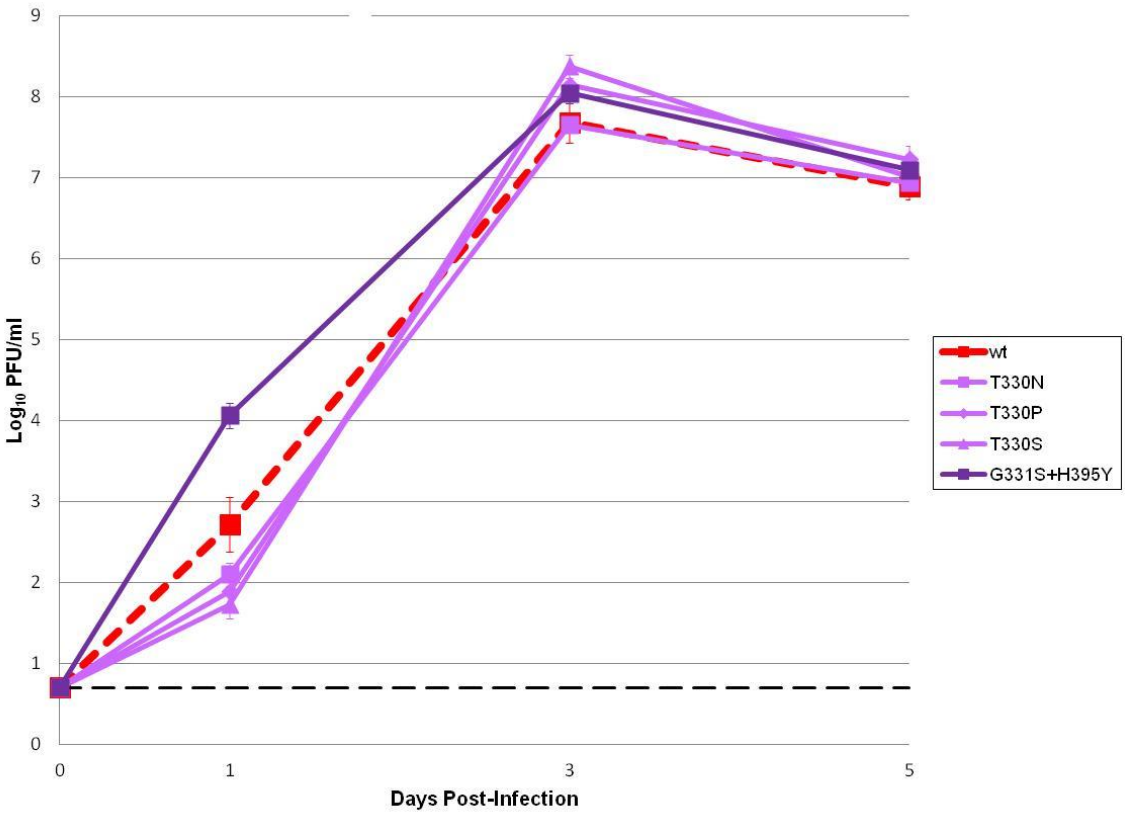

Figure 21: Replication of WNV EIII BC Loop Mutants in Vero Cells

Growth kinetics of WNV wild-type and EIII BC surface loop mutants in Vero cells. Dashed black line = limit of detection. Error bars = standard deviation.

	Days Post-Infection			
	0	**1**	**3**	**5**
ANOVA	N/A	0.000	0.016	0.221
WNV NY99ic Strain				
T330N	N/A	1.000	1.000	1.000
T330P	N/A	0.405	1.000	1.000
T330S	N/A	0.041	0.008	1.000
G331S+H395Y	N/A	0.000	1.000	1.000

Table 23: Statistical Analysis of WNV EIII BC Loop Mutant Replication Kinetics in Vero Cells

Significance values obtained by one-way ANOVA with Bonferroni post-hoc analysis comparing each strain to the wild-type control. N/A = not applicable. Green = mutant is significantly higher than the wild-type control. Red = mutant is significantly lower than the wild-type control. White = mutant is not significantly different than the wild-type control. Threshold for significance = 0.05.

All DE loop mutants were able to replicate in Vero cells (Figure 22). At 1 day post infection T366M, T366P, A367P, N368I, and N368S are 1.0-1.4$\log_{10}$ pfu/ml below NY99ic wild-type. Similarly, A367S, A367T, N368K, N368T, and N368Y are 1.9-2.0log10 pfu/ml below NY99ic wild-type at 1 day post-infection, being either below or just above the limit of detection. No strains differ from NY99ic wild-type by 1.0$\log_{10}$ pfu/ml or more at 3 days post-infection. At 5 days post-infection, A367D, A367T, and N368D are 1.0-1.2$\log_{10}$ pfu/ml below NY99ic wild-type, and A367G and T366R are both 2.2$\log_{10}$ pfu/ml below NY99ic wild-type.

All of the mutant/timepoint combinations that differ from NY99ic wild-type by at least 1.0$\log_{10}$ pfu/ml are also statistically different from NY99ic wild-type except for N368D at 5 days post-infection (Table 24). In addition, there are three mutants that differ from NY99ic wild-type by less than 1.0$\log_{10}$ pfu/ml at 3 days post-infection but are statistically different from NY99ic wild-type at that timepoint: T366A with a 0.7$\log_{10}$ pfu/ml excess, N368I with a 0.8$\log_{10}$ pfu/ml deficit, and N368Y with a 0.9$\log_{10}$ pfu/ml deficit.

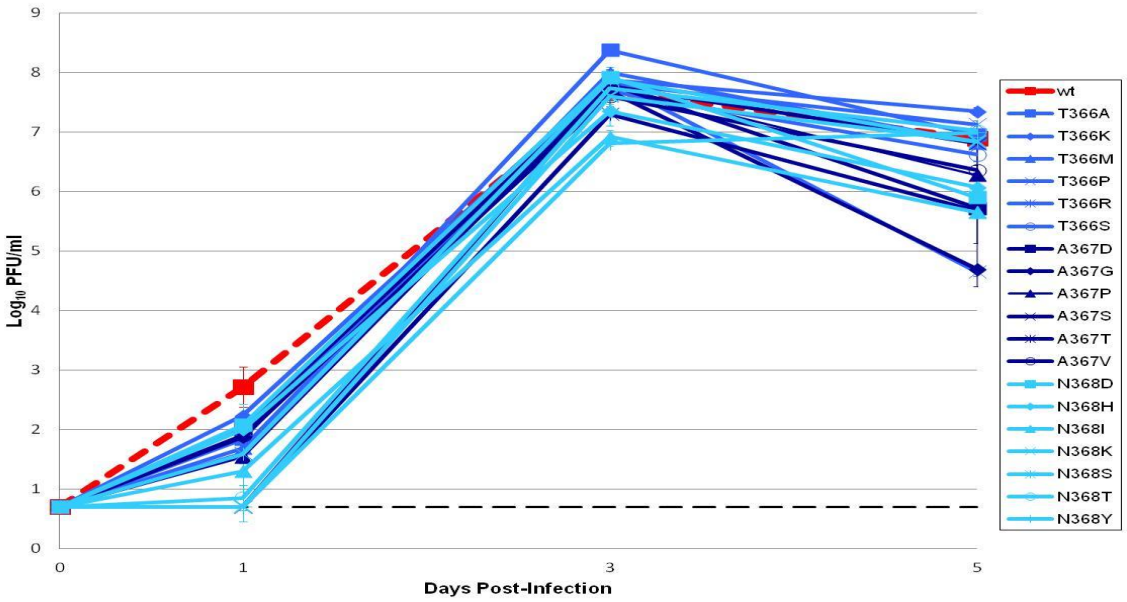

Figure 22: Replication of WNV EIII DE Loop Mutants in Vero Cells

Growth kinetics of WNV wild-type and EIII DE surface loop mutants in Vero cells. Dashed black line = limit of detection. Error bars = standard deviation.

	Days Post-Infection			
	0	**1**	**3**	**5**
ANOVA	N/A	0.000	0.000	0.000
WNV NY99ic Strain				
T366A	N/A	0.204	0.008	1.000
T366K	N/A	1.000	1.000	1.000
T366M	N/A	0.025	1.000	1.000
T366P	N/A	0.007	1.000	1.000
T366R	N/A	0.463	1.000	0.000
T366S	N/A	1.000	1.000	1.000
A367D	N/A	1.000	1.000	0.020
A367G	N/A	0.330	1.000	0.000
A367P	N/A	0.003	1.000	1.000
A367S	N/A	0.000	1.000	1.000
A367T	N/A	0.000	1.000	0.010
A367V	N/A	0.463	1.000	1.000
N368D	N/A	1.000	1.000	0.181
N368H	N/A	1.000	1.000	1.000
N368I	N/A	0.000	0.002	0.007
N368K	N/A	0.000	1.000	1.000
N368S	N/A	0.006	1.000	1.000
N368T	N/A	0.000	1.000	1.000
N368Y	N/A	0.000	0.000	1.000

Table 24: Statistical Analysis of WNV EIII DE Loop Mutant Replication Kinetics in Vero Cells

Significance values obtained by one-way ANOVA with Bonferroni post-hoc analysis comparing each strain to the wild-type control. N/A = not applicable. Green = mutant is significantly higher than the wild-type control. Red = mutant is significantly lower than the wild-type control. White = mutant is not significantly different than the wild-type control. Threshold for significance = 0.05.

Mouse Virulence

The relative virulence of viable mutants varied widely by residue within the surface loops (Table 25). On the N-terminal loop, mutants encoding threonine at either S306 or K307 were significantly attenuated (50% and 75% survival following 100 pfu challenge, respectively, compared to 13% survival for the wild-type), but other viable mutants at those residues retained virulence comparable to the wild-type. The neighboring residue A308 was virulent with all mutations tested, including the A308T mutation. In the BC loop, substitutions at T330 resulted in no loss of virulence, but the G331S+H395Y mutant was completely attenuated at the 100pfu dose tested. Finally, in the DE loop, residues T366 and A367 were mutated without impacting virulence. In contrast, four of seven attempted mutations at residue N368 caused statistically significant attenuation (N368I resulted in 63% survival, N368K resulted in 38% survival, N368T resulted in 88% survival, and N368Y resulted in 100% survival).

WNV NY99ic Strain	Survival		AST±SD
	%	Alive/Total	
Wild-type	13	1/8	8.3±1.4
S306A	13	1/8	8.9±1.2
S306L	0	0/8	9.6±1.2
S306P	0	0/8	8.4±2.0
S306T	50*	4/8	9.8±2.4
K307M	0	0/8	9.6±2.0
K307N	0	0/8	7.6±0.7
K307Q	13	1/8	9.1±2.0
K307R	13	1/8	11.0±2.1*
K307T+T129S	75*	6/8	11.5±2.1*
A308D	13	1/8	11.0±4.1
A308G	0	0/8	9.5±1.9
A308P	38	3/8	8.2±1.6
A308S	13	1/8	7.7±0.8
A308T	0	0/8	8.8±1.3
A308V	0	0/8	8.6±1.4
T330N	25	2/8	9.3±3.9
T330P	38	3/8	8.2±0.4
T330S	0	0/8	8.4±0.9
G331S+H395Y	100*	8/8	N/A
T366A	13	1/8	8.6±1.0
T366K	0	0/8	9.6±2.3
T366M	25	2/8	8.0±0.6
T366P	25	2/8	9.8±2.9
T366R	13	1/8	8.7±0.8
T366S	0	0/8	8.8±1.9
A367D	0	0/8	8.1±1.0
A367G	0	0/8	9.8±1.8
A367P	13	1/8	7.6±0.5
A367S	0	0/8	8.8±1.8
A367T	0	0/8	9.3±1.2
A367V	13	1/8	9.3±1.3
N368D	25	2/8	9.0±0.6
N368H	0	0/8	9.3±1.8
N368I	63*	5/8	9.3±0.6
N368K	38*	3/8	11.0±1.9*
N368S	0	0/8	9.3±2.2
N368T	88*	7/8	10.0±N/A
N368Y	100*	8/8	N/A

Table 25: Virulence of WNV EIII Surface Loop Mutants in a Swiss Webster Mouse Model

Survival data for WNV wild-type and EIII surface loop mutants in 3-4-week-old Swiss Webster mice. AST is in days.* = p-value <0.05compared to wild type values using the Kaplan Meier log rank test (% Survival column) or the Bonferroni post-hoc test following one-way ANOVA (AST±SD column).

DISCUSSION

Residue C305 yielded no viable mutants, which was expected given its critical role in a cysteine bridge.(200) The other N-terminal residues each tolerated the full range of attempted substitutions. Residue S306, which has previously been implicated as an antigenic determinant by crystallography and yeast display epitope mapping, but which has not been tested in the context of infectious virus, had very little impact on virulence or replication in Vero cells.(65, 137) The exception was S306T, which was attenuated in mice despite having no decrease in titer in Vero cells. Antigenically, S306 mutations had widespread impacts on neutralization by 5H10 and polyclonal anti-EIII serum but not on neutralization by 7H2.

Substitutions at residue K307 had minor impacts on virulence and replication in Vero cells but a strong impact on antigenicity. Like S306T, the K307T+T129S mutant replicated like wild-type in Vero cells but was attenuated in mice. It is difficult to speculate why the S306T and K307T mutants were attenuated but the other mutants at those residues were not. Threonine was slightly smaller than lysine and the other substitutions at K307, but other than that, threonine is less different from the wild-type amino acid than at least one mutant that retained virulence in terms of category, size, pI, and hydropathy index (See Appendix B). In contrast to its apparently minor role in WNV EIII structure and function, K307 was very important antigenically, and was in fact the only residue in this set for which all mutants resulted in moderate or weak neutralization by 5H10, 7H2, and anti-EIII serum. These results are in agreement with previously published data regarding residue K307.(138)

Mutations at residue A308 did not strongly impact replication in Vero cells or mouse virulence. All of the attempted mutants were viable, replicated to high titers in Vero cells, and were virulent in mice. The strongest antigenic change came from the

A308D mutant, which was also the only charged substitution. A308G and A308S resulted in moderate neutralization by 5H10 and A308P resulted in weak neutralization by 7H2. G and P are each amino acids with unique structural/chemical characteristics (G because it is not chiral and has a single hydrogren as its side chain, and P because its side chain binds its amino group to form a ring, often resulting in kinks or turns in a protein), although the antigenic impact of A308S is less easily explained by the physiochemical properties of the amino acid.

The BC loop was overall quite different from the N-terminal loop. Consistent with earlier studies, residues in this loop appear to play major roles in antigenicity and/or structure and function of EIII.(140) The T330 mutants behaved essentially as expected. None of the T330 mutants had any deleterious effect on replication in Vero cells or virulence in mice except for T330P, which was slightly (although not statistically) attenuated in mice. Antigenically, T330 had wisespread impact on 5H10 and polyclonal anti-EIII serum neutralization but T330N decreased 7H2 neutralization to moderate levels.

Two of the three BC loop residues investigated here (G331 and D333) had previously been characterized, based on a much smaller number of mutations, as functionally and/or structurally critical.(140) In the case of G331, only two of the six possible mutants investigated here and in earlier studies were viable. One, G331A, had been studied previously, but G331S had not yet been characterized. Alanine and serine are the two amino acids closest in size to glycine, so it is perhaps not surprising that those were viable if residue 331 is important to the conformation of the BC loop. G331S grew to high titers in Vero cells, which was surprising considering that G331A grows to lower titers compared to wild-type in Vero cells. They are both strongly attenuated in mice.(140) The cause for the G331S mutant's strong replication *in vitro* in light of its attenuation *in vivo* is not currently known. Both G331A and G331S were critical antigenic determinants. It seems likely that residue G331 has an important antigenic role,

but that its inability to tolerate substitution without severe attenuation means that neutralization-resistant mutants with variation at residue G331 are unlikely to ever be selected for. The role of the G331S mutant's H395Y mutation is unknown. The only naturally occurring H395Y strain (accession DQ823112) was obtained from the kidney of a crow collected in New York during May 2004, and no characterization has been done beyond sequencing.(220) Mutagenesis of residue F309 during other studies in our laboratory has also been associated with selection of variants also encoding H395Y (E. I. Bovshik and D. W. C. Beasley, unpublished), suggesting that this mutation may have some compensating effect for mutations at or close to the EIII surface.

An attempt to recover seven different D333 mutants was made, but only two (D333E and D333N) were viable. These two mutants had already been described in earlier studies. Both replicated to lower titers than wild-type NY99ic in Vero cells, were attenuated in mice (especially D333N), and had a substantial impact on neutralization by anti-WNV EIII MAbs and polyclonal sera.(140) Like residue G331, D333 appears to be antigenically critical but unlikely to be selected for due to its critical functional or structural role. Upon examining the physical characteristics of the amino acids that yielded viable and non-viable virus, it was noticed that both glutamatic acid and asparagine are the most similar to aspartic acid in terms of hydropathy (See Appendix B).

The DE loop residues seemed to be less involved antigenically than the N-terminal or BC loop residues. The exception was T366, which was important for 5H10 neutralization but less so for 7H2 or polyclonal anti-EIII neutralization. None of the T366 mutants were strongly affected in terms of either Vero growth or mouse virulence. While it seems unlikely that a T366 mutant could escape from the pressure of a polyclonal response to WVN EIII, it is does appear that selective pressure from a monoclonal antibody could lead to the emergence of a T366 mutant within a pool of virus. It is worth noting that a naturally occurring T366A variant does exist, confirming that variation at residue T366 is a real possibility and that the neutralization resistance

demonstrated by these mutants could pose an issue for an anti-WNV EIII monoclonal antibody therapy.

The A367 mutants replicated to high titer in Vero cells and are virulent in mice. The one acidic substitution tested, A367D, had a weak neutralization phenotype with both 7H2 and the anti-WNV EIII serum, although it retained strong neutralization by 5H10. Overall, the changes to A367 had scattered impacts on 5H10 and polyclonal anti-EIII neutralization but only minimal impacts on 7H2 neutralization. It appears that A367 is capable of causing antibody escape and that changes are well tolerated, raising the possibility that it may be possible to select for resistant A367 mutants from a wild-type population.

Residue N368 has only minor antigenic importance. Changes to N368 caused scattered and minor loss of neutralization by 5H10 and polyclonal anti-EIII serum, but had essentially no impact on 7H2 neutralization. Functionally, four of the seven N368 mutants were significantly attenuated in mice. Two of these attenuated mutants, N3698K and N368T, grew to a peak titer of within $0.1\log_{10}$pfu/ml of wild-type in Vero cells, but allowed 38% and 88% survival in mice, respectively. The N368I and N368Y mutants grew to $0.8\text{-}0.9\log_{10}$pfu/ml lower titers than wild-type in Vero cells, and they allowed 63% and 100% survival, respectively. This may mean that residue N368 has a slightly different role when replicating in an *in vitro* primate cell compared to an *in vivo* mouse cell, perhaps due to utilization of different receptors. The remaining mutants replicated normally in Vero cells and were virulent in mice. There is no obvious pattern separating the attenuated mutants from the virulent mutants in terms of category, size, pI, or hydropathy (See Appendix B).

In summary, there appeared to be a range of distinct roles for the residues of the surface loops, although all were involved in antigenicity of EIII to at least some extent. Structurally and functionally, residue C305 in the N-terminal loop and residues G331 and D333 in the BC loop appear to be critical given that no or very few, primarily

conservative, mutations at those sites resulted in viable virus in Vero cells. Changes at residue N368 had no impact on viability in Vero cells, but did result in attenuation in mice. Mutations at other surface loop residues were able to vary with no strong consequences. Antigenically, the workload appeared to be more evenly spread: 100% of S306, K307, T330, and T366 mutants resulted in moderate or weak neutralization by 5H10, 100% of K307 mutants resulted in moderate or weak neutralization by 7H2, and 100% of S306, K307, and T330 mutants resulted in moderate or weak neutralization by polyclonal anti-EIII serum. A367 and N368 were close, with 83% and 66% of mutants resulting in moderate to weak polyclonal anti-EIII neutralization, respectively. Residues K307 and T332 were thus especially important, as they were the only two that resulted in widespread escape from neutralization by both 5H10 and 7H2 monoclonal antibodies and by polyclonal anti-EIII serum. Furthermore, the fact that S306 and T330 were important to neutralization by 5H10 and polyclonal anti-EIII serum but not by 7H2 might indicate that the rabbit neutralizing antibody response to recombinant WNV EIII might be more "5H10-like" than "7H2-like".

Taken together, this seems to indicate that residues C305 and N368 have not been selected for antibody resistance because they are only moderately important in an antigenic sense but are extremely important in a structural and/or functional sense. Residues G331 and D333 contribute to the epitopes recognized by neutralizing antibodies , but they have not been selected for antibody neutralization resistance because they are too important functionally and any changes acquired for the sake of antibody escape would most probably be too costly in terms of fitness. The remaining residues that have not been selected for resistance to antibody neutralization are A308 and T366. The reason for A308 not being selected for neutralization resistance may be that it has only scattered antigenic importance so the majority of mutations acquired are unlikely to be selected for under antigenic pressure. T366, on the other hand, resulted in widespread resistance to 5H10 neutralization but only scattered resistance to neutralization 7H2 and

polyclonal anti-EIII serum, suggesting that its selection under antigenic pressure would be highly dependent on which antibody was used (as opposed to K307 or T332, which could likely be selected for by most anti-EIII surface loop antibodies).

Chapter 6: Homologous and Heterologous Protection from WNV EIII Subunit Vaccination with Variable Surface Loop Residues

RATIONALE AND APPROACH

Several promising studies have demonstrated that vaccination with WNV EIII can protect against lethal challenge in mouse models.(161-165) However, in each one of these studies the amino acid sequence of the EIII protein used for vaccination exactly matched the amino acid sequence of EIII in the challenge virus; no attempt was made to address the impact of naturally occurring EIII variation or the potential for the selection of an EIII variant within an infected patient with previous vaccination. Previous studies of WNV demonstrated that single amino acid differences in EIII can impact *in vitro* neutralization by anti-WNV EIII serum.(139) Although the *in vivo* impact of EIII amino acid sequence variation on neutralization by polyclonal anti-EIII serum has not been evaluated for WNV, it has been evaluated for related flaviviruses. One study used EIII from two strains of DENV-3 virus for vaccination of mice and demonstrated that small differences in EIII sequence can impact antigenicity and immunogenicity with dot blot, ELISA, PRNT, and survival data.(172) Similar results were from serum monkeys immunized with EIII from DENV-1 or DENV-2 virus and then analyzed via PRNT for their ability to neutralize viruses of the same species but different genotype.(173) This work aimed to address whether differences in WNV EIII sequence affect *in vivo* protection.

Groups of 3-4-week-old female Swiss Webster mice were vaccinated with WNV NY99 EIII, WNV SA58 EIII, or a PBS control. All immunizations were given with Freund's incomplete adjuvant. These two strains were chosen because they are from the two different WNV lineages responsible for major outbreaks of human disease (NY99 is linage 1 and SA58 is lineage 2) and because SA58 naturally has the T332K change that

results in *in vitro* escape from neutralization by anti-WNV EIII serum.(139) There are two additional differences in the EIII sequences of NY99 and SA58: NY99 has L312 while SA58 has A312, and NY99 has A369 while SA58 has S369. Neither of these two residues are thought to contribute strongly to antigenicity.(139) Vaccination took place at two week intervals with doses of 8µg and 25µg. The first dose was lower than the second dose because of accidental sample loss during the emulsification process for the first dose. Two weeks after the final dose, a small blood sample was collected to measure levels of binding and neutralizing antibody. Binding antibody levels were used to divide vaccinated animals into the homologous and heterologous challenge groups such that each group had approximately even numbers of high, medium, and lower responders. Survival of homologous and heterologous challenge was observed, and relationships between antibody levels and survival were examined.

Of note, when the experiment was initially conducted, none of the PBS-vaccinated, NY99ic-challenged mice died, but all four of the PBS-vaccinated, SA58-challenged mice died. It was initially feared that an error had been made during the sample preparation and that the NY99ic-challenged mice had not actually received any virus. However, when pre- and post-challenge serum samples from the PBS-vaccinated, NY99ic-challenged mice were analyzed via ELISA it was seen that the NY99ic-challenged animals did, in fact, seroconvert (data not shown). It was later discovered that the supplier had discovered *Streptococcus spp.* Group B and *Klebsiella pneumoniae* in some of their animal colonies around the time this experiment was conducted. Whether or how these bacteria might have affected the immune system of the mice and led to their resistance to NY99ic (but not SA58) infection is not known. However, the vaccination and challenge schedule for NY99ic was repeated with a second set of animals that succumbed to infection as expected, and the data from that second experiment is included here for all NY99ic-challenged cohorts.

RESULTS

Antibody Response to WNV EIII Vaccination

NY99 EIII vaccination generated a strong anti-EIII IgG binding antibody response (Figure 23 and Table 26). The homologously binding antibody signal was significantly higher than the heterologously binding antibody signal at all dilutions measured by the ELISA.

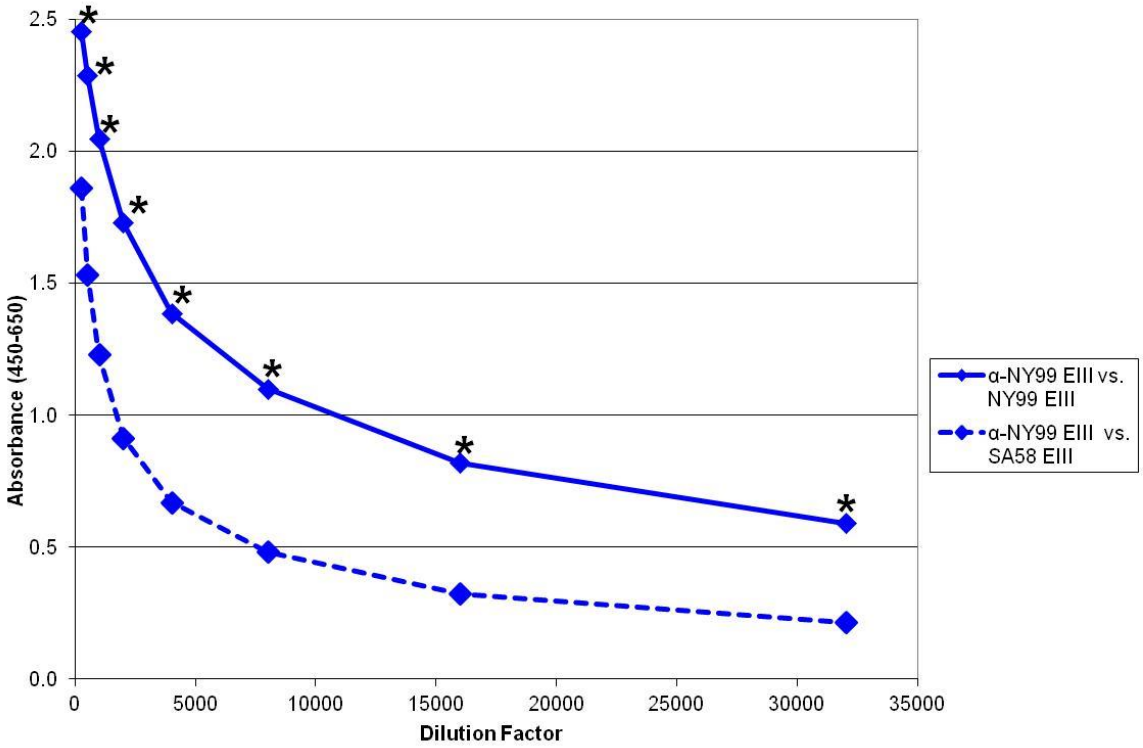

Figure 23: Homologous and Heterologous Binding Antibody Generated by NY99 EIII Vaccination

ELISA results demonstrating the levels of anti-NY99 EIII and anti-SA58 EIII binding antibody generated by NY99 EIII vaccination. * = p-value <0.05 by unpaired Student's T-test.

Serum Group	ELISA Antigen	Logarithmic Equation	R^2 Value	Binding IgG Titer
α-NY99 EIII	NY99 EIII	y=-0.405ln(x)+4.7677	0.9946	87,079
α-NY99 EIII	SA58 EIII	y=-0.344ln(x)+3.6405	0.9724	24,069

Table 26: Binding IgG Antibody Titers Generated by NY99 EIII Vaccination

Reciprocal titers of binding IgG generated by NY99 EIII vaccination. Titer given as the dilution factor at which the absorbance value is 0.17 (twice the highest absorbance measured from PBS-vaccinated mice).

Vaccination with SA58 EIII produced a more balanced homologous and heterologous binding antibody response than NY99 EIII vaccination at all dilutions tested (Figure 24). The levels of anti-NY99 EIII binding antibody generated by SA58 EIII vaccination compared to NY99 EIII vaccination were statistically indistinguishable at all but the most concentrated serum dilution. The same is true for anti-SA58 EIII binding antibody levels. However, the ratios of the calculated anti-NY99 EIII titers to anti-SA58 EIII titers were quite similar (3.6 for NY99 EIII-vaccinated mice and 3.2 for SA58 EIII-vaccinated mice) (Table 27). It is interesting to note that both vaccinations induce higher binding antibody levels against NY99 EIII than SA58 EIII. Results of the ELISA using anti-PBS serum are not shown, but confirmed that the negative control groups had no detectable antibody able to bind recombinant EIII protein from either WNV strain.

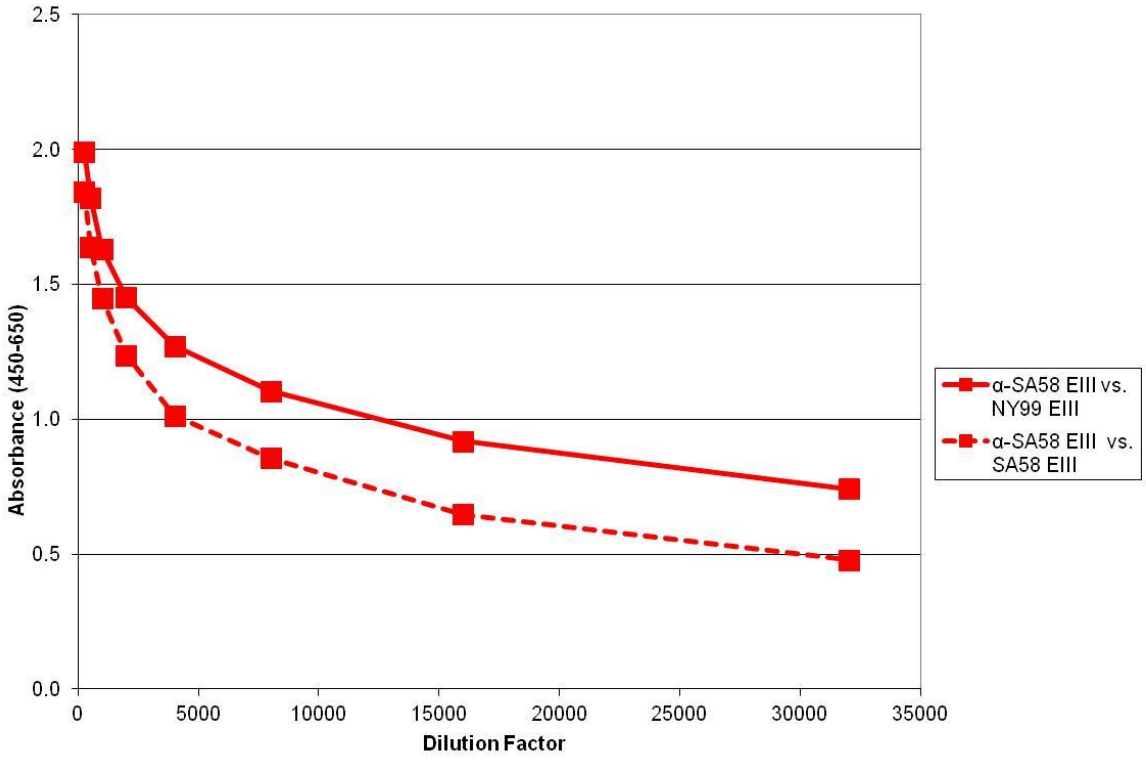

Figure 24: Homologous and Heterologous Binding Antibody Generated by SA58 EIII Vaccination

ELISA results demonstrating the levels of anti-NY99 EIII and anti-SA58 EIII binding antibody generated by SA58 EIII vaccination. * = p-value <0.05 by unpaired Student's T-test.

Serum Group	ELISA Antigen	Logarithmic Equation	R^2 Value	Binding IgG Titer
α-SA58 EIII	NY99 EIII	y=-0.258ln(x)+3.4169	0.9999	292,109
α-SA58 EIII	SA58 EIII	y=-0.283ln(x)+3.3982	0.9989	89,955

Table 27: Binding IgG Antibody Titers Generated by SA58 EIII Vaccination

Reciprocal titers of binding IgG generated by SA58 EIII vaccination. Titer given as the dilution factor at which the absorbance value is 0.17 (twice the highest absorbance measured from PBS-vaccinated mice).

PRNT results from pre-challenge serum demonstrated that both NY99 EIII and SA58 EIII vaccination generated antibody capable of neutralizing WNV (Table 28). As was the case with binding antibody, the NY99 EIII vaccination resulted in a larger difference in homologous vs. heterologous antibody levels than SA58 EIII vaccination, and the anti-SA58 antibody was lower than the anti-NY99 antibody with both vaccinations. Those trends, while interesting, had no statistical significance (one-way ANOVA p-value for non-PBS-vaccinated cohorts = 0.419).

Vaccine	$PRNT_{50}$ vs. NY99 Virus	$PRNT_{50}$ vs. SA58 Virus
NY99 EIII	197±196	137±161
SA58 EIII	121±154	117±148
PBS	<40	<40

Table 28: Homologous and Heterologous Neutralizing Antibody Generated by NY99 EIII and SA58 EIII Vaccination

PRNT results demonstrating the levels of anti-NY99 and anti-SA58 neutralizing antibody generated by NY99 EIII and SA58 EIII vaccination.

Survival of Homologous or Heterologous WNV Challenge

Both the NY99 challenge and SA58 challenge resulted in lower heterologous protection compared to homologous protection (Table 29). For both sets, homologous challenge resulted in 90% survival and heterologous protection resulted in approximately 70% survival. Survival rates for both homologous and heterologous protection were significantly different from the PBS control vaccination, but were not statistically different from each other (NY99-challenged mice p=0.239, SA58-challenged mice p=0.189). There was statistically significant variation in AST between all six cohorts (one-way ANOVA p=0.000). According to Bonferroni post-hoc analysis, AST for the

heterologous SA58 EIII-vaccinated, NY99-challenged cohort was significantly different from both the heterologous NY99 EIII-vaccinated, SA58-challenge cohort (p=0.003) and both of the PBS-vaccinated cohorts (p=0.001). Note that the homologously challenged cohorts were not included in the post-hoc analysis due to having only a single data point.

Vaccine	Challenge	Survival		AST±SD
		%	Alive/Total	
NY99 EIII	NY99	90	9/10	20.0±N/A
SA58 EIII	NY99	70	7/10	15.7±2.5
PBS	NY99	20	1/5	9.3±1.0
NY99 EIII	SA58	67	6/9	10.0±1.0
SA58 EIII	SA58	90	9/10	12.0±N/A
PBS	SA58	0	0/4	9.0±0.8

Table 29: Homologous and Heterologous Protection Following WNV EIII Vaccination

Survival data for NY99 and SA58 homologous and heterologous protection following EIII vaccination in 3-4-week-old Swiss Webster mice. AST is in days.

Relationship Between Survival Outcomes and Antibody Response

Following the results of the challenge, the ELISA and PRNT data from the pre-challenge serum was re-analyzed to look for any potential patterns in which mice survived the challenge and which mice succumbed to infection. First, the mice that were vaccinated with NY99 EIII and challenged with the homologous NY99 EIII virus, resulting in 90% survival, were analyzed (Figure 25). In this group, the total anti-EIII IgG binding antibody response of the surviving mice against NY99 EIII was stronger than the response against SA58 EIII. It was also observed that the single mouse that succumbed to homologous NY99 challenge had very low levels of binding antibody against either NY99 EIII or SA58 EIII. There was no statistically significant variation between the four datasets in Figure 25, however this may be due to the fact that there is only a single reading in each of the two 'anti-NY99 EIII vs. NY99 deaths' datasets. In fact, the calculated NY99 EIII-binding IgG titer of the surviving animals was 15.6-fold

higher than the NY99 EIII-binding IgG titer of the mouse that succumbed to infection (Table 30)

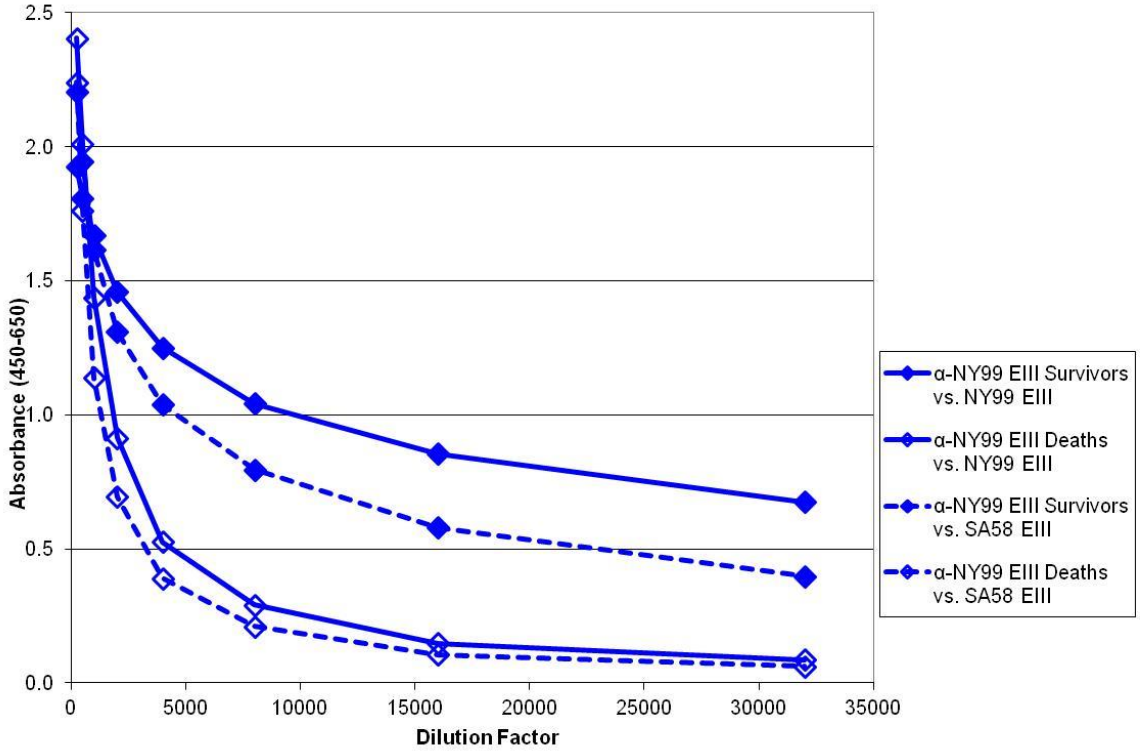

Figure 25: Homologous and Heterologous Binding Antibody Generated by NY99 EIII Vaccination in Homologous NY99 Challenge Cohort

ELISA results demonstrating the levels of anti-NY99 EIII and anti-SA58 EIII binding antibody generated by NY99 EIII vaccination in cohort of mice that received homologous NY99 challenge. Closed markers = survivors. Open markers = Deaths. Solid lines = NY99 EIII binding antibody. Dashed lines = SA58 EIII binding antibody. * = $p < 0.05$ by one-way ANOVA.

Serum Group	ELISA Antigen	Logarithmic Equation	R^2 Value	Binding IgG Titer	Fold Difference (Survivors / Deaths)
α-NY99 EIII vs. NY99 Virus, Survivor(s)	NY99 EIII	y=-0.268ln(x)+3.4675	0.9945	220,600	15.6
α-NY99 EIII vs. NY99 Virus, Death(s)	NY99 EIII	y=-0.504ln(x)+4.9864	0.9377	14,134	
α-NY99 EIII vs. NY99 Virus, Survivor(s)	SA58 EIII	y=-0.381ln(x)+4.2669	0.9926	46,771	3.1
α-NY99 EIII vs. NY99 Virus, Death(s)	SA58 EIII	y=-0.457ln(x)+4.4566	0.9043	15,052	

Table 30: Binding IgG Antibody Titers in NY99 EIII-Vaccinated, NY99-Challenged Mice

Reciprocal titers of binding IgG generated by NY99 EIII vaccination in mice that were subsequently challenged with NY99 virus. Titer given as the dilution factor at which the absorbance value is 0.17 (twice the highest absorbance measured from PBS-vaccinated mice).

Next, the mice that received the SA58 EIII vaccination and the heterologous NY99 challenge were examined (Figure 26). Unlike the mice that succumbed to homologous NY99 challenge, the mice the succumbed to heterologous NY99 challenge did not have a low anti-EIII IgG binding antibody response. In fact, the mice that succumbed to infection had slightly higher anti-EIII IgG binding antibody responses than the mice that survived. Again, there was no statistically significant difference between the four datasets. Calculated anti-NY99 EIII and anti-SA58 EIII binding IgG titers were approximately equal for the surviving mice and the mice that succumbed (Table 31).

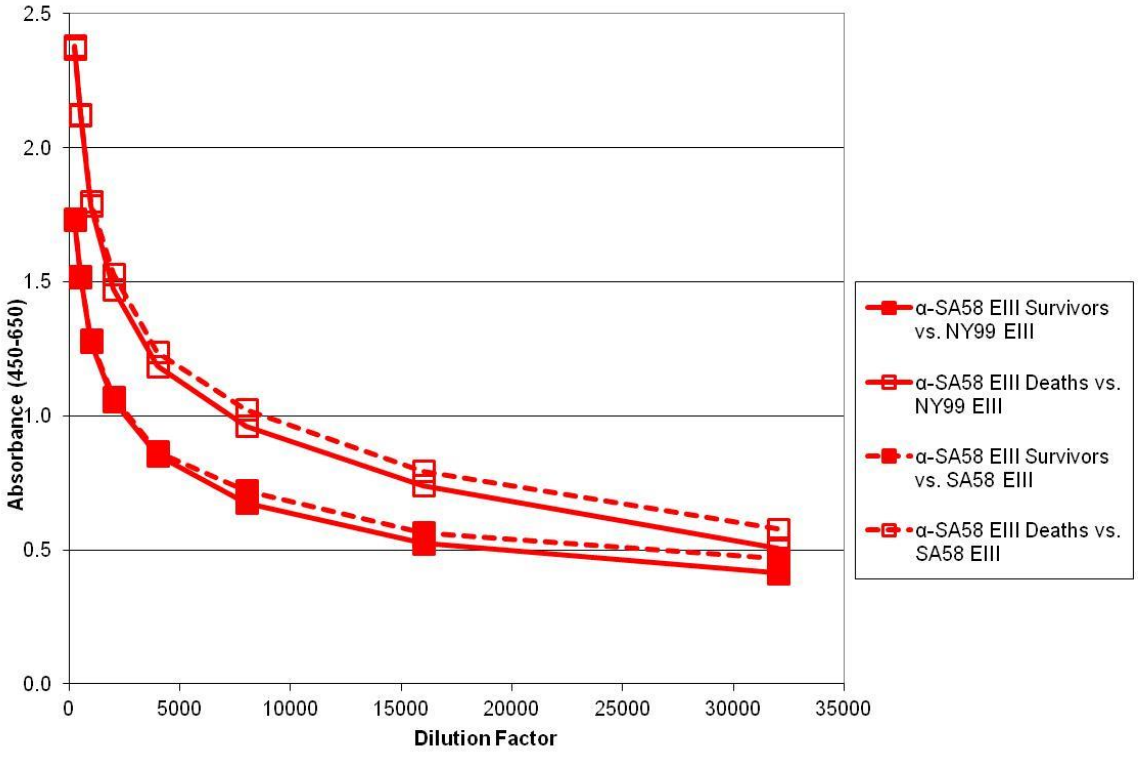

Figure 26: Homologous and Heterologous Binding Antibody Generated by SA58 EIII Vaccination in Heterologous NY99 Challenge Cohort

ELISA results demonstrating the levels of anti-NY99 EIII and anti-SA58 EIII binding antibody generated by SA58 EIII vaccination in cohort of mice that received heterologous NY99 challenge. Closed markers = survivors. Open markers = Deaths. Solid lines = NY99 EIII binding antibody. Dashed lines = SA58 EIII binding antibody. * = $p < 0.05$ by one-way ANOVA.

Serum Group	ELISA Antigen	Logarithmic Equation	R^2 Value	Binding IgG Titer	Fold Difference (Survivors / Deaths)
α-SA58 EIII vs. NY99 Virus, Survivor(s)	NY99 EIII	y=-0.278ln(x)+3.2167	0.9888	57,489	0.9
α-SA58 EIII vs. NY99 Virus, Death(s)	NY99 EIII	y=-0.391ln(x)+4.5017	0.9942	64,765	
α-SA58 EIII vs. NY99 Virus, Survivor(s)	SA58 EIII	y=-0.266ln(x)+3.1449	0.9858	71,958	0.9
α-SA58 EIII vs. NY99 Virus, Death(s)	SA58 EIII	y=-0.375ln(x)+4.4113	0.9957	81,645	

Table 31: Binding IgG Antibody Titers in SA58 EIII-Vaccinated, NY99-Challenged Mice

Reciprocal titers of binding IgG generated by SA58 EIII vaccination in mice that were subsequently challenged with NY99 virus. Titer given as the dilution factor at which the absorbance value is 0.17 (twice the highest absorbance measured from PBS-vaccinated mice).

The binding antibody response of the NY99 EIII vaccinated, SA58 virus challenged cohort was also analyzed (Figure 27). In this heterologous challenge group, both the survivors and the mice that succumbed generated more homologous anti-EIII IgG binding antibody against NY99 EIII than heterologous anti-EIII IgG binding antibody against SA58 EIII. The mice that succumbed did have a lower level of anti-EIII IgG binding antibody against NY99 EIII, but they did not have especially low levels of anti-EIII IgG binding antibody against SA58 EIII. However, unlike the previous two groups which had been NY99-challenged, these NY99 EIII-vaccinated, SA58-challenged dataset did have significant variation between the groups, and there was significance and all dilutions tested. This is despite the fact that calculated binding IgG titers between surviving and succumbing mice were fairly even (Table 32) These calculated titer datapoints are consistent, however, with the lack of significance between the absorbance signals of the surviving and succumbing mice for either EIII antigen at any dilution tested.

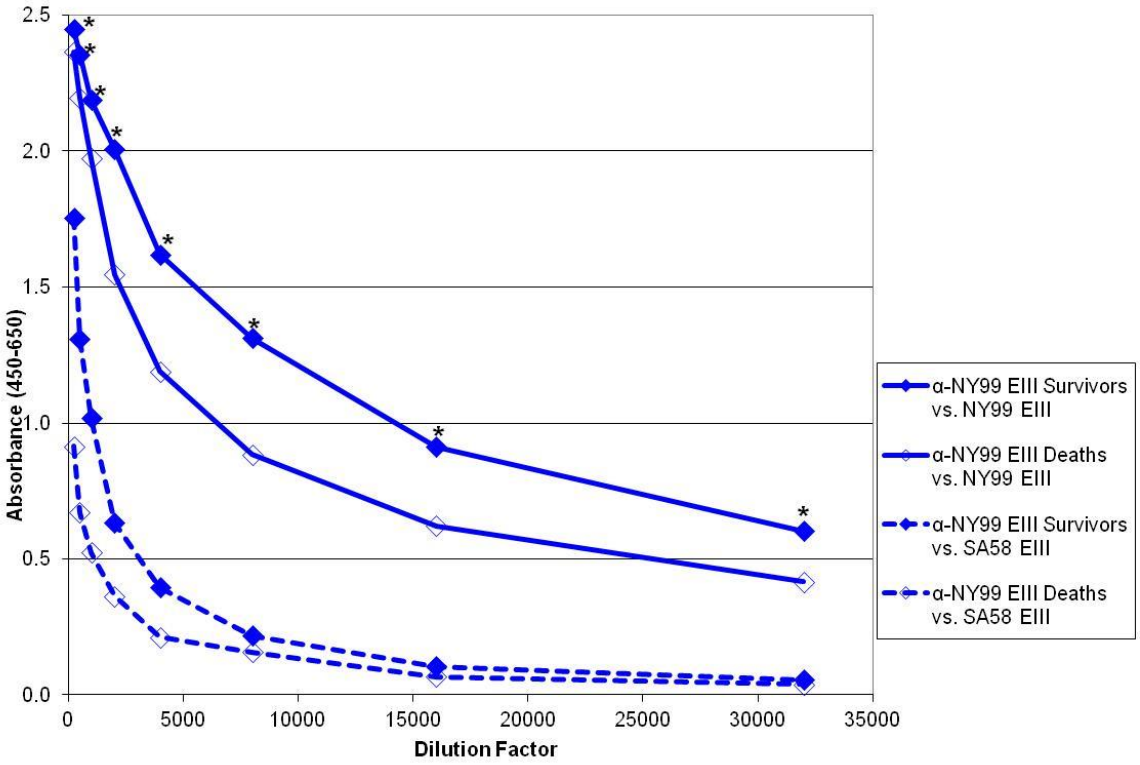

Figure 27: Homologous and Heterologous Binding Antibody Generated by NY99 EIII Vaccination in Heterologous SA58 Challenge Cohort

ELISA results demonstrating the levels of anti-NY99 EIII and anti-SA58 EIII binding antibody generated by NY99 EIII vaccination in cohort of mice that received heterologous SA58 challenge. Closed markers = survivors. Open markers = Deaths. Solid lines = NY99 EIII binding antibody. Dashed lines = SA58 EIII binding antibody. * = $p < 0.05$ by one-way ANOVA.

Serum Group	ELISA Antigen	Logarithmic Equation	R^2 Value	Binding IgG Titer	Fold Difference (Survivors / Deaths)
α-NY99 EIII vs.SA58 Virus, Survivor(s)	NY99 EIII	y=-0.397ln(x)+4.8392	0.9666	128,182	2.5
α-NY99 EIII vs.SA58 Virus, Death(s)	NY99 EIII	y=-0.432ln(x)+4.8598	0.9902	51,845	
α-NY99 EIII vs.SA58 Virus, Survivor(s)	SA58 EIII	y=-0.353ln(x)+3.4915	0.9373	12,202	1.5
α-NY99 EIII vs.SA58 Virus, Death(s)	SA58 EIII	y=-0.179ln(x)+1.7874	0.9434	8,398	

Table 32: Binding IgG Antibody Titers in NY99 EIII-Vaccinated, SA58-Challenged Mice

Reciprocal titers of binding IgG generated by NY99 EIII vaccination in mice that were subsequently challenged with SA58 virus. Titer given as the dilution factor at which the absorbance value is 0.17 (twice the highest absorbance measured from PBS-vaccinated mice).

Finally, the binding antibody response of the SA58 EIII vaccinated, SA58 challenged cohort was analyzed (Figure 28). The homologous survivors had a strong anti-NY99 EIII and anti-SA58 EIII binding antibody response. The mouse that died, on the other hand, had virtually undetectable binding antibody levels against both NY99 EII and SA58 EIII. There was significant variation between the four datasets at the two most concentrated serum dilutions, however because there was only a single mouse in the 'succumbed' categories post-hoc Bonferroni analysis could not be performed to confirm the significant difference between the binding antibody response of the surviving and succumbing mice. That difference is, however, strongly supported by the binding IgG endpoint titer (Table 33).

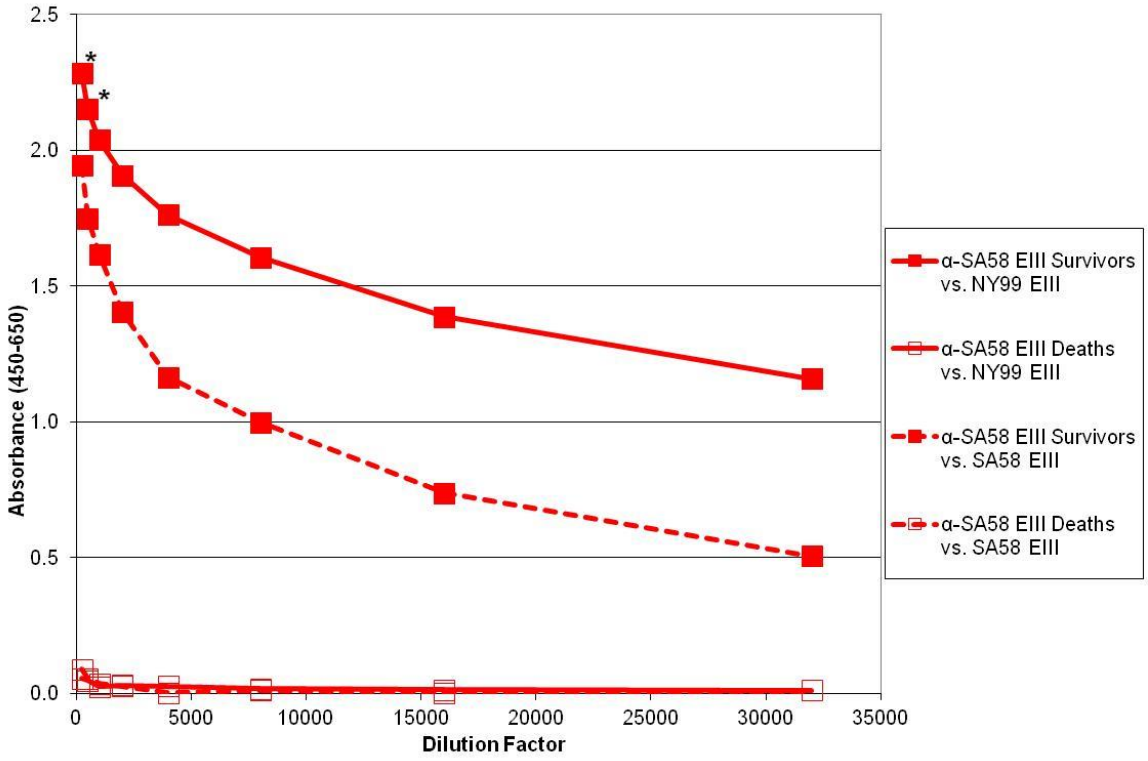

Figure 28: Homologous and Heterologous Binding Antibody Generated by SA58 EIII Vaccination in Homologous SA58 Challenge Cohort

ELISA results demonstrating the levels of anti-NY99 EIII and anti-SA58 EIII binding antibody generated by SA58 EIII vaccination in cohort of mice that received homologous SA58 challenge. Closed markers = survivors. Open markers = Deaths. Solid lines = NY99 EIII binding antibody. Dashed lines = SA58 EIII binding antibody. * = $p < 0.05$ by one-way ANOVA.

Serum Group	ELISA Antigen	Logarithmic Equation	R^2 Value	Bindng IgG Titer	Fold Difference (Survivors / Deaths)
α-SA58 EIII vs.SA58 Virus, Survivor(s)	NY99 EIII	y=-0.226ln(x)+3.5801	0.9826	3,573,078	~40,000,000,000
α-SA58 EIII vs.SA58 Virus, Death(s)	NY99 EIII	y=-0.008ln(x)+0.0954	0.8725	0	
α-SA58 EIII vs.SA58 Virus, Survivor(s)	SA58 EIII	y=-0.296ln(x)+3.6169	0.9947	114,112	165,300
α-SA58 EIII vs.SA58 Virus, Death(s)	SA58 EIII	y=-0.017ln(x)+0.1637	0.8492	1	

Table 33: Binding IgG Antibody Titers in SA58 EIII-Vaccinated, SA58-Challenged Mice

Reciprocal titers of binding IgG generated by SA58 EIII vaccination in mice that were subsequently challenged with SA58 virus. Titer given as the dilution factor at which the absorbance value is 0.17 (twice the highest absorbance measured from PBS-vaccinated mice).

After analyzing the importance of anti-EIII IgG binding antibody, the impact of neutralizing antibody on the outcome of homologous or heterologous challenge was examined (Table 34). Similar to the binding antibody results, it was found that the mice the succumbed to homologous challenge had very low neutralizing antibody titers that were either below or just at the limit of detection of 40. The mice that succumbed to heterologous challenge, on the other hand, had strong neutralizing antibody responses. The NY99 EIII vaccinated, SA58 challenged mice that succumbed to infection had average $PRNT_{50}$ titers of 267 against NY99 and 140 against SA58. The SA58 EIII vaccinated, NY99 challenged mice that succumbed to infection had average $PRNT_{50}$ titers of 273 against NY99 and 293 against SA58. There was no statistically significant variation in $PRNT_{50}$ values between the groups (one-way ANOVA p=0.156)

Vaccine	Challenge	Outcome	$PRNT_{50}$ vs. NY99 Virus	$PRNT_{50}$ vs. SA58 Virus
NY99 EIII	NY99	Alive (n=9)	140±210	176±211
NY99 EIII	NY99	Dead (n=1)	40±0	40±0
SA58 EIII	NY99	Alive (n=7)	123±102	57±56
SA58 EIII	NY99	Dead (n=3)	273±325	293±303
PBS	NY99	Alive (n=1)	<40	<40
PBS	NY99	Dead (n=4)	<40	<40
NY99 EIII	SA58	Alive (n=6)	273±209	93±73
NY99 EIII	SA58	Dead (n=3)	267±92	140±159
SA58 EIII	SA58	Alive (n=9)	80±101	109±93
SA58 EIII	SA58	Dead (n=1)	<40	<40
PBS	SA58	Alive (n=0)	N/A	N/A
PBS	SA58	Dead (n=4)	<40	<40

Table 34: Homologous and Heterologous Neutralizing Antibody Generated by NY99 EIII and SA58 EIII Vaccination and Analyzed by the Result of Homologous or Heterologous Challenge

PRNT results demonstrating the impact of neutralizing antibody on the outcome of homologous or heterologous challenge following NY99 EIII or SA58 EIII vaccination.

DISCUSSION

This study demonstrated that the exact sequence of the WNV EIII immunizing antigen has important implications for immunogenicity and protection. Immunization with either recombinant protein generated higher levels of anti-EIII IgG binding antibody against NY99 EIII, suggesting that NY99 EIII might be more antigenic than SA58 EIII. Immunization with NY99 EIII generated higher levels of anti-EIII IgG binding antibodies against both NY99 EIII and SA58 EIII than did SA58 EIII vaccination, suggesting that NY99 EIII might be more immunogenic than SA58 EIII. A similar pattern in PRNT results also suggested that NY99 EIII may be more immunogenic than SA58 EIII in Swiss Webster mice. This was consistent with the earlier studies of DENV EIII vaccination, which demonstrated that different strains generate different strengths of antibody response and that homologous binding and neutralization is not always stronger then heterologous binding and neutralization.(172, 173)

Although not statistically significant, there was a trend of decreased heterologous protection, with a difference of approximately 20%. Mice that were vaccinated with WNV NY99 EIII and challenged with either WNV NY99 or Japanese encephalitis virus Beijing-1 also demonstrated a 20% loss of protection with the heterologous challenge.(162) The NY99 EIII and SA58 EIII sequences differed at 3 of 115 residues, while NY99 EIII and Japanese encephalitis virus Beijing-1 differed at 28 of 105 residues including the equivalents of residues 312, 332, and 369. The lack of statistical significance may be due to the wide range of strong to weak responders in each cohort of Swiss Webster mice. Although this variability can make interpretation of data from outbred mice more challenging, it more accurately represents the genetic diversity in the human population than an inbred model would.

The mice the succumbed to homologous infection generated a weak antibody response to vaccination. The mice that succumbed to heterologous infection, on the other

hand, produced normal levels of binding and neutralizing antibodies. This could indicate that even individuals who seroconvert following EIII vaccination could be at risk of infection if changes at key antigenic residues (T332) are tolerated with little or no apparent loss of virulence. Given that naturally occurring T332 variants have been detected in both lineage 1 and lineage 2 strains, on multiple continents, and in multiple host species over the course of decades, the potential impact of T332 variation in particular should be taken into consideration when evaluating the potential of an EIII subunit vaccine.(192-194, 196, 197)

Chapter 7: Overall Conclusions and Future Directions

This study analyzed the functional and antigenic importance of specific surface residues in WNV EIII. It was found that residue 312, which is located immediately following the C-terminus of the A strand, contributed very little to antibody neutralization or the functional role of EIII. Within the surface loops, all of the residues except for C305 tolerated at least some change. Given that C305 forms a disulfide bond with C336, it was expected that all attempted substitutions at that site would be lethal to the virus.(142) Of the remaining residues studied (S306, K307, A308, T330, G331, T332, D333, T366, A367, and N368), all had at least some impact on antibody neutralization, although not necessarily for every substitution or antibody tested. Residues T332 and K307 seemed to be the most important residues from an antigenic standpoint because substitutions at those residues almost universally resulted in escape from neutralization by polyclonal serum raised against recombinant WNV EIII and from the two monoclonal antibodies 5H10 and 7H2. Residues S306, T330 and T366 were important for neutralization by 5H10 but not as much for 7H2. Residues S306 and T330 were also important for anti-EIII serum neutralization, suggesting that neutralizing antibodies the immune response to an EIII-subunit vaccine (at least in a rabbit) are skewed more toward the 5H10 epitope than the 7H2 epitope. It is also consistent with 5H10 and 7H2 having overlapping but not identical epitopes. Importantly, changes at residues T332 and K307 were well tolerated by the virus, and changes at residue T332 have been found in naturally occurring strains, and led to resistance to neutralization by monoclonal and polyclonal anti-EIII antibodies both *in vitro* and *in vivo*.(144, 192-197)

While impacts on antibody-mediated neutralization were widespread, mutations at only a few residues led to decreased growth in cell culture or attenuation in a mouse model. Residues G331 and D333 only tolerated a few of the attempted substitutions, and, while N368 tolerated all attempted substitutions, changes at any of those three residues

led to attenuation in mice (Figure 29). When mapped onto a NMR structure of WNV EIII, these residues formed a continuous patch despite their separation in the sequence of WNV EIII. This patch appeared to form a "canyon" that ran between the more prominent "peak" residues K307, T330, T332, and T366. While the peaks played a more important antigenic role, the canyon appeared to be more critical to the structure and function of WNV EIII. This may be due to a functional role (the canyon residues are interacting with the receptor) or a structural role (the peaks are interacting with the receptor, but changing the canyon residues alters the position of the peaks in some critical way).

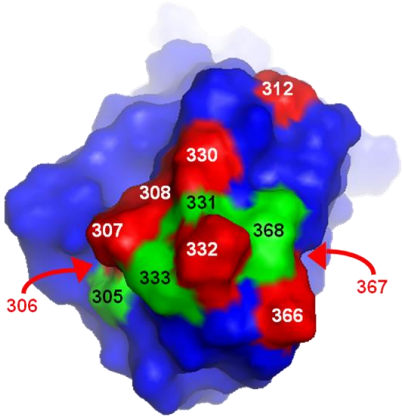

Figure 29: Location of Virulence and Viability Determinants in WNV EIII

Green = Known virulence/viability determinants. Red = Neighboring residues. Blue = Other EIII residues. Image generated using the PyMol Graphics System, Version 1.3, Schrödinger, LLC with PDB ID 1S6N.

It is worth noting that, although the G331/D333/N368 functional patch appears continuous in the NMR structure of recombinant WNV EIII, that is not necessarily the case in all available structures that incorporate WNV EIII (Figure 30). In fact, two of the eight x-ray diffraction- and electron microscopy- generated structures that contain WNV EIII do not even show residue G331 as being surface exposed and thus available to form a continuous patch. That NY99ic was viable with all attempted N368 mutations (with half of them attenuating the virus in mice) while G331 and D333 were extremely restricted in Vero cells (and highly attenuated in mice) might be explained by the slight physical separation of N368 from G331/D333 in the x-ray diffraction- and electron microscopy-derived structures.

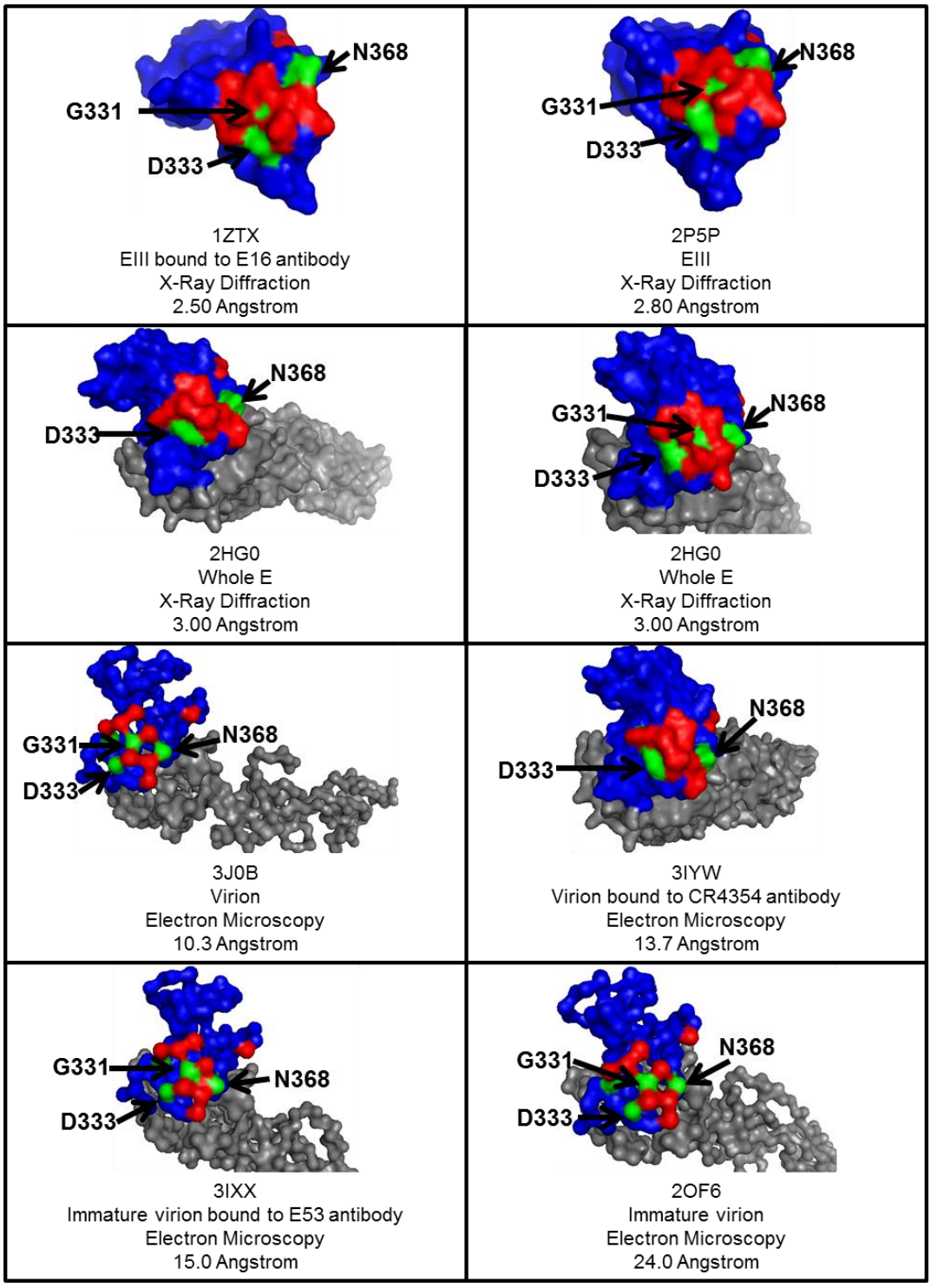

Figure 30: X-Ray Diffraction and Electron Microscopy Structures Containing WNV EIII

Grey = EI+EII, blue = EIII residues not addressed in this dissertation, green = structurally or functionally critical residues (C305, G331, D333, and N368), red = structurally and functionally non-critical residues (S306, K307, A308, T330, T332, T366, and A367). Residues G331, D333, and N368 are labeled when visible. Bound antibodies are not included in the images. Images generated using the PyMol Graphics System, Version 1.3, Schrödinger, LLC.

The functional explanation is consistent with the so-called canyon hypothesis, first put forth by Michael Rossmann in 1985 in the context of the common cold virus.(221) Rossmann suggested that, at their 5-fold axes of symmetry, the structural proteins of picornaviruses form deep (~25 angstrom), narrow canyons that allow access by the cellular receptor protein but not the Fab fragment of antibodies. This would allow the virus to avoid immune detection at its critical receptor binding site, mitigating the selective pressure to mutate the receptor binding residues in the canyon to avoid antibody binding at the cost of decreased receptor binding ability. Because the interaction with the cellular receptor took place in the canyon, the peaks would be left free to mutate in response to the selective pressures of the immune response.(221-224) Four major lines of evidence in support of the canyon hypothesis in *Picornaviridae* have been proposed:(223)

1. The canyon residues are better conserved than the peak residues, consistent with their high functional importance and low antigenic importance.(225, 226)
2. Plant and insect viruses do not generally have these canyons, perhaps because they are not exposed to the selective pressure of neutralizing antibodies and thus do not need to hide their receptor-binding residues in a canyon.(227, 228)
3. Mutation of canyon residues affects receptor binding.(229)
4. Antiviral compounds are capable of blocking receptor binding by inducing conformational changes in the canyon residues.(230)

One key difference between the proposed WNV "canyon" and the picornavirus canyon is the depth: the picornavirus canyon is approximately 25 angstroms deep, while the difference between the G331/D333/N368 patch and the surrounding K307/T330/T332/T366 "peaks" is closer to 4-5 angstroms, and the peaks do not completely encircle the functional residues. Influenza, however, has also been proposed

to use a canyon- like strategy to protect its receptor pocket, and that canyon is only 8 angstroms deep.(231) Given that the surface of the flavivirus virion is relatively flat, lacking the spike proteins found in so many viruses, perhaps WNV has been able to achieve the same end (protecting the functional receptor binding residues that must be conserved by surrounding them with protruding residues that can change in response to antibody-mediated selective pressures with minimal impact on viral fitness) using a modified means more suited to a virus with a smoother surface. Furthermore, as was the case with the picornaviruses, the key determinants of viability and virulence are much more strongly conserved between viruses than the neighboring residues are (Table 35). Although the experiments described in this dissertation did not directly address the question of receptor binding, they demonstrated that the "canyon" residues are more important to WNV viability and virulence than the "peak" residues, and given WNV EIII's putative receptor binding function it seems likely that changes in virulence and viability are a function of changes in receptor binding ability.(81, 191) Although insect-only flaviviruses are known to exist, structural data about the envelope protein or whole virion is not currently available. Although the previously described importance of glycosylation makes it unlikely that DC-SIGN is interacting with the EIII canyon, a cryo-EM reconstruction of DENV-2 with DC-SIGN demonstrated that DC-SIGN bound the glycosylation sites on E in such a way that left EIII available to bind some other receptor.(77, 78, 232) The proposed receptor $\alpha_v\beta_3$ integrin, on the other hand, does bind EIII, and the antagonistic effect of soluble EIII on WNV infection of Vero and C6/36 cells leaves open the possibility that as yet unidentified receptors may also interact with EIII via the G331-D333-N368 "canyon".(81, 191) Future studies determining the identity of the WNV receptor(s) and the structure of receptor-bound WNV may help determine the role of the proposed WNV EIII canyon and elucidate whether the canyon hypothesis can be applies to flavivirus receptor binding. The G331-D333-N368 "canyon" may also be an attractive target for drug design.

		305	306	307		308	330	331	332	333	366	367	368
Mosquito-Borne	**DENV-1**	C	T	G	-	S	E	G	T	D	-	K	E
	DENV-2	C	T	G	-	K	E	G	D	G	-	K	D
	DENV-3	C	L	N	-	T	K	G	E	D	-	K	E
	DENV-4	C	S	G	-	K	E	G	A	G	-	T	N
	MVEV	C	T	E	-	K	T	G	S	D	T	A	N
	JEV	C	T	E	-	K	S	G	S	D	S	A	N
	WNV	C	S	K	-	A	T	G	T	D	T	A	N
	ILHV	C	K	G	-	T	T	G	T	D	A	K	S
	SLEV	C	D	S	-	A	T	G	S	N	G	A	N
	YFV	C	T	D	-	K	P	K	G	-	-	N	D
Tick-	**TBEV**	C	D	K	T	K	S	G	T	-	-	N	G
	LGTV	C	D	K	T	K	S	G	T	-	-	N	G
	POWV	C	D	K	A	K	T	G	S	D	-	N	G
	KFDV	C	E	G	S	K	T	G	S	-	-	T	G

Table 35: Alignment of Key Surface Loop Residues in Mosquito-Borne and Tick-Borne Flaviviruses

Amino acid alignment of flavivirus surface loop residues. Alignment data kindly provided by Dr. David Beasley. Unlabeled column between 307 and 308 represents a residue position commonly found in tick-borne but not mosquito-borne flaviviruses. Amino acid numbering is based on WNV E.

Appendix A: Recipes for Growth Media

VERO GROWTH MEDIA

500ml Minimum Essential Medium Eagle (1x) (Cellgro, Manassas, VA)

40ml Heat-Inactivated Bovine Growth Serum (HyClone, Logan, UT)

5ml Penicillin (10,000IU/ml) Streptomycin (10,000µg/ml) (Cellgro, Manassas, VA)

5ml MEM Non-Essential Amino Acid Solution (100x) (Sigma, St. Louis, MO)

1.5ml L-Glutamine (200mM) (Gibco, Brazil)

VERO MAINTENANCE MEDIA

500ml Minimum Essential Medium Eagle (1x) (Cellgro, Manassas, VA)

10ml Heat-Inactivated Bovine Growth Serum (HyClone, Logan, UT)

5ml Penicillin (10,000IU/ml) Streptomycin (10,000µg/ml) (Cellgro, Manassas, VA)

5ml MEM Non-Essential Amino Acid Solution (100x) (Sigma, St. Louis, MO)

1.5ml L-Glutamine (200mM) (Gibco, Brazil)

2X VERO MAINTENANCE MEDIA

500ml Modified Eagle Medium (2x) (Gibco, Grand Island, NY)

20ml Heat-Inactivated Bovine Growth Serum (HyClone, Logan, UT)

10ml Penicillin (10,000IU/ml) Streptomycin (10,000µg/ml) (Cellgro, Manassas, VA)

10ml MEM Non-Essential Amino Acid Solution (100x) (Sigma, St. Louis, MO)

3ml L-Glutamine (200mM) (Gibco, Brazil)

2.5ml Phenol Red (0.5%) (Sigma, St. Louis, MO)

DEF GROWTH MEDIA

500ml Minimum Essential Medium Eagle (1x) (Cellgro, Manassas, VA)

50ml Heat-Inactivated Fetal Bovine Serum (HyClone, Logan, UT)

5ml Penicillin (10,000IU/ml) Streptomycin (10,000µg/ml) (Cellgro, Manassas, VA)

DEF MAINTENANCE MEDIA

500ml Minimum Essential Medium Eagle (1x) (Cellgro, Manassas, VA)

10ml Heat-Inactivated Fetal Bovine Serum (HyClone, Logan, UT)

5ml Penicillin (10,000IU/ml) Streptomycin (10,000µg/ml) (Cellgro, Manassas, VA)

C6/36 GROWTH MEDIA

500ml Minimum Essential Medium Eagle (1x) (Cellgro, Manassas, VA)

50ml Heat-Inactivated Fetal Bovine Serum (Hyclone, Logan, UT)

25ml Tryptose Phosphate Broth (2x)

5ml Penicillin (10,000IU/ml) Streptomycin (10,000µg/ml) (Cellgro, Manassas, VA)

5ml Sodium Pyruvate (100mM) (Sigma, St. Louis, MO)

MEM Non-Essential Amino Acid Solution (100x) (Sigma, St. Louis, MO)

C6/36 MAINTENANCE MEDIA

500ml Minimum Essential Medium Eagle (1x) (Cellgro, Manassas, VA)

10ml Heat-Inactivated Fetal Bovine Serum (Hyclone, Logan, UT)

25ml Tryptose Phosphate Broth (2x)

5ml Penicillin (10,000IU/ml) Streptomycin (10,000µg/ml) (Cellgro, Manassas, VA)

5ml Sodium Pyruvate (100mM) (Sigma, St. Louis, MO)

MEM Non-Essential Amino Acid Solution (100x) (Sigma, St. Louis, MO)

2X TRYPTOSE PHOSPHATE BROTH

20g Tryptose (Difco, Detroit, MI)

2g Glucose (Sigma, St. Louis, MO)

5g NaCl (Fisher, Fair Lawn, NJ)

2.5g Na_2HPO_4 (Sigma, St. Louis, MO)

Bring up to 500ml with ddH_2O. Adjust pH to 7.3. Sterilize with 0.22µm filter.

LB/AMP MEDIA

LB (2%) (Fisher, Fair Lawn, NJ)

Ampicillin (100µg/ml) (Fisher, Fair Lawn, NJ)

LB/AMP PLATE

LB (2%) (Fisher, Fair Lawn, NJ)

Bacto Agar (1.5%) (BD, Sparks, MD)

Ampicillin (100µg/ml) (Fisher, Fair Lawn, NJ)

IPTG (500µM) (Fisher, Fair Lawn, NJ)

5-bromo-4-chloro-3-indolyl β-D-galactopyranoside (X-GAL) (5µg/ml) (Bioline, Taunton, MA)

Appendix B: Physical and Chemical Characteristics of Amino Acids

Code	Amino Acid	Category	Mass	pI	Hydropathy Index
A	Alanine	Hyrophobic - aliphatic	89	6.01	7.8
C	Cysteine	Neutral - polar	121	5.07	1.9
D	Aspartic Acid	Acidic	133	2.77	5.3
E	Glutamic Acid	Acidic	147	3.22	6.3
F	Phenylalanine	Hyrophobic - aromatic	165	5.48	3.9
G	Glycine	Unique	75	5.97	7.2
H	Histidine	Basic	155	7.59	2.3
I	Isoleucine	Hyrophobic - aliphatic	131	6.02	5.3
K	Lysine	Basic	146	9.74	5.9
L	Leucine	Hyrophobic - aliphatic	131	5.98	9.1
M	Methionine	Neutral - polar	149	5.74	2.3
N	Asparagine	Neutral - polar	132	5.41	4.3
P	Proline	Unique	115	6.48	5.2
Q	Glutamine	Neutral - polar	146	5.65	4.2
R	Arginine	Basic	174	10.76	5.1
S	Serine	Neutral - polar	105	5.68	6.8
T	Threonine	Neutral - polar	119	5.87	5.9
V	Valine	Hyrophobic - aliphatic	117	5.97	6.6
W	Tryptophan	Hyrophobic - aromatic	204	5.89	1.4
Y	Tyrosine	Hyrophobic - aromatic	181	5.66	3.2

Table 36: Physical and Chemical Characteristics of Amino Acids

Relevant properties of amino acids. Mass, pI, and Hydropathy Index data are taken from the Lenhinger Principles of Biochemistry textbook, 4th edition.(233) Category is taken from the Sigma-Aldrich website.(234)

Appendix C: Permissions for Use of Copyrighted Materials

FIGURE 1

Copyright Clearance Center RightsLink®

Home | Account Info | Help

AMERICAN SOCIETY FOR MICROBIOLOGY

Title: The Unique Transmembrane Hairpin of Flavivirus Fusion Protein E Is Essential for Membrane Fusion
Author: Richard Fritz, Janja Blazevic, Christian Taucher et al.
Publication: Journal of Virology
Publisher: American Society for Microbiology
Date: May 1, 0001
Copyright © 2011, American Society for Microbiology

Logged in as:
Jessica Plante
Account #:
3000684774
LOGOUT

Permissions Request

ASM authorizes an advanced degree candidate to republish the requested material in his/her doctoral thesis or dissertation. If your thesis, or dissertation, is to be published commercially, then you must reapply for permission.

BACK | CLOSE WINDOW

Copyright © 2013 Copyright Clearance Center, Inc. All Rights Reserved. Privacy statement.
Comments? We would like to hear from you. E-mail us at customercare@copyright.com

FIGURE 2A

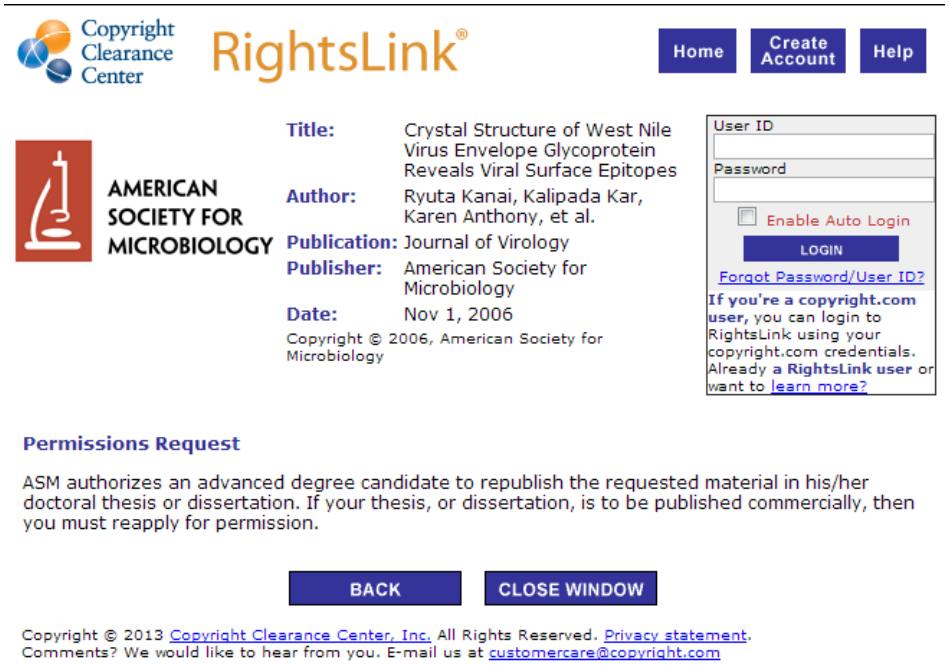

Copyright Clearance Center RightsLink®

Home | Create Account | Help

AMERICAN SOCIETY FOR MICROBIOLOGY

Title: Crystal Structure of West Nile Virus Envelope Glycoprotein Reveals Viral Surface Epitopes
Author: Ryuta Kanai, Kalipada Kar, Karen Anthony, et al.
Publication: Journal of Virology
Publisher: American Society for Microbiology
Date: Nov 1, 2006
Copyright © 2006, American Society for Microbiology

User ID
Password
Enable Auto Login
LOGIN
Forgot Password/User ID?
If you're a copyright.com user, you can login to RightsLink using your copyright.com credentials. Already **a RightsLink user** or want to learn more?

Permissions Request

ASM authorizes an advanced degree candidate to republish the requested material in his/her doctoral thesis or dissertation. If your thesis, or dissertation, is to be published commercially, then you must reapply for permission.

BACK | CLOSE WINDOW

Copyright © 2013 Copyright Clearance Center, Inc. All Rights Reserved. Privacy statement.
Comments? We would like to hear from you. E-mail us at customercare@copyright.com

FIGURE 2B

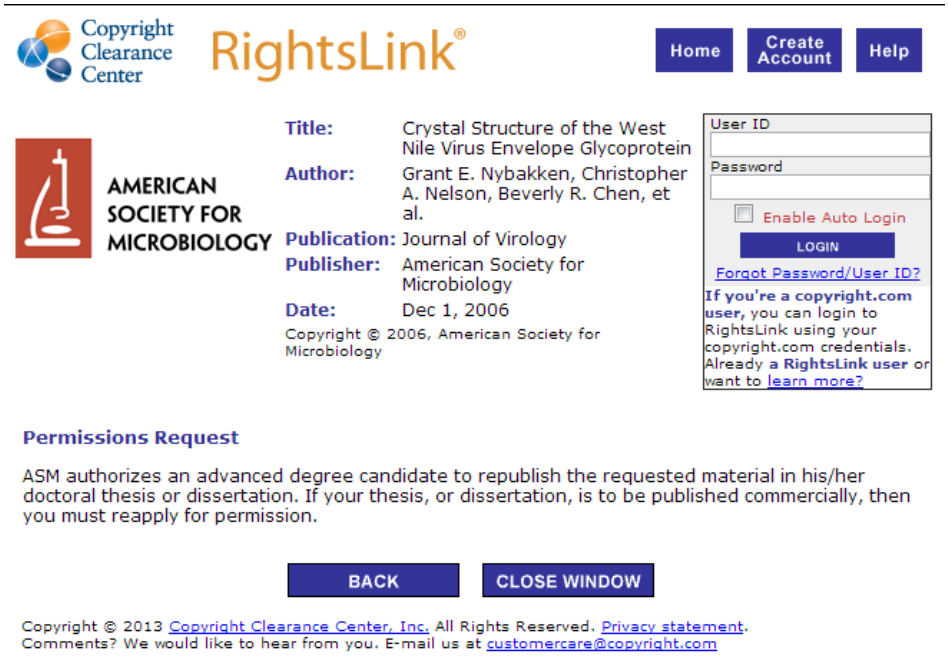
Copyright Clearance Center
RightsLink®
Home
Create Account
Help
AMERICAN SOCIETY FOR MICROBIOLOGY
Title: Crystal Structure of the West Nile Virus Envelope Glycoprotein
Author: Grant E. Nybakken, Christopher A. Nelson, Beverly R. Chen, et al.
Publication: Journal of Virology
Publisher: American Society for Microbiology
Date: Dec 1, 2006
Copyright © 2006, American Society for Microbiology
User ID
Password
Enable Auto Login
LOGIN
Forgot Password/User ID?
If you're a copyright.com user, you can login to RightsLink using your copyright.com credentials. Already a RightsLink user or want to learn more?
Permissions Request
ASM authorizes an advanced degree candidate to republish the requested material in his/her doctoral thesis or dissertation. If your thesis, or dissertation, is to be published commercially, then you must reapply for permission.
BACK
CLOSE WINDOW
Copyright © 2013 Copyright Clearance Center, Inc. All Rights Reserved. Privacy statement.
Comments? We would like to hear from you. E-mail us at customercare@copyright.com

References

1. **Smithburn KC, Hughes TP, Burke AW, Paul JH.** 1940. A Neurotropic Virus Isolated From the Blood of a Native of Uganda. American Journal of Tropical Medicine and Hygeine **s1-20:**471-492.
2. **Goldblum N, Jasinska-Klingberg W, Klingberg Ma, Marberg K, Sterk Vv.** 1956. The natural history of West Nile Fever. I. Clinical observations during an epidemic in Israel. Am J Hyg **64:**259-269.
3. **Flatau E, Kohn D, Daher O, Varsano N.** 1981. West Nile fever encephalitis. Isr J Med Sci **17:**1057-1059.
4. **McIntosh BM, Jupp PG, Dos Santos I, Meenehan GM.** 1976. Epidemics of West Nile and Sindbis viruses in South Africa with *Culex (Culex) univittatus* Theobald as vector South African Journal of Science **72:**295-300.
5. **Goldblum N, Sterk VV, Paderski B.** 1954. West Nile fever; the clinical features of the disease and the isolation of West Nile virus from the blood of nine human cases. Am J Hyg **59:**89-103.
6. **Weinbren MP.** 1955. The occurrence of West Nile virus in South Africa. S Afr Med J **29:**1092-1097.
7. **Hannoun C, Panthier R, Mouchet J, Eouzan JP.** 1964. Isolation In France Of The West Nile Virus From Patients And From The Vector *Culex Modestus Ficalbi*. C R Hebd Seances Acad Sci **259:**4170-4172.
8. **Jupp PG, Blackburn NK, Thompson DL, Meenehan GM.** 1986. Sindbis and West Nile virus infections in the Witwatersrand-Pretoria region. S Afr Med J **70:**218-220.
9. **Morrill JC, Johnson BK, Hyams C, Okoth F, Tukei PM, Mugambi M, Woody J.** 1991. Serological evidence of arboviral infections among humans of coastal Kenya. J Trop Med Hyg **94:**166-168.
10. **Tsai TF, Popovici F, Cernescu C, Campbell GL, Nedelcu NI.** 1998. West Nile encephalitis epidemic in southeastern Romania. Lancet **352:**767-771.
11. **Savage HM, Ceianu C, Nicolescu G, Karabatsos N, Lanciotti R, Vladimirescu A, Laiv L, Ungureanu A, Romanca C, Tsai TF.** 1999. Entomologic and avian investigations of an epidemic of West Nile fever in Romania in 1996, with serologic and molecular characterization of a virus isolate from mosquitoes. Am J Trop Med Hyg **61:**600-611.
12. **Hubálek Z, Halouzka J.** 1999. West Nile fever--a reemerging mosquito-borne viral disease in Europe. Emerg Infect Dis **5:**643-650.
13. **Lanciotti RS, Roehrig JT, Deubel V, Smith J, Parker M, Steele K, Crise B, Volpe KE, Crabtree MB, Scherret JH, Hall RA, MacKenzie JS, Cropp CB, Panigrahy B, Ostlund E, Schmitt B, Malkinson M, Banet C, Weissman J, Komar N, Savage HM, Stone W, McNamara T, Gubler DJ.** 1999. Origin of

the West Nile virus responsible for an outbreak of encephalitis in the northeastern United States. Science **286:**2333-2337.

14. **Steinhauer J.** September 25, 1999. African Virus May Be Culprit in Mosquito-Borne Illness in New York Region, New York Times.

15. **Centers for Disease Control and Prevention.** 1999. West Nile-like Virus in the United States. http://www.cdc.gov/media/pressrel/r990924.htm

16. **ArboNET** 2013, posting date. West Nile virus disease cases and deaths reported to CDC by year and clinical presentation, 1999-2012. Centers for Disease Control and Prevention. http://www.cdc.gov/westnile/resources/pdfs/cummulative/99_2012_CasesAndDeathsClinicalPresentationHumanCases.pdf

17. **Campbell GL, Marfin AA, Lanciotti RS, Gubler DJ.** 2002. West Nile virus. Lancet Infect Dis **2:**519-529.

18. **Komar N, Clark GG.** 2006. West Nile virus activity in Latin America and the Caribbean. Rev Panam Salud Publica **19:**112-117.

19. **Ulloa A, Ferguson HH, Méndez-Sánchez JD, Danis-Lozano R, Casas-Martínez M, Bond JG, García-Zebadúa JC, Orozco-Bonilla A, Juárez-Ordaz JA, Farfan-Ale JA, García-Rejón JE, Rosado-Paredes EP, Edwards E, Komar N, Hassan HK, Unnasch TR, Rodríguez-Pérez MA.** 2009. West Nile virus activity in mosquitoes and domestic animals in Chiapas, México. Vector Borne Zoonotic Dis **9:**555-560.

20. **Morales MA, Barrandeguy M, Fabbri C, Garcia JB, Vissani A, Trono K, Gutierrez G, Pigretti S, Menchaca H, Garrido N, Taylor N, Fernandez F, Levis S, Enría D.** 2006. West Nile virus isolation from equines in Argentina, 2006. Emerg Infect Dis **12:**1559-1561.

21. **Pauvolid-Corrêa A, Morales MA, Levis S, Figueiredo LT, Couto-Lima D, Campos Z, Nogueira MF, da Silva EE, Nogueira RM, Schatzmayr HG.** 2011. Neutralising antibodies for West Nile virus in horses from Brazilian Pantanal. Mem Inst Oswaldo Cruz **106:**467-474.

22. **Artsob H, Lindsay R, Drebot M.** 2006. Biodiversity-related aspects of West Nile virus and its cycle in nature. Biodiversity **7:**18-23.

23. **Gubler DJ.** 2007. The continuing spread of West Nile virus in the western hemisphere. Clin Infect Dis **45:**1039-1046.

24. **Bakonyi T, Ivanics E, Erdélyi K, Ursu K, Ferenczi E, Weissenböck H, Nowotny N.** 2006. Lineage 1 and 2 strains of encephalitic West Nile virus, central Europe. Emerg Infect Dis **12:**618-623.

25. **Platonov AES, T.A.Karan,L.S.Rusakova,N.V.Shishkina,L.V.** 2008. New outbreak of West Nile fever in Volgograd, Russia, in 2007. Unpublished, listed in NCBI with sequence data.

26. **Valiakos G, Touloudi A, Athanasiou LV, Giannakopoulos A, Iacovakis C, Birtsas P, Spyrou V, Dalabiras Z, Petrovska L, Billinis C.** 2012. Serological

and molecular investigation into the role of wild birds in the epidemiology of West Nile virus in Greece. Virol J **9:**266.

27. **Papa A, Bakonyi T, Xanthopoulou K, Vázquez A, Tenorio A, Nowotny N.** 2011. Genetic characterization of West Nile virus lineage 2, Greece, 2010. Emerg Infect Dis **17:**920-922.

28. **Magurano F, Remoli ME, Baggieri M, Fortuna C, Marchi A, Fiorentini C, Bucci P, Benedetti E, Ciufolini MG, Rizzo C, Piga S, Salcuni P, Rezza G, Nicoletti L.** 2012. Circulation of West Nile virus lineage 1 and 2 during an outbreak in Italy. Clin Microbiol Infect **18:**E545-547.

29. **Aliota MT, Jones SA, Dupuis AP, Ciota AT, Hubalek Z, Kramer LD.** 2012. Characterization of Rabensburg virus, a flavivirus closely related to West Nile virus of the Japanese encephalitis antigenic group. PLoS One **7:**e39387.

30. **Ebel G, Kramer L.** 2009. West Nile Virus: Molecular Epidemiology and Diversity, p. 25-43, West Nile Encephalitis Virus Infection. Springer New York.

31. **Hubálek Z, Halouzka J, Juricová Z, Sebesta O.** 1998. First isolation of mosquito-borne West Nile virus in the Czech Republic. Acta Virol **42:**119-120.

32. **Hubálek Z, Savage HM, Halouzka J, Juricová Z, Sanogo YO, Lusk S.** 2000. West Nile virus investigations in South Moravia, Czechland. Viral Immunol **13:**427-433.

33. **Hubálek Z, Rudolf I, Bakonyi T, Kazdová K, Halouzka J, Sebesta O, Sikutová S, Juricová Z, Nowotny N.** 2010. Mosquito (Diptera: *Culicidae*) surveillance for arboviruses in an area endemic for West Nile (Lineage Rabensburg) and Tahyna viruses in Central Europe. J Med Entomol **47:**466-472.

34. **Aliota MT, Kramer LD.** 2012. Replication of West Nile virus, Rabensburg lineage in mammalian cells is restricted by temperature. Parasit Vectors **5:**293.

35. **Lvov DK, Butenko AM, Gromashevsky VL, Kovtunov AI, Prilipov AG, Kinney R, Aristova VA, Dzharkenov AF, Samokhvalov EI, Savage HM, Shchelkanov MY, Galkina IV, Deryabin PG, Gubler DJ, Kulikova LN, Alkhovsky SK, Moskvina TM, Zlobina LV, Sadykova GK, Shatalov AG, Lvov DN, Usachev VE, Voronina AG.** 2004. West Nile virus and other zoonotic viruses in Russia: examples of emerging-reemerging situations. Arch Virol Suppl**:**85-96.

36. **Platonov AES, T.A.Fedorova,M.V. Karan,L.S.Frolov,A.I., Malenko GV, Levina LS, Pogodina VV.** 2008. West Nile-like virus in amphibian and mosquitoes in Volgograd, Russia. Unpublished, listed in NCBI with sequence data.

37. **May FJ, Davis CT, Tesh RB, Barrett AD.** 2011. Phylogeography of West Nile virus: from the cradle of evolution in Africa to Eurasia, Australia, and the Americas. J Virol **85:**2964-2974.

38. **Bondre VP, Jadi RS, Mishra AC, Yergolkar PN, Arankalle VA.** 2007. West Nile virus isolates from India: evidence for a distinct genetic lineage. J Gen Virol **88:**875-884.

39. **Scherret JH, Poidinger M, Mackenzie JS, Broom AK, Deubel V, Lipkin WI, Briese T, Gould EA, Hall RA.** 2001. The relationships between West Nile and Kunjin viruses. Emerg Infect Dis **7:**697-705.

40. **Vazquez A, Sanchez-Seco MP, Ruiz S, Molero F, Hernandez L, Moreno J, Magallanes A, Tejedor CG, Tenorio A.** 2010. Putative new lineage of west nile virus, Spain. Emerg Infect Dis **16:**549-552.

41. **McLean RG, Ubico SR, Docherty DE, Hansen WR, Sileo L, McNamara TS.** 2001. West Nile virus transmission and ecology in birds. Ann N Y Acad Sci **951:**54-57.

42. **Komar N, Langevin S, Hinten S, Nemeth N, Edwards E, Hettler D, Davis B, Bowen R, Bunning M.** 2003. Experimental infection of North American birds with the New York 1999 strain of West Nile virus. Emerg Infect Dis **9:**311-322.

43. **Prevention CfDCa.** Species of dead birds in which West Nile virus has been detected, United States, 1999-2012.

44. **Bin H, Grossman Z, Pokamunski S, Malkinson M, Weiss L, Duvdevani P, Banet C, Weisman Y, Annis E, Gandaku D, Yahalom V, Hindyieh M, Shulman L, Mendelson E.** 2001. West Nile fever in Israel 1999-2000: from geese to humans. Ann N Y Acad Sci **951:**127-142.

45. **Malkinson M, Weisman Y, Pokamonski S, King R, Deubel V.** 2001. Intercontinental transmission of West Nile virus by migrating white storks. Emerg Infect Dis **7:**540.

46. **Brault AC, Huang CY, Langevin SA, Kinney RM, Bowen RA, Ramey WN, Panella NA, Holmes EC, Powers AM, Miller BR.** 2007. A single positively selected West Nile viral mutation confers increased virogenesis in American crows. Nat Genet **39:**1162-1166.

47. **Reed LM, Johansson MA, Panella N, McLean R, Creekmore T, Puelle R, Komar N.** 2009. Declining mortality in American crow (*Corvus brachyrhynchos*) following natural West Nile virus infection. Avian Dis **53:**458-461.

48. **Tiawsirisup S, Platt KB, Tucker BJ, Rowley WA.** 2005. Eastern cottontail rabbits (*Sylvilagus floridanus*) develop West Nile virus viremias sufficient for infecting select mosquito species. Vector Borne Zoonotic Dis **5:**342-350.

49. **Platt KB, Tucker BJ, Halbur PG, Tiawsirisup S, Blitvich BJ, Fabiosa FG, Bartholomay LC, Rowley WA.** 2007. West Nile virus viremia in eastern chipmunks (*Tamias striatus*) sufficient for infecting different mosquitoes. Emerg Infect Dis **13:**831-837.

50. **Klenk K, Snow J, Morgan K, Bowen R, Stephens M, Foster F, Gordy P, Beckett S, Komar N, Gubler D, Bunning M.** 2004. Alligators as West Nile virus amplifiers. Emerg Infect Dis **10:**2150-2155.

51. **Centers for Disease Control and Prevention.** Mosquito species in which West Nile virus has been detected, United States, 1999-2012. http://www.cdc.gov/westnile/resources/pdfs/Mosquito%20Species%201999-2012.pdf

52. **Hamer GL, Kitron UD, Goldberg TL, Brawn JD, Loss SR, Ruiz MO, Hayes DB, Walker ED.** 2009. Host selection by *Culex pipiens* mosquitoes and West Nile virus amplification. Am J Trop Med Hyg **80:**268-278.

53. **Garcia-Rejon JE, Blitvich BJ, Farfan-Ale JA, Loroño-Pino MA, Chi Chim WA, Flores-Flores LF, Rosado-Paredes E, Baak-Baak C, Perez-Mutul J, Suarez-Solis V, Fernandez-Salas I, Beaty BJ.** 2008. Host-feeding preference of the mosquito, *Culex quinquefasciatus*, in Yucatan State, Mexico Journal of Insect Science **10**.

54. **Thiemann TC, Wheeler SS, Barker CM, Reisen WK.** 2011. Mosquito host selection varies seasonally with host availability and mosquito density. PLoS Negl Trop Dis **5:**e1452.

55. **Styer LM, Kent KA, Albright RG, Bennett CJ, Kramer LD, Bernard KA.** 2007. Mosquitoes inoculate high doses of West Nile virus as they probe and feed on live hosts. PLoS Pathog **3:**1262-1270.

56. **Turell MJ, O'Guinn M, Oliver J.** 2000. Potential for New York mosquitoes to transmit West Nile virus. Am J Trop Med Hyg **62:**413-414.

57. **Sardelis MR, Turell MJ, Dohm DJ, O'Guinn ML.** 2001. Vector competence of selected North American *Culex* and *Coquillettidia* mosquitoes for West Nile virus. Emerg Infect Dis **7:**1018-1022.

58. **Southam CM, Moore AE.** 1954. Induced Virus Infections in Man by the Egypt Isolates of West Nile Virus. The American Journal of Tropical Medicine and Hygiene **3:**19-50.

59. **Unlu I, Mackay AJ, Roy A, Yates MM, Foil LD.** 2010. Evidence of vertical transmission of West Nile virus in field-collected mosquitoes. J Vector Ecol **35:**95-99.

60. **Anderson JF, Main AJ.** 2006. Importance of vertical and horizontal transmission of West Nile virus by *Culex pipiens* in the Northeastern United States. J Infect Dis **194:**1577-1579.

61. **Anderson JF, Andreadis TG, Main AJ, Ferrandino FJ, Vossbrinck CR.** 2006. West Nile virus from female and male mosquitoes (Diptera: Culicidae) in subterranean, ground, and canopy habitats in Connecticut. J Med Entomol **43:**1010-1019.

62. **Davis CT, Ebel GD, Lanciotti RS, Brault AC, Guzman H, Siirin M, Lambert A, Parsons RE, Beasley DW, Novak RJ, Elizondo-Quiroga D, Green EN, Young DS, Stark LM, Drebot MA, Artsob H, Tesh RB, Kramer LD, Barrett AD.** 2005. Phylogenetic analysis of North American West Nile virus isolates, 2001-2004: evidence for the emergence of a dominant genotype. Virology **342:**252-265.

63. **Nybakken GE, Nelson CA, Chen BR, Diamond MS, Fremont DH.** 2006. Crystal structure of the West Nile virus envelope glycoprotein. J Virol **80:**11467-11474.

64. **Ebel GD, Carricaburu J, Young D, Bernard KA, Kramer LD.** 2004. Genetic and phenotypic variation of West Nile virus in New York, 2000-2003. Am J Trop Med Hyg **71:**493-500.

65. **Nybakken GE, Oliphant T, Johnson S, Burke S, Diamond MS, Fremont DH.** 2005. Structural basis of West Nile virus neutralization by a therapeutic antibody. Nature **437:**764-769.

66. **Kilpatrick AM, Meola MA, Moudy RM, Kramer LD.** 2008. Temperature, viral genetics, and the transmission of West Nile virus by *Culex pipiens* mosquitoes. PLoS Pathog **4:**e1000092.

67. **Richards SL, Lord CC, Pesko KN, Tabachnick WJ.** 2010. Environmental and biological factors influencing *Culex pipiens quinquefasciatus* (Diptera: Culicidae) vector competence for West Nile Virus. Am J Trop Med Hyg **83:**126-134.

68. **Anderson JF, Main AJ, Andreadis TG, Wikel SK, Vossbrinck CR.** 2003. Transstadial transfer of West Nile virus by three species of ixodid ticks (Acari: Ixodidae). J Med Entomol **40:**528-533.

69. **Reisen WK, Brault AC, Martinez VM, Fang Y, Simmons K, Garcia S, Omi-Olsen E, Lane RS.** 2007. Ability of transstadially infected *Ixodes pacificus* (Acari: Ixodidae) to transmit West Nile virus to song sparrows or western fence lizards. J Med Entomol **44:**320-327.

70. **Hutcheson HJ, Gorham CH, Machain-Williams C, Loroño-Pino MA, James AM, Marlenee NL, Winn B, Beaty BJ, Blair CD.** 2005. Experimental transmission of West Nile virus (Flaviviridae: Flavivirus) by *Carios capensis* ticks from North America. Vector Borne Zoonotic Dis **5:**293-295.

71. **Mumcuoglu KY, Banet-Noach C, Malkinson M, Shalom U, Galun R.** 2005. Argasid ticks as possible vectors of West Nile virus in Israel. Vector Borne Zoonotic Dis **5:**65-71.

72. **Pöhlmann S, Soilleux EJ, Baribaud F, Leslie GJ, Morris LS, Trowsdale J, Lee B, Coleman N, Doms RW.** 2001. DC-SIGNR, a DC-SIGN homologue expressed in endothelial cells, binds to human and simian immunodeficiency viruses and activates infection in trans. Proc Natl Acad Sci U S A **98:**2670-2675.

73. **Granelli-Piperno A, Pritsker A, Pack M, Shimeliovich I, Arrighi JF, Park CG, Trumpfheller C, Piguet V, Moran TM, Steinman RM.** 2005. Dendritic cell-specific intercellular adhesion molecule 3-grabbing nonintegrin/CD209 is abundant on macrophages in the normal human lymph node and is not required for dendritic cell stimulation of the mixed leukocyte reaction. J Immunol **175:**4265-4273.

74. **Geijtenbeek TB, Torensma R, van Vliet SJ, van Duijnhoven GC, Adema GJ, van Kooyk Y, Figdor CG.** 2000. Identification of DC-SIGN, a novel dendritic

cell-specific ICAM-3 receptor that supports primary immune responses. Cell **100:**575-585.

75. **Tassaneetrithep B, Burgess TH, Granelli-Piperno A, Trumpfheller C, Finke J, Sun W, Eller MA, Pattanapanyasat K, Sarasombath S, Birx DL, Steinman RM, Schlesinger S, Marovich MA.** 2003. DC-SIGN (CD209) mediates dengue virus infection of human dendritic cells. J Exp Med **197:**823-829.

76. **Navarro-Sanchez E, Altmeyer R, Amara A, Schwartz O, Fieschi F, Virelizier JL, Arenzana-Seisdedos F, Desprès P.** 2003. Dendritic-cell-specific ICAM3-grabbing non-integrin is essential for the productive infection of human dendritic cells by mosquito-cell-derived dengue viruses. EMBO Rep **4:**723-728.

77. **Davis CW, Nguyen HY, Hanna SL, Sánchez MD, Doms RW, Pierson TC.** 2006. West Nile virus discriminates between DC-SIGN and DC-SIGNR for cellular attachment and infection. J Virol **80:**1290-1301.

78. **Davis CW, Mattei LM, Nguyen HY, Ansarah-Sobrinho C, Doms RW, Pierson TC.** 2006. The location of asparagine-linked glycans on West Nile virions controls their interactions with CD209 (dendritic cell-specific ICAM-3 grabbing nonintegrin). J Biol Chem **281:**37183-37194.

79. **Chu JJ, Ng ML.** 2004. Interaction of West Nile virus with alpha v beta 3 integrin mediates virus entry into cells. J Biol Chem **279:**54533-54541.

80. **Chu JJ, Ng ML.** 2003. Characterization of a 105-kDa plasma membrane associated glycoprotein that is involved in West Nile virus binding and infection. Virology **312:**458-469.

81. **Lee JW, Chu JJ, Ng ML.** 2006. Quantifying the specific binding between West Nile virus envelope domain III protein and the cellular receptor alphaVbeta3 integrin. J Biol Chem **281:**1352-1360.

82. **Medigeshi GR, Hirsch AJ, Streblow DN, Nikolich-Zugich J, Nelson JA.** 2008. West Nile virus entry requires cholesterol-rich membrane microdomains and is independent of alphavbeta3 integrin. J Virol **82:**5212-5219.

83. **Schmidt K, Keller M, Bader BL, Korytár T, Finke S, Ziegler U, Groschup MH.** 2013. Integrins modulate the infection efficiency of West Nile virus into cells. J Gen Virol **94:**1723-1733.

84. **Gollins SW, Porterfield JS.** 1985. Flavivirus infection enhancement in macrophages: an electron microscopic study of viral cellular entry. J Gen Virol **66 (Pt 9):**1969-1982.

85. **Chu JJ, Ng ML.** 2004. Infectious entry of West Nile virus occurs through a clathrin-mediated endocytic pathway. J Virol **78:**10543-10555.

86. **Fritz R, Blazevic J, Taucher C, Pangerl K, Heinz FX, Stiasny K.** 2011. The unique transmembrane hairpin of flavivirus fusion protein E is essential for membrane fusion. J Virol **85:**4377-4385.

87. **Wengler G, Beato M.** 1979. In vitro translation of 42 S virus-specific RNA from cells infected with the flavivirus West Nile virus. Virology **96:**516-529.

88. **Wengler G, Czaya G, Färber PM, Hegemann JH.** 1991. In vitro synthesis of West Nile virus proteins indicates that the amino-terminal segment of the NS3 protein contains the active centre of the protease which cleaves the viral polyprotein after multiple basic amino acids. J Gen Virol **72 (Pt 4):**851-858.

89. **Falgout B, Markoff L.** 1995. Evidence that flavivirus NS1-NS2A cleavage is mediated by a membrane-bound host protease in the endoplasmic reticulum. J Virol **69:**7232-7243.

90. **Nowak T, Färber PM, Wengler G.** 1989. Analyses of the terminal sequences of West Nile virus structural proteins and of the in vitro translation of these proteins allow the proposal of a complete scheme of the proteolytic cleavages involved in their synthesis. Virology **169:**365-376.

91. **Chu PW, Westaway EG.** 1985. Replication strategy of Kunjin virus: evidence for recycling role of replicative form RNA as template in semiconservative and asymmetric replication. Virology **140:**68-79.

92. **Malet H, Egloff MP, Selisko B, Butcher RE, Wright PJ, Roberts M, Gruez A, Sulzenbacher G, Vonrhein C, Bricogne G, Mackenzie JM, Khromykh AA, Davidson AD, Canard B.** 2007. Crystal structure of the RNA polymerase domain of the West Nile virus non-structural protein 5. J Biol Chem **282:**10678-10689.

93. **Ray D, Shah A, Tilgner M, Guo Y, Zhao Y, Dong H, Deas TS, Zhou Y, Li H, Shi PY.** 2006. West Nile virus 5'-cap structure is formed by sequential guanine N-7 and ribose 2'-O methylations by nonstructural protein 5. J Virol **80:**8362-8370.

94. **Selisko B, Dutartre H, Guillemot JC, Debarnot C, Benarroch D, Khromykh A, Desprès P, Egloff MP, Canard B.** 2006. Comparative mechanistic studies of de novo RNA synthesis by flavivirus RNA-dependent RNA polymerases. Virology **351:**145-158.

95. **Guyatt KJ, Westaway EG, Khromykh AA.** 2001. Expression and purification of enzymatically active recombinant RNA-dependent RNA polymerase (NS5) of the flavivirus Kunjin. J Virol Methods **92:**37-44.

96. **Steffens S, Thiel HJ, Behrens SE.** 1999. The RNA-dependent RNA polymerases of different members of the family Flaviviridae exhibit similar properties in vitro. J Gen Virol **80 (Pt 10):**2583-2590.

97. **Ng ML, Tan SH, Chu JJ.** 2001. Transport and budding at two distinct sites of visible nucleocapsids of West Nile (Sarafend) virus. J Med Virol **65:**758-764.

98. **Mackenzie JM, Westaway EG.** 2001. Assembly and maturation of the flavivirus Kunjin virus appear to occur in the rough endoplasmic reticulum and along the secretory pathway, respectively. J Virol **75:**10787-10799.

99. **Stadler K, Allison SL, Schalich J, Heinz FX.** 1997. Proteolytic activation of tick-borne encephalitis virus by furin. J Virol **71:**8475-8481.

100. **Mukherjee S, Lin TY, Dowd KA, Manhart CJ, Pierson TC.** 2011. The infectivity of prM-containing partially mature West Nile virus does not require the activity of cellular furin-like proteases. J Virol **85:**12067-12072.

101. **Schneider BS, Soong L, Girard YA, Campbell G, Mason P, Higgs S.** 2006. Potentiation of West Nile encephalitis by mosquito feeding. Viral Immunol **19:**74-82.

102. **Styer LM, Lim PY, Louie KL, Albright RG, Kramer LD, Bernard KA.** 2011. Mosquito saliva causes enhancement of West Nile virus infection in mice. J Virol **85:**1517-1527.

103. **Lim PY, Behr MJ, Chadwick CM, Shi PY, Bernard KA.** 2011. Keratinocytes are cell targets of West Nile virus in vivo. J Virol **85:**5197-5201.

104. **Johnston LJ, Halliday GM, King NJ.** 2000. Langerhans cells migrate to local lymph nodes following cutaneous infection with an arbovirus. J Invest Dermatol **114:**560-568.

105. **Armah HB, Wang G, Omalu BI, Tesh RB, Gyure KA, Chute DJ, Smith RD, Dulai P, Vinters HV, Kleinschmidt-DeMasters BK, Wiley CA.** 2007. Systemic distribution of West Nile virus infection: postmortem immunohistochemical study of six cases. Brain Pathol **17:**354-362.

106. **Omalu BI, Shakir AA, Wang G, Lipkin WI, Wiley CA.** 2003. Fatal fulminant pan-meningo-polioencephalitis due to West Nile virus. Brain Pathol **13:**465-472.

107. **Paddock CD, Nicholson WL, Bhatnagar J, Goldsmith CS, Greer PW, Hayes EB, Risko JA, Henderson C, Blackmore CG, Lanciotti RS, Campbell GL, Zaki SR.** 2006. Fatal hemorrhagic fever caused by West Nile virus in the United States. Clin Infect Dis **42:**1527-1535.

108. **Hunsperger EA, Roehrig JT.** 2006. Temporal analyses of the neuropathogenesis of a West Nile virus infection in mice. J Neurovirol **12:**129-139.

109. **Brown AN, Kent KA, Bennett CJ, Bernard KA.** 2007. Tissue tropism and neuroinvasion of West Nile virus do not differ for two mouse strains with different survival rates. Virology **368:**422-430.

110. **Samuel MA, Diamond MS.** 2005. Alpha/beta interferon protects against lethal West Nile virus infection by restricting cellular tropism and enhancing neuronal survival. J Virol **79:**13350-13361.

111. **Verma S, Lo Y, Chapagain M, Lum S, Kumar M, Gurjav U, Luo H, Nakatsuka A, Nerurkar VR.** 2009. West Nile virus infection modulates human brain microvascular endothelial cells tight junction proteins and cell adhesion molecules: Transmigration across the in vitro blood-brain barrier. Virology **385:**425-433.

112. **Roe K, Kumar M, Lum S, Orillo B, Nerurkar VR, Verma S.** 2012. West Nile virus-induced disruption of the blood-brain barrier in mice is characterized by the degradation of the junctional complex proteins and increase in multiple matrix metalloproteinases. J Gen Virol **93:**1193-1203.

113. **Wang S, Welte T, McGargill M, Town T, Thompson J, Anderson JF, Flavell RA, Fikrig E, Hedrick SM, Wang T.** 2008. Drak2 contributes to West Nile virus entry into the brain and lethal encephalitis. J Immunol **181:**2084-2091.

114. **Verma S, Kumar M, Gurjav U, Lum S, Nerurkar VR.** 2010. Reversal of West Nile virus-induced blood-brain barrier disruption and tight junction proteins degradation by matrix metalloproteinases inhibitor. Virology **397:**130-138.

115. **Wang P, Dai J, Bai F, Kong KF, Wong SJ, Montgomery RR, Madri JA, Fikrig E.** 2008. Matrix metalloproteinase 9 facilitates West Nile virus entry into the brain. J Virol **82:**8978-8985.

116. **Wang T, Town T, Alexopoulou L, Anderson JF, Fikrig E, Flavell RA.** 2004. Toll-like receptor 3 mediates West Nile virus entry into the brain causing lethal encephalitis. Nat Med **10:**1366-1373.

117. **Sultana H, Neelakanta G, Foellmer HG, Montgomery RR, Anderson JF, Koski RA, Medzhitov RM, Fikrig E.** 2012. Semaphorin 7A contributes to West Nile virus pathogenesis through TGF-β1/Smad6 signaling. J Immunol **189:**3150-3158.

118. **de Vries HE, Blom-Roosemalen MC, van Oosten M, de Boer AG, van Berkel TJ, Breimer DD, Kuiper J.** 1996. The influence of cytokines on the integrity of the blood-brain barrier in vitro. J Neuroimmunol **64:**37-43.

119. **Fiala M, Looney DJ, Stins M, Way DD, Zhang L, Gan X, Chiappelli F, Schweitzer ES, Shapshak P, Weinand M, Graves MC, Witte M, Kim KS.** 1997. TNF-alpha opens a paracellular route for HIV-1 invasion across the blood-brain barrier. Mol Med **3:**553-564.

120. **Chu JJ, Ng ML.** 2003. The mechanism of cell death during West Nile virus infection is dependent on initial infectious dose. J Gen Virol **84:**3305-3314.

121. **Ramanathan MP, Chambers JA, Pankhong P, Chattergoon M, Attatippaholkun W, Dang K, Shah N, Weiner DB.** 2006. Host cell killing by the West Nile Virus NS2B-NS3 proteolytic complex: NS3 alone is sufficient to recruit caspase-8-based apoptotic pathway. Virology **345:**56-72.

122. **Mostashari F, Bunning ML, Kitsutani PT, Singer DA, Nash D, Cooper MJ, Katz N, Liljebjelke KA, Biggerstaff BJ, Fine AD, Layton MC, Mullin SM, Johnson AJ, Martin DA, Hayes EB, Campbell GL.** 2001. Epidemic West Nile encephalitis, New York, 1999: results of a household-based seroepidemiological survey. Lancet **358:**261-264.

123. **Centers for Disease Control and Prevention.** June 15 2010, posting date. West Nile Virus Statistics, Surveillance, and Control Archive. http://www.cdc.gov/ncidod/dvbid/westnile/surv&control.htm

124. **Brown JA, Factor DL, Tkachenko N, Templeton SM, Crall ND, Pape WJ, Bauer MJ, Ambruso DR, Dickey WC, Marfin AA.** 2007. West Nile viremic blood donors and risk factors for subsequent West Nile fever. Vector Borne Zoonotic Dis **7:**479-488.

125. **Zou S, Foster GA, Dodd RY, Petersen LR, Stramer SL.** 2010. West Nile fever characteristics among viremic persons identified through blood donor screening. J Infect Dis **202:**1354-1361.

126. **Custer B, Kamel H, Kiely NE, Murphy EL, Busch MP.** 2009. Associations between West Nile virus infection and symptoms reported by blood donors identified through nucleic acid test screening. Transfusion **49:**278-288.

127. **Pealer LN, Marfin AA, Petersen LR, Lanciotti RS, Page PL, Stramer SL, Stobierski MG, Signs K, Newman B, Kapoor H, Goodman JL, Chamberland ME, Team WNVTI.** 2003. Transmission of West Nile virus through blood transfusion in the United States in 2002. N Engl J Med **349:**1236-1245.

128. **Sejvar JJ, Haddad MB, Tierney BC, Campbell GL, Marfin AA, Van Gerpen JA, Fleischauer A, Leis AA, Stokic DS, Petersen LR.** 2003. Neurologic manifestations and outcome of West Nile virus infection. JAMA **290:**511-515.

129. **Sampson BA, Ambrosi C, Charlot A, Reiber K, Veress JF, Armbrustmacher V.** 2000. The pathology of human West Nile Virus infection. Hum Pathol **31:**527-531.

130. **Guarner J, Shieh WJ, Hunter S, Paddock CD, Morken T, Campbell GL, Marfin AA, Zaki SR.** 2004. Clinicopathologic study and laboratory diagnosis of 23 cases with West Nile virus encephalomyelitis. Hum Pathol **35:**983-990.

131. **Roehrig JT, Staudinger LA, Hunt AR, Mathews JH, Blair CD.** 2001. Antibody prophylaxis and therapy for flavivirus encephalitis infections. Ann N Y Acad Sci **951:**286-297.

132. **Throsby M, Geuijen C, Goudsmit J, Bakker AQ, Korimbocus J, Kramer RA, Clijsters-van der Horst M, de Jong M, Jongeneelen M, Thijsse S, Smit R, Visser TJ, Bijl N, Marissen WE, Loeb M, Kelvin DJ, Preiser W, ter Meulen J, de Kruif J.** 2006. Isolation and characterization of human monoclonal antibodies from individuals infected with West Nile Virus. J Virol **80:**6982-6992.

133. **Diamond MS, Shrestha B, Marri A, Mahan D, Engle M.** 2003. B cells and antibody play critical roles in the immediate defense of disseminated infection by West Nile encephalitis virus. J Virol **77:**2578-2586.

134. **Diamond MS, Sitati EM, Friend LD, Higgs S, Shrestha B, Engle M.** 2003. A critical role for induced IgM in the protection against West Nile virus infection. J Exp Med **198:**1853-1862.

135. **Oliphant T, Nybakken GE, Austin SK, Xu Q, Bramson J, Loeb M, Throsby M, Fremont DH, Pierson TC, Diamond MS.** 2007. Induction of epitope-specific neutralizing antibodies against West Nile virus. J Virol **81:**11828-11839.

136. **Busch MP, Kleinman SH, Tobler LH, Kamel HT, Norris PJ, Walsh I, Matud JL, Prince HE, Lanciotti RS, Wright DJ, Linnen JM, Caglioti S.** 2008. Virus and antibody dynamics in acute west nile virus infection. J Infect Dis **198:**984-993.

137. **Oliphant T, Engle M, Nybakken GE, Doane C, Johnson S, Huang L, Gorlatov S, Mehlhop E, Marri A, Chung KM, Ebel GD, Kramer LD, Fremont DH, Diamond MS.** 2005. Development of a humanized monoclonal antibody with therapeutic potential against West Nile virus. Nat Med **11:**522-530.

138. **Beasley DW, Barrett AD.** 2002. Identification of neutralizing epitopes within structural domain III of the West Nile virus envelope protein. J Virol **76:**13097-13100.

139. **Li L, Barrett AD, Beasley DW.** 2005. Differential expression of domain III neutralizing epitopes on the envelope proteins of West Nile virus strains. Virology **335:**99-105.

140. **Zhang S, Bovshik EI, Maillard R, Gromowski GD, Volk DE, Schein CH, Huang CY, Gorenstein DG, Lee JC, Barrett AD, Beasley DW.** 2010. Role of BC loop residues in structure, function and antigenicity of the West Nile virus envelope protein receptor-binding domain III. Virology **403:**85-91.

141. **Zlatkovic J, Stiasny K, Heinz FX.** 2011. Immunodominance and functional activities of antibody responses to inactivated West Nile virus and recombinant subunit vaccines in mice. J Virol **85:**1994-2003.

142. **Volk DE, Beasley DW, Kallick DA, Holbrook MR, Barrett AD, Gorenstein DG.** 2004. Solution structure and antibody binding studies of the envelope protein domain III from the New York strain of West Nile virus. J Biol Chem **279:**38755-38761.

143. **Choi KS, Nah JJ, Ko YJ, Kim YJ, Joo YS.** 2007. The DE loop of the domain III of the envelope protein appears to be associated with West Nile virus neutralization. Virus Res **123:**216-218.

144. **Zhang S, Vogt MR, Oliphant T, Engle M, Bovshik EI, Diamond MS, Beasley DWC.** 2009. Development of resistance to passive therapy with a potently neutralizing humanized monoclonal antibody against West Nile virus. Journal of Infectious Diseases **200:**202-205.

145. **Crill WD, Roehrig JT.** 2001. Monoclonal antibodies that bind to domain III of dengue virus E glycoprotein are the most efficient blockers of virus adsorption to Vero cells. J Virol **75:**7769-7773.

146. **He RT, Innis BL, Nisalak A, Usawattanakul W, Wang S, Kalayanarooj S, Anderson R.** 1995. Antibodies that block virus attachment to Vero cells are a major component of the human neutralizing antibody response against dengue virus type 2. J Med Virol **45:**451-461.

147. **Oliphant T, Nybakken GE, Engle M, Xu Q, Nelson CA, Sukupolvi-Petty S, Marri A, Lachmi BE, Olshevsky U, Fremont DH, Pierson TC, Diamond MS.** 2006. Antibody recognition and neutralization determinants on domains I and II of West Nile Virus envelope protein. J Virol **80:**12149-12159.

148. **Pierson TC, Xu Q, Nelson S, Oliphant T, Nybakken GE, Fremont DH, Diamond MS.** 2007. The stoichiometry of antibody-mediated neutralization and enhancement of West Nile virus infection. Cell Host Microbe **1:**135-145.

149. **Thompson BS, Moesker B, Smit JM, Wilschut J, Diamond MS, Fremont DH.** 2009. A therapeutic antibody against west nile virus neutralizes infection by blocking fusion within endosomes. PLoS Pathog **5:**e1000453.

150. **Vogt MR, Moesker B, Goudsmit J, Jongeneelen M, Austin SK, Oliphant T, Nelson S, Pierson TC, Wilschut J, Throsby M, Diamond MS.** 2009. Human monoclonal antibodies against West Nile virus induced by natural infection neutralize at a postattachment step. J Virol **83:**6494-6507.

151. **Kaufmann B, Vogt MR, Goudsmit J, Holdaway HA, Aksyuk AA, Chipman PR, Kuhn RJ, Diamond MS, Rossmann MG.** 2010. Neutralization of West Nile virus by cross-linking of its surface proteins with Fab fragments of the human monoclonal antibody CR4354. Proc Natl Acad Sci U S A **107:**18950-18955.

152. **Ben-Nathan D, Lustig S, Tam G, Robinzon S, Segal S, Rager-Zisman B.** 2003. Prophylactic and therapeutic efficacy of human intravenous immunoglobulin in treating West Nile virus infection in mice. J Infect Dis **188:**5-12.

153. **Ben-Nathan D, Gershoni-Yahalom O, Samina I, Khinich Y, Nur I, Laub O, Gottreich A, Simanov M, Porgador A, Rager-Zisman B, Orr N.** 2009. Using high titer West Nile intravenous immunoglobulin from selected Israeli donors for treatment of West Nile virus infection. BMC Infect Dis **9:**18.

154. **Saquib R, Randall H, Chandrakantan A, Spak CW, Barri YM.** 2008. West Nile virus encephalitis in a renal transplant recipient: the role of intravenous immunoglobulin. Am J Kidney Dis **52:**e19-21.

155. **Makhoul B, Braun E, Herskovitz M, Ramadan R, Hadad S, Norberto K.** 2009. Hyperimmune gammaglobulin for the treatment of West Nile virus encephalitis. Isr Med Assoc J **11:**151-153.

156. **Haley M, Retter AS, Fowler D, Gea-Banacloche J, O'Grady NP.** 2003. The role for intravenous immunoglobulin in the treatment of West Nile virus encephalitis. Clin Infect Dis **37:**e88-90.

157. **Penn RG, Guarner J, Sejvar JJ, Hartman H, McComb RD, Nevins DL, Bhatnagar J, Zaki SR.** 2006. Persistent neuroinvasive West Nile virus infection in an immunocompromised patient. Clin Infect Dis **42:**680-683.

158. **Levi ME, Quan D, Ho JT, Kleinschmidt-Demasters BK, Tyler KL, Grazia TJ.** 2010. Impact of rituximab-associated B-cell defects on West Nile virus meningoencephalitis in solid organ transplant recipients. Clin Transplant **24:**223-228.

159. **Smeraski CA, Siddharthan V, Morrey JD.** 2011. Treatment of spatial memory impairment in hamsters infected with West Nile virus using a humanized monoclonal antibody MGAWN1. Antiviral Res **91:**43-49.

160. **Beigel JH, Nordstrom JL, Pillemer SR, Roncal C, Goldwater DR, Li H, Holland PC, Johnson S, Stein K, Koenig S.** 2010. Safety and pharmacokinetics of single intravenous dose of MGAWN1, a novel monoclonal antibody to West Nile virus. Antimicrob Agents Chemother **54:**2431-2436.

161. **Chu JHJ, Chiang CCS, Ng ML.** 2007. Immunization of flavivirus West Nile recombinant envelope domain III protein induced specific immune response and protection against West Nile virus infection. Journal of Immunology **178:**2699-2705.

162. **Martina BE, Koraka P, van den Doel P, van Amerongen G, Rimmelzwaan GF, Osterhaus AD.** 2008. Immunization with West Nile virus envelope domain III protects mice against lethal infection with homologous and heterologous virus. Vaccine **26:**153-157.

163. **Alonso-Padilla J, de Oya NJ, Blázquez AB, Escribano-Romero E, Escribano JM, Saiz JC.** 2011. Recombinant West Nile virus envelope protein E and domain III expressed in insect larvae protects mice against West Nile disease. Vaccine **29:**1830-1835.

164. **Dunn MD, Rossi SL, Carter DM, Vogt MR, Mehlhop E, Diamond MS, Ross TM.** 2010. Enhancement of anti-DIII antibodies by the C3d derivative P28 results in lower viral titers and augments protection in mice. Virol J **7:**95.

165. **Spohn G, Jennings GT, Martina BE, Keller I, Beck M, Pumpens P, Osterhaus AD, Bachmann MF.** 2010. A VLP-based vaccine targeting domain III of the West Nile virus E protein protects from lethal infection in mice. Virol J **7:**146.

166. **Halstead SB, O'Rourke EJ.** 1977. Dengue viruses and mononuclear phagocytes. I. Infection enhancement by non-neutralizing antibody. J Exp Med **146:**201-217.

167. **Halstead SB, O'Rourke EJ, Allison AC.** 1977. Dengue viruses and mononuclear phagocytes. II. Identity of blood and tissue leukocytes supporting in vitro infection. J Exp Med **146:**218-229.

168. **Roehrig JT, Bolin RA, Kelly RG.** 1998. Monoclonal antibody mapping of the envelope glycoprotein of the dengue 2 virus, Jamaica. Virology **246:**317-328.

169. **Beasley DW, Aaskov JG.** 2001. Epitopes on the dengue 1 virus envelope protein recognized by neutralizing IgM monoclonal antibodies. Virology **279:**447-458.

170. **Lin B, Parrish CR, Murray JM, Wright PJ.** 1994. Localization of a neutralizing epitope on the envelope protein of dengue virus type 2. Virology **202:**885-890.

171. **Gromowski GD, Barrett AD.** 2007. Characterization of an antigenic site that contains a dominant, type-specific neutralization determinant on the envelope protein domain III (ED3) of dengue 2 virus. Virology **366:**349-360.

172. **Zulueta A, Martín J, Hermida L, Alvarez M, Valdés I, Prado I, Chinea G, Rosario D, Guillén G, Guzmán MG.** 2006. Amino acid changes in the recombinant Dengue 3 Envelope domain III determine its antigenicity and immunogenicity in mice. Virus Res **121:**65-73.

173. **Bernardo L, Fleitas O, Pavón A, Hermida L, Guillén G, Guzman MG.** 2009. Antibodies induced by dengue virus type 1 and 2 envelope domain III

recombinant proteins in monkeys neutralize strains with different genotypes. Clin Vaccine Immunol **16:**1829-1831.

174. **Seino KK, Long MT, Gibbs EP, Bowen RA, Beachboard SE, Humphrey PP, Dixon MA, Bourgeois MA.** 2007. Comparative efficacies of three commercially available vaccines against West Nile Virus (WNV) in a short-duration challenge trial involving an equine WNV encephalitis model. Clin Vaccine Immunol **14:**1465-1471.

175. **Minke JM, Siger L, Karaca K, Austgen L, Gordy P, Bowen R, Renshaw RW, Loosmore S, Audonnet JC, Nordgren B.** 2004. Recombinant canarypoxvirus vaccine carrying the prM/E genes of West Nile virus protects horses against a West Nile virus-mosquito challenge. Arch Virol Suppl**:**221-230.

176. **Siger L, Bowen RA, Karaca K, Murray MJ, Gordy PW, Loosmore SM, Audonnet JC, Nordgren RM, Minke JM.** 2004. Assessment of the efficacy of a single dose of a recombinant vaccine against West Nile virus in response to natural challenge with West Nile virus-infected mosquitoes in horses. Am J Vet Res **65:**1459-1462.

177. **Johnson BW, Chambers TV, Crabtree MB, Arroyo J, Monath TP, Miller BR.** 2003. Growth characteristics of the veterinary vaccine candidate ChimeriVax-West Nile (WN) virus in Aedes and Culex mosquitoes. Med Vet Entomol **17:**235-243.

178. **Davis BS, Chang GJ, Cropp B, Roehrig JT, Martin DA, Mitchell CJ, Bowen R, Bunning ML.** 2001. West Nile virus recombinant DNA vaccine protects mouse and horse from virus challenge and expresses in vitro a noninfectious recombinant antigen that can be used in enzyme-linked immunosorbent assays. J Virol **75:**4040-4047.

179. **Mukhopadhyay S, Kim BS, Chipman PR, Rossmann MG, Kuhn RJ.** 2003. Structure of West Nile virus. Science **302:**248.

180. **Hanna SL, Pierson TC, Sanchez MD, Ahmed AA, Murtadha MM, Doms RW.** 2005. N-linked glycosylation of west nile virus envelope proteins influences particle assembly and infectivity. J Virol **79:**13262-13274.

181. **Beasley DW, Davis CT, Whiteman M, Granwehr B, Kinney RM, Barrett AD.** 2004. Molecular determinants of virulence of West Nile virus in North America. Arch Virol Suppl**:**35-41.

182. **Shirato K, Miyoshi H, Goto A, Ako Y, Ueki T, Kariwa H, Takashima I.** 2004. Viral envelope protein glycosylation is a molecular determinant of the neuroinvasiveness of the New York strain of West Nile virus. J Gen Virol **85:**3637-3645.

183. **Beasley DW, Whiteman MC, Zhang S, Huang CY, Schneider BS, Smith DR, Gromowski GD, Higgs S, Kinney RM, Barrett AD.** 2005. Envelope protein glycosylation status influences mouse neuroinvasion phenotype of genetic lineage 1 West Nile virus strains. J Virol **79:**8339-8347.

184. **Shirato K, Miyoshi H, Kariwa H, Takashima I.** 2006. The kinetics of proinflammatory cytokines in murine peritoneal macrophages infected with envelope protein-glycosylated or non-glycosylated West Nile virus. Virus Res **121:**11-16.

185. **Arjona A, Ledizet M, Anthony K, Bonafé N, Modis Y, Town T, Fikrig E.** 2007. West Nile virus envelope protein inhibits dsRNA-induced innate immune responses. J Immunol **179:**8403-8409.

186. **Moudy RM, Payne AF, Dodson BL, Kramer LD.** 2011. Requirement of glycosylation of West Nile virus envelope protein for infection of, but not spread within, Culex quinquefasciatus mosquito vectors. Am J Trop Med Hyg **85:**374-378.

187. **Murata R, Eshita Y, Maeda A, Maeda J, Akita S, Tanaka T, Yoshii K, Kariwa H, Umemura T, Takashima I.** 2010. Glycosylation of the West Nile Virus envelope protein increases in vivo and in vitro viral multiplication in birds. Am J Trop Med Hyg **82:**696-704.

188. **Totani M, Yoshii K, Kariwa H, Takashima I.** 2011. Glycosylation of the envelope protein of West Nile Virus affects its replication in chicks. Avian Dis **55:**561-568.

189. **Kanai R, Kar K, Anthony K, Gould LH, Ledizet M, Fikrig E, Marasco WA, Koski RA, Modis Y.** 2006. Crystal structure of west nile virus envelope glycoprotein reveals viral surface epitopes. J Virol **80:**11000-11008.

190. **Yu S, Wuu A, Basu R, Holbrook MR, Barrett AD, Lee JC.** 2004. Solution structure and structural dynamics of envelope protein domain III of mosquito- and tick-borne flaviviruses. Biochemistry **43:**9168-9176.

191. **Chu JJH, Rajamanonmani R, Li J, Bhuvananakantham R, Lescar J, Ng ML.** 2005. Inhibition of West Nile virus entry by using a recombinant domain III from the envelope glycoprotein. Journal of General Virology **86:**405-412.

192. **McMullen AR, Albayrak H, May FJ, Davis CT, Beasley DW, Barrett AD.** 2013. Molecular evolution of lineage 2 West Nile virus. J Gen Virol **94:**318-325.

193. **Beasley DW, Li L, Suderman MT, Barrett AD.** 2002. Mouse neuroinvasive phenotype of West Nile virus strains varies depending upon virus genotype. Virology **296:**17-23.

194. **Sapkal GN, Harini S, Ayachit VM, Fulmali PV, Mahamuni SA, Bondre VP, Gore MM.** 2011. Neutralization escape variant of West Nile virus associated with altered peripheral pathogenicity and differential cytokine profile. Virus Res **158:**130-139.

195. **Bernardin F, Stramer,S., Caglioti,S., Busch,M.P. and Delwart,E.** 2010. Phylogenetic analysis of WNV in US blood donors during the 2003-2007 epidemic seasons Blood Systems Research Institute and University of California San Francisco.

196. **Pybus OG, Suchard MA, Lemey P, Bernardin FJ, Rambaut A, Crawford FW, Gray RR, Arinaminpathy N, Stramer SL, Busch MP, Delwart EL.** 2012. Unifying the spatial epidemiology and molecular evolution of emerging epidemics. Proc Natl Acad Sci U S A **109:**15066-15071.

197. **Armstrong PM, Vossbrinck CR, Andreadis TG, Anderson JF, Pesko KN, Newman RM, Lennon NJ, Birren BW, Ebel GD, Henn MR.** 2011. Molecular evolution of West Nile virus in a northern temperate region: Connecticut, USA 1999-2008. Virology **417:**203-210.

198. **Herring BL, Bernardin F, Caglioti S, Stramer S, Tobler L, Andrews W, Cheng L, Rampersad S, Cameron C, Saldanha J, Busch MP, Delwart E.** 2007. Phylogenetic analysis of WNV in North American blood donors during the 2003-2004 epidemic seasons. Virology **363:**220-228.

199. **Nowak T, Wengler G.** 1987. Analysis of disulfides present in the membrane proteins of the West Nile flavivirus. Virology **156:**127-137.

200. **Volk DE, Lee YC, Li X, Thiviyanathan V, Gromowski GD, Li L, Lamb AR, Beasley DW, Barrett AD, Gorenstein DG.** 2007. Solution structure of the envelope protein domain III of dengue-4 virus. Virology **364:**147-154.

201. **Beasley DW, Davis CT, Guzman H, Vanlandingham DL, Travassos da Rosa AP, Parsons RE, Higgs S, Tesh RB, Barrett AD.** 2003. Limited evolution of West Nile virus has occurred during its southwesterly spread in the United States. Virology **309:**190-195.

202. **De Kruif CA, Throsby M.** 2006. Binding molecules capable of neutralizing West Nile virus and uses thereof United States.

203. **ArboNET** 2013, posting date. West Nile virus disease cases reported to CDC by state, 1999-2012. Centers for Disease Control and Prevention. [Online.]

204. **Godsey MS, Burkhalter K, Young G, Delorey M, Smith K, Townsend J, Levy C, Mutebi JP.** 2012. Entomologic investigations during an outbreak of West Nile virus disease in Maricopa County, Arizona, 2010. Am J Trop Med Hyg **87:**1125-1131.

205. **Gibney KB, Colborn J, Baty S, Bunko Patterson AM, Sylvester T, Briggs G, Stewart T, Levy C, Komatsu K, MacMillan K, Delorey MJ, Mutebi JP, Fischer M, Staples JE.** 2012. Modifiable risk factors for West Nile virus infection during an outbreak--Arizona, 2010. Am J Trop Med Hyg **86:**895-901.

206. **McMullen AR, May FJ, Li L, Guzman H, Bueno R, Dennett JA, Tesh RB, Barrett AD.** 2011. Evolution of new genotype of West Nile virus in North America. Emerg Infect Dis **17:**785-793.

207. **Keller BC, Fredericksen BL, Samuel MA, Mock RE, Mason PW, Diamond MS, Gale M.** 2006. Resistance to alpha/beta interferon is a determinant of West Nile virus replication fitness and virulence. J Virol **80:**9424-9434.

208. **Botha EM, Markotter W, Wolfaardt M, Paweska JT, Swanepoel R, Palacios G, Nel LH, Venter M.** 2008. Genetic determinants of virulence in pathogenic lineage 2 West Nile virus strains. Emerg Infect Dis **14:**222-230.

209. **Bertolotti L, Kitron U, Goldberg TL.** 2007. Diversity and evolution of West Nile virus in Illinois and the United States, 2002-2005. Virology **360:**143-149.

210. **Añez G, Grinev A, Chancey C, Ball C, Akolkar N, Land KJ, Winkelman V, Stramer SL, Kramer LD, Rios M.** 2013. Evolutionary dynamics of West Nile virus in the United States, 1999-2011: phylogeny, selection pressure and evolutionary time-scale analysis. PLoS Negl Trop Dis **7:**e2245.

211. **Grinev A, Rios M.** 2006. Genetic variability of West Nile virus (WNV) in blood donor populations during four consecutive epidemics (2002 to 2005) in the USA

212. **Lin TY, Dowd KA, Manhart CJ, Nelson S, Whitehead SS, Pierson TC.** 2012. A novel approach for the rapid mutagenesis and directed evolution of the structural genes of west nile virus. J Virol **86:**3501-3512.

213. **Lee E, Lobigs M.** 2000. Substitutions at the putative receptor-binding site of an encephalitic flavivirus alter virulence and host cell tropism and reveal a role for glycosaminoglycans in entry. J Virol **74:**8867-8875.

214. **Chu JJ, Leong PW, Ng ML.** 2005. Characterization of plasma membrane-associated proteins from Aedes albopictus mosquito (C6/36) cells that mediate West Nile virus binding and infection. Virology **339:**249-260.

215. **Paingankar MS, Gokhale MD, Deobagkar DN.** 2010. Dengue-2-virus-interacting polypeptides involved in mosquito cell infection. Arch Virol **155:**1453-1461.

216. **Ren J, Ding T, Zhang W, Song J, Ma W.** 2007. Does Japanese encephalitis virus share the same cellular receptor with other mosquito-borne flaviviruses on the C6/36 mosquito cells? Virol J **4:**83.

217. **Klimstra WB, Ryman KD, Johnston RE.** 1998. Adaptation of Sindbis virus to BHK cells selects for use of heparan sulfate as an attachment receptor. J Virol **72:**7357-7366.

218. **Mandl CW, Kroschewski H, Allison SL, Kofler R, Holzmann H, Meixner T, Heinz FX.** 2001. Adaptation of tick-borne encephalitis virus to BHK-21 cells results in the formation of multiple heparan sulfate binding sites in the envelope protein and attenuation in vivo. J Virol **75:**5627-5637.

219. **Lee E, Hall RA, Lobigs M.** 2004. Common E protein determinants for attenuation of glycosaminoglycan-binding variants of Japanese encephalitis and West Nile viruses. J Virol **78:**8271-8280.

220. **Snapinn KW, Holmes EC, Young DS, Bernard KA, Kramer LD, Ebel GD.** 2007. Declining growth rate of West Nile virus in North America. J Virol **81:**2531-2534.

221. **Rossmann MG, Arnold E, Erickson JW, Frankenberger EA, Griffith JP, Hecht HJ, Johnson JE, Kamer G, Luo M, Mosser AG.** 1985. Structure of a

human common cold virus and functional relationship to other picornaviruses. Nature **317:**145-153.

222. **Rossmann MG.** 1989. The canyon hypothesis. Hiding the host cell receptor attachment site on a viral surface from immune surveillance. J Biol Chem **264:**14587-14590.

223. **Rossmann MG.** 1994. Viral cell recognition and entry. Protein Sci **3:**1712-1725.

224. **Rossmann MG, He Y, Kuhn RJ.** 2002. Picornavirus-receptor interactions. Trends Microbiol **10:**324-331.

225. **Rossmann MG, Palmenberg AC.** 1988. Conservation of the putative receptor attachment site in picornaviruses. Virology **164:**373-382.

226. **Chapman MS, Rossmann MG.** 1993. Comparison of surface properties of picornaviruses: strategies for hiding the receptor site from immune surveillance. Virology **195:**745-756.

227. **Harrison SC, Olson AJ, Schutt CE, Winkler FK, Bricogne G.** 1978. Tomato bushy stunt virus at 2.9 A resolution. Nature **276:**368-373.

228. **Abad-Zapatero C, Abdel-Meguid SS, Johnson JE, Leslie AG, Rayment I, Rossmann MG, Suck D, Tsukihara T.** 1980. Structure of southern bean mosaic virus at 2.8 A resolution. Nature **286:**33-39.

229. **Colonno RJ, Condra JH, Mizutani S, Callahan PL, Davies ME, Murcko MA.** 1988. Evidence for the direct involvement of the rhinovirus canyon in receptor binding. Proc Natl Acad Sci U S A **85:**5449-5453.

230. **Pevear DC, Fancher MJ, Felock PJ, Rossmann MG, Miller MS, Diana G, Treasurywala AM, McKinlay MA, Dutko FJ.** 1989. Conformational change in the floor of the human rhinovirus canyon blocks adsorption to HeLa cell receptors. J Virol **63:**2002-2007.

231. **Wiley DC, Skehel JJ.** 1987. The structure and function of the hemagglutinin membrane glycoprotein of influenza virus. Annu Rev Biochem **56:**365-394.

232. **Pokidysheva E, Zhang Y, Battisti AJ, Bator-Kelly CM, Chipman PR, Xiao C, Gregorio GG, Hendrickson WA, Kuhn RJ, Rossmann MG.** 2006. Cryo-EM reconstruction of dengue virus in complex with the carbohydrate recognition domain of DC-SIGN. Cell **124:**485-493.

233. **Nelson DL, Cox MM.** 2005. Lehninger Principles of Biochemistry, 4 ed. W. H. Freeman and Company, New York, NY.

234. **Sigma-Aldrich** 2013, posting date. Amino Acids Reference Chart. http://www.sigmaaldrich.com/life-science/metabolomics/learning-center/amino-acid-reference-chart.html

Vita

Jessica Ann Plante was born Jessica Ann Lewis on November 21, 1985 in Livermore, California. She is the only child of Linda Ann Lewis and Charles David Lewis. Jessica graduated from Livermore High School in 2003 and earned her Bachelor of Science degree in microbiology from the University of California at Davis in 2006. Jessica spent one year working at Lawrence Livermore National Laboratory before moving to Galveston, Texas to begin graduate school in 2007. During her studies Jessica has been supported by fellowships from the Sealy Center for Vaccine Development and the NIH T32 Biodefense Training Program. Jessica also earned an Edward S. Reynolds award and a McLaughlin travel award.

Permanent address: 13 Manor Way, Galveston, Texas, 77550

This dissertation was typed by Jessica Ann Plante.